2011

Kinetics and Mechanisms of Release by Redox-Active Liposomes in Drug Delivery

Jerimiah Forsythe
Louisiana State University and Agricultural and Mechanical College, jforsy2@lsu.edu

KINETICS AND MECHANISMS OF RELEASE BY REDOX-ACTIVE LIPOSOMES IN DRUG DELIVERY

A Dissertation

Submitted to the Graduate Faculty of the
Louisiana State University and
Agricultural and Mechanical College
in partial fulfillment of the
requirements for the degree of
Doctor of Philosophy

in

The Department of Chemistry

By
Jerimiah Forsythe
B.S., Colorado State University, 2002
M.S., Washington State University, 2005
August 2011

DEDICATION

This dissertation is dedicated to my loving wife:

Carley Petrie Forsythe

And to my family:

My Mom, Cathy Forsythe

My Dad, Robert Forsythe

My Brother, Brandon Forsythe

ACKNOWLEDGMENTS

As I sit down to write this one last final part to this dissertation, the memories and experiences to reach this point come flooding back to me. It has been an interesting journey and not one I would have ever thought possible without the encouragement and support of so many different people. There was many points during my entire graduate career where I considered quitting or turning back as the prospects of continuing forward on this path were simply too daunting. There were, however, many interesting and wonderful times to, but all through it, I learned a lot about myself. This journey has taught me to think, analyze, and when all else fails, isolate all the variables or try another approach.

I would like to express my deepest gratitude to my advisor, Dr. Robin L. McCarley for his support and guidance over the years. I had no inkling the direction my research would take or what I was getting myself into after our first meeting to discuss possible research topics. When starting with an open-ended question, one never knows what the results or the direction will be. In all honesty, a more appropriate title for this document would be "Adventures in Chemistry" from the sheer breadth of topics covered, researched, and pondered. In the end, despite all of the frustrations, articles, research, time, sweat, swearing, and confusion, this project has made me a better scientist and most of all, the critical ability to think and analyze.

I would also like to thank Dr. Bruce Parkinson who had a huge influence and hand in where I am today. Again, I would like to express my deepest gratitude for all of the years of support, advice, guidance, and most importantly the encouragement to pursue a graduate education. I honestly had no idea what I was getting myself into when I started as an undergraduate researcher in your lab – all I knew was that I wanted to do research and the opportunities you gave me have taken me all the way to this point.

To the McCarley research group, thank you for your support and friendship. The group is certainly dynamic and ever changing. I'll remember all of our lab cleaning sessions, gatherings, and conferences for years to come. I finally have an appreciation for organic chemistry after working so closely with a lot of synthetic organic chemists. Who knew an analytical group would gravitate toward a hybrid analytical/organic group and that I would ever perform an actual synthesis of an organic compound on my own!

To my committee members, Dr. David Spivak, Dr. Jayne Garno, and last-minute-substitution Dr. John Pojman – thank you for taking the time to assist me with my dissertation, for sitting in on my defense talk, and for your insightful questions and comments. To my Dean's representative, Dr. Fred Sheldeon, thank you for taking the time to sit on my committee for both my general exam and my final defense.

I would also like to thank all of those who have taken the time to assist with instruments, concepts, theories, and synthesis advice that helped me through the course of my research. Thank you especially to Dr. Sreelatha Balamurugan, Dr. Raphael Cueto, Dr. Dale Treleaven, and Dr. Vince LiCata.

Finally to my family, without your support and love, I would not be where I am today. Thank you, to both of my parents for your sacrifices to help me with my education and everything else you have done and provided for me.

Last and most importantly, thank you to my dear wife Carley. Thank you for putting up with me for the past year. I know this entire process has been difficult for both of us, including late nights and weekends at the lab or stuck in front of the computer writing, but here we are, on the other side. Now the real adventures begin…

TABLE OF CONTENTS

LIST OF TABLES

LIST OF FIGURES

LIST OF SCHEMES

LIST OF ABBREVIATIONS AND SYMBOLS

ANTS	1-aminonaphthalene-3,6,8-trisulfonic acid
DEPE	1,2-dielaidoyl-*sn*-glycero-3-phosphoethanolamine
DLiPE	1,2-dilinoleoyl-*sn*-glycero-3-phosphoethanolamine
DLS	Dynamic light scattering
DOPC	1,2-dioleoyl-*sn*-glycero-3-phosphocholine
DOPE	1,2-dioleoyl-*sn*-glycero-3-phosphoethanolamine
DOPE-Me	1,2-dioleoyl-*sn*-glycero-3-phosphoethanolamine-N-methyl
DPA	Dipicolinic acid
DPPE	1,2-dipalmitoyl-*sn*-glycero-3-phosphoethanolamine
DPX	*N*, *N'*-*p*-xylylenebis-(pyridinium bromide)
DSPE	1,2-distearoyl-*sn*-glycero-3-phosphoethanolamine
EDTA	Ethylenediaminetetraacetic acid
EPR	Enhanced permeability and retention
$FADH_2$	1,5-dihydro-flavin adenine dinucleotide
$L\alpha$	Lamellar liquid crystalline
$L\beta$	Lamellar gel
H_{II}	Inverted hexagonal, inverted micelle
MPS	Mononuclear phagocyte system
NAD(P)H	Nicotinamide adenine dinucleotide (with or without phosphate)
NBD	7-nitrobenz-2-oxa-1,3-diazol-4-yl
NQO1	NAD(P)H: quinone oxidoreductase type 1
PC	Phosphatidylcholine

PE	Phosphatidylethanolamine
PEG	Poly(ethylene glycol)
Q_3-DLiPE	Trimethy-locked, quinone capped 1,2-dilinoleoyl-*sn*-glycero-3-phosphoethanolamine
Q_0-DOPE	Quinone capped 1,2-dioleoyl-*sn*-glycero-3-phosphoethanolamine
Q_3-DOPE	Trimethyl-locked, quinone capped 1,2-dioleoyl-*sn*-glycero-3-phosphoethanolamine
RES	Reticulo-endothelial system
Rh	Rhodamine
T_H	Hexagonal phase transition temperature, lipid phase change from $L\alpha \rightarrow H_{II}$
T_M	Chain melting temperature, lipid phase change from $L\beta \rightarrow L\alpha$
TES	(2-[2-hydroxy-1,1-bis(hydroxymethyl)ethyl)amino]ethanesulfonic acid

ABSTRACT

Liposomes have had a long and fruitful application of drug delivery devices in the treatment of select tumors and cancer types. Third-generation liposomes possess endogenous triggering methods that hold the ability for site-specific unloading of liposomal contents, thus providing necessary temporal and spatial control over contents release that can be tuned to match the drug efficacy for decreased side effects during treatment. Of these new endogenous triggers, redox-active liposomes that can be triggered to unload contents via two-electron reduction by enzymes or chemical means have demonstrated promise for the encapsulation and delivery of cargo.

The research project undertaken involved the study in the mechanisms responsible for the unloading of contents from redox-active, trimethyl-locked, quinone-capped DOPE (Q_3-DOPE) liposomes. It is envisioned that the local environment surrounding the liposomes is responsible for the phase behavior and rate of contents unloading due to the influence of the phase conversion of DOPE. Once the capping quinone headgroup is removed via lactone formation, lamellar phase DOPE liposomes are expected to come into close approach, aggregate, and release their contents by phase conversion to non-lamellar inverted hexagonal phase DOPE. To that end, the research here involved measurement of the rate of phase conversion through (1) study of the experimental temperature differences on the phase conversion temperature to drive contents unloading and (2) the effects of Hofmeister anion salts on the rate of contents unloading. Study of both of these lead to the hypothesis that the interfacial water layer is critical in the close approach and aggregation rate of lamellar DOPE liposomes and the presence of the Hofmeister anions assists in regulation of the water layer.

CHAPTER 1

INTRODUCTION

1.1 Research Goals and Aims

The goal of this research is to investigate the kinetics of release following the stimuli-responsive reduction of a redox-active liposomal system. In particular, the question of how to control the temporal and spatial guest release through the manipulation of the phase transition behavior of phosphatidylethanolamine (PE) lipids by temperature, salt concentration, and anions of the Hofmeister series will be investigated.

Ever since the observations of A. D. Banghamn in 1965 that dispersions of phospholipids in aqueous medium spontaneously form closed bilayer structures,[1] liposomes have advanced to be major components of biophysical research and a diverse collection of commercial applications including pharmaceutical carriers. Liposome-based therapeutics have had a significant impact on the treatment of select cancers, fungal infections, and even as a delivery device for influenza vaccines.[2] As of 2007, more than 150 companies have been actively researching liposome-based therapeutics, yielding 11 clinically-approved, liposome-encapsulated pharmaceutical formulations.[3] In analytical sciences, liposomes are being developed as components in new analytical systems, such as liposome-based immunoassays and nanoscale-scale analytical devices for reagent delivery or isolated reaction sites for sensitive reactions.[4] Regardless of this considerable interest in liposomes and their applications, there are still a number of novel methods that can be applied to liposomal systems to study the underlying biophysical effects that the lipid subunits have on the behavior of the system.

Currently, the clinical utility of most conventional liposome-based therapeutics is limited either by the inability to actively deliver appropriate therapeutic drug concentrations to the target tissues or by severe and harmful toxic effects on normal, healthy organs and tissues. In order to

circumvent these issues, “selective” delivery of liposome-based therapeutics to target only those organs, tissues, or cells affected by disease needs to be developed. By using environmental triggers that are present at the desired delivery site, liposome-based therapeutics can be directed to diseased sites and actively unload their contents rather than relying on the passive diffusion delivery method of conventional liposomes.[5] Through active delivery, liposomal carriers can be developed that have a tunability over the release profile to adapt it to match the therapeutic profile to the drug being delivered. The McCarley research group has previously developed a redox-triggerable lipid capable of forming liposomes and encapsulating cargo. However, the redox-lipid remains unexplored for the kinetic release profile in different salt concentrations, salt components, and temperature.

The first aim of this research is to establish the standard behavior and mechanism of release of the redox-active quinone capped phosphatidylethanolamine (PE) lipid, known as Q_3-DOPE. Pure Q_3-DOPE liposomes were prepared using a standard buffer of pH 7.4 50 mM phosphate and 75 mM KCl. Quenched, non-fluorescent concentrations of calcein dye were used as a probe to assess the encapsulation ability and stability of the liposomes. Leakage that leads to dequenching of the calcein was followed by fluorescence spectroscopy after introduction of a chemical reducing agent, sodium dithionite ($Na_2S_2O_4$), to reduce and remove the capping headgroup via a trimethyl lock-facilitated lactonization reaction. Dynamic light scattering (DLS), zeta potential, and UV-vis spectroscopy were used to further characterize the Q_3-DOPE liposomes to establish its hosting and the mechanism and kinetics of guest release upon reduction.

The second aim of this research is to investigate environmental changes to the Q_3-DOPE liposomes in order to influence the kinetics and rate of content release. In addition, the key interest of the second aim was the observation of the release kinetics following a Hofmeister salt

series with a common K^+. The hypothesis in the use of Hofmeister salts is to influence the phase transition temperature (T_H) of the DOPE lipid, either favoring or disfavoring the fusion of DOPE liposomes and the release of the quenched calcein probe. In addition, the role of temperature was first probed due to the low T_H of the DOPE lipid, reported to be between – 4 and 16 °C.[6] Based on the results of the temperature study, a second lipid, DLiPE with a T_H = – 15 °C,[7] was prepared with the capping quinone headgroup for Q_3-DLiPE.

The third goal of this research is to investigate the differences in quinone structure of the capping headgroup. The geminal methyls in the trimethyl lock were found to be important in the rate for which the lactone is released from the lipid. Without the *gem*-methyls, the Q_1-DOPE experiences an exceptionally slow rate of probe release due to the slow release rate of the lactone from the headgroup. Further removal of all methyl groups on the quinone for Q_0-DOPE results in no observable release of any contents over a period of over 24 hrs.

Ultimately, Q_3-DOPE liposomes will be used as drug or reagent delivery vehicles that operate by reductive activation, either enzymatically or chemically, to unload an encapsulated cargo. The findings here allow for development of an understanding of the underlying behavior of the DOPE that contributes to the release kinetics of the Q_3-DOPE system and to further influence the kinetics by careful selection of environmental factors and the type of lipid used in the redox-active liposome system for content delivery.

1.2 Review of Liposomes and Responsive Systems for Delivery

1.2.1 Challenges for Drug Delivery

For liposomes to fulfill requirements as drug carriers and delivery agents, they must meet two criteria. First, the encapsulated cargo must remain inside the liposome and not prematurely leak. Early leakage hampers the inherit benefits of lowering the drug toxicity by liposomal encapsulation, as well as decreasing the concentration of the drug available at the target site.

Secondly, as the most common introduction of liposomal carriers into the body is through intravenous injection into the vascular system, the liposomes must avoid components of the mononuclear phagocyte system (MPS)[8] (previously known as the reticulo-endothelial system or RES)[2] that is responsible for the capture and removal of foreign objects from circulating blood.[9] While the behavior of the MPS can be exploited for delivery of antiparasitic and antimicrobial drugs to treat localized infections of the MPS, longer blood circulation times are required to take advantage of the leaky tumor vasculature and poor lymphatic drainage of tumors.[10,11] The leaky tumor vasculature and poor lymphatic system of cancerous tumors, known as the enhanced permeability and retention (EPR) effect, results in accumulation of particles and objects on the order of 100 nm in the interstitial area of tumors, permitting the accumulation of liposomes.[12] Once the liposomes reach their target site, the contained drug must be unloaded into the region. This can be done by either passive diffusion of the drug or by an active trigger designed to disrupt or destroy the lipid bilayer, resulting in rapid release of the drug.

1.2.2 Liposome-Based Delivery Systems

The clinical utility of the majority of conventional chemotherapeutics is limited by either the inability of drugs to reach target tissues in sufficient therapeutic concentrations, or the drugs themselves have severe to toxic effects on normal, healthy organs and tissues. Thus, the full therapeutic potential of many drugs cannot be completely exploited. Many different methods have been developed to overcome these problems, one of which focuses on sequestering the drug inside a biocompatible container that can then be selectively delivered to target organs, tissues, or cells affected by disease. Liposomes, by design, are biocompatible due to the lipid composition of the barrier separating the interior from the exterior of the container. The lipid bilayer allows hydrophobic drugs to reside within the hydrophobic region of the lipid layers while water-soluble drugs can be encapsulated completely inside the liposome interior.

Conventional liposomes or first-generation liposomes, upon intravenous administration, are rapidly (<6 hours) recognized by components of the MPS; opsonins are bound to the liposome surface and these opsonin-liposome complexes are removed from blood circulation via the liver and lymph nodes.[2] Interestingly, their capture by the MPS can be used to effectively deliver antimicrobial and antiparasitic drugs to treat infections of the MPS. Early methods to prevent opsonination involved manipulation of the bilayer fluidity, as the incorporation of cholesterol into the bilayer along with careful selection of lipids containing saturated acyl chains was observed to yield liposomes with an increased stability in blood when compared to non-cholesterol-containing bilayers or bilayers containing unsaturated acyl chain lipids.[13] It was also noted that the size and lamellarity of liposomes had influence over the rate of clearance from the blood as larger liposomes were eliminated from the blood more rapidly than were smaller liposomes.[2] Finally, the surface charge of the liposome can be varied through the incorporation of positively or negatively charged lipids. However, the addition of charge to the liposome surface had consequences, as clearance times of both negatively and positively charged liposomes were faster than those of neutral liposomes.[4]

As of 2007, there were five approved conventional liposomal drug delivery systems based on lipid cholesterol formulations.[8] The most widely known is Doxil (liposome Doxorubicin) for the treatment of Kaposi's sarcoma and Myocet (Doxorubicin) for the treatment of breast cancer. Another formulation, called Depocyt, is for the treatment of lymphomatous meningitis, and Liposomal-Annamycin for treatment of fungal infections in immuno-compromised patients. There are 14 different conventional liposome formulations in clinical trials, with the main focus on the treatment of various cancers.[8]

In order to overcome or slow opsonin binding to the liposome surface, second-generation liposomes were developed based on the work of T.M. Allen and D. Papahadjopoulos. Water-

soluble poly(ethylene glycol), PEG, groups were anchored to a cross-liked lipid and incorporated into liposome surfaces.[14] These second-generation liposomes are called sterically stabilized or "stealth" liposomes and experience significantly improved blood circulation times (up to 24 hours).[15] Longer-circulating liposomes can passively accumulate inside tumor tissues by taking advantage of the enhanced permeability and retention (EPR) effect.[10] The EPR effect results from the porous endothelial vasculature and poor lymphatic drainage of the tumor that draws blood and leads to concentration of small (100–200 nm in diameter) objects, such as liposomes, into the tumor region.[12] PEGylated cationic liposomes have also been found to slow or inhibit the MPS response and have become a major cornerstone in the development of non-viral DNA delivery;[16] and have recently been investigated for the liposome-mediated delivery of small interfering RNA (siRNA).[17] Alternatives to PEG, such as protective polymers,[18] biodegradable polymers[19] and even amino acids,[20] are being investigated as possible next-generation, long-circulating liposomes that have a modifiable degradation time, permitting further applications of this type of liposome.

The first approved PEG liposome is DOXIL/Caelyx (liposomal Doxorubicin) for the treatment of Kaposi's sarcoma and recurrent ovarian cancer.[8] Nearly all of the cardiotoxic side-effects from conventional Doxorubicin have decreased occurrence with the use of Doxorubicin PEG liposomes. Further applications of DOXIL/Caelyx are currently in progress to study treatment of myeloma, breast cancer and recurrent high-grade glioma. Several other PEG liposome-based formulations are in clinical trials for the treatment of neck and lung cancer, acute myeloid leukemia, multiple sclerosis and prostate cancer.[8,21]

While passive release of drugs from liposome systems has had significant impact on the treatment of cancers, the current first- and second-generation liposomes do not come without side effects, with the most common being hand-foot syndrome associated with liposomal

treatment.[22] There also remains the question of the kinetics of release of the drug from the liposome through passive diffusion routes, as it is difficult to determine the ratio between free and encapsulated drug residing in the extracellular fluid of tumors.[23] Matching toxic drugs to an effective dosing model for passive diffusion is limited at best, providing severe side effects, such as bone-marrow and other organ toxicities.[5] Recent efforts in liposomal research address both of these issues by focusing on stimuli-responsive liposomes with a programmed self-destructive pathway to actively unload their contents after reaching a specific site. Stimuli-responsive liposomes offer the ability to tune the rate of drug release to match the efficacy profile of the drug to improve the effectiveness of treatment.[24]

1.2.3 Triggered Release

Triggered or stimuli-responsive systems rely on the stimulus to be present or to reach the target site at sufficient concentrations or intensities to result in the triggering of the system to begin its self-programmed destruction path. Ideally, the stimulus is not present at other locations so as to prevent premature or unwanted opening of the liposome and delivery of the pharmaceutical agents to non-diseased tissues. Upon the occurrence of the stimulus event, the liposomes can be designed to either fuse with other liposomes and lipid bilayers to unload the interior cargo or for the lipid bilayer of the liposome to become permeable to its contents. Previous stimuli-responsive systems have exploited both external (exogenous) triggers, such as temperature[25,26] or radiation,[27,28] or internal (endogenous) triggers, such as pH[29,30] or enzyme activity.[31,32]

The simplest approach for temperature-sensitive liposomes takes advantage of lipids with different phase transition temperatures (T_H) or different chain melting temperatures (T_M) by either selecting lipids with various chain lengths or chain saturation.[33] Heating a lipid beyond its T_H induces a change in the phase of the lipid, causing them to undergo a phase transition from a

lamellar to a non-lamellar form, thereby disrupting the lipid bilayer and causing content release to occur. Lipids can be selected with different T_M values, creating a liposome that can have permeable regions at elevated temperatures, permitting the drug to diffuse outside of the liposome.[34,35] Also, temperature-sensitive polymers, such as poly(organophosphazenes), change conformation at temperatures from 32 to 44 °C and have previously been incorporated into liposomes for successful release of liposome contents at elevated temperatures.[36]

Light-sensitive liposomes have had two primary different development pathways, one focused on the use of light to cleave a photoresponsive headgroup from the lipid, while the other has focused on light-driven polymerization of functional groups on the acyl hydrocarbon chains. For the photoresponsive headgroup, Zhang and Smith attached 6-nitroveratryl-oxycarbonyl chloride (NVOC-Cl) to DOPE and upon exposure to 300–nm light, released the headgroup and CO_2 from the DOPE.[28] The DOPE liposomes then have to undergo membrane fusion and release their contents via lipid phase transition. A 20–minute exposure with 300 nm light from a 150 W lamp, resulted in release of approximately 50% of the contents after 40 minutes (pH 5 and 37 °C).[28] Alternatively, liposomes can be made permeable by polymerizable lipids, as in the case with lipids containing a photosensitive group, 10-(2',4'-hexadienoyloxy)decanoyl attached to the lipid hydrocarbon chains of PC lipids.[37] Photopolymerization of the acyl hydrocarbon chains was achieved with 1–2 min exposure to 258–nm light, demonstrating approximately 40% release of contents after 30 seconds after the termination of light exposure (pH 7 and 37 °C).[38]

The utility of exogenous triggers is limited by the ability of the stimulus to reach the responsive liposomes at a significant amount as to trigger the content unloading mechanism of the liposomes. For example, with light-sensitive liposomes, the activation of the liposome is limited by the distance light can penetrate into the skin. Studies have demonstrated that on average, approximately half low wavelength light can reach the epidermis layer, which has an

average depth of 0.05 mm.[39] Thus, light responsive liposomes are limited to sites near the surface of skin and require the use of wavelengths and intensities of light that are potentially harmful to the outer epidermis. Complex medical engineering is required for the application of light to regions of the body deeper than the epidermis layer of skin. Temperature sensitive liposomes require less engineering to deliver the stimulus to the site, as it can be as simple as selectively heating a region of the body that contains the site of delivery. Like light penetration into the skin, the question arises of how far temperature can penetrate into the body and be comfortably maintained for the period of time required to trigger and unload the liposomal contents. For example, heating the interior of a limb to a constant 40 °C for several hours may not be the most comfortable form of treatment, especially considering that the exterior temperature may be significantly higher.

With endogenous triggers, such as pH or enzymatic activity, the stimulus is already present at the target site; stimuli-responsive liposomes would only have to be administered while the design of the system would facilitate delivery and release of the drug from the liposome. An endogenous trigger would not be limited to a region where the applied stimulus could reach, permitting the delivery of drugs to sites within the body that would otherwise be inaccessible to light or elevated temperature.

A number of pH-triggered liposomes have been developed over the past thirty years.[40,41] This interest comes from the observed decrease in pH in many of the physiological and pathological processes that occur in liposome uptake and delivery, such as endosome trafficking,[42] tumor growth,[43] and inflammation.[44] Mechanisms for pH-triggered liposomes include lamellar to non-lamellar phase states from protonation of negatively charged lipids, protonation of negative peptides or polymers, hydrolysis of bilayer-stabilizing lipids to destabilizing lipids, and pH-sensitive surfactants.[45] The difficulty in developing pH-responsive

liposomes stems from the small pH changes, usually 0.4 to 0.8 units more acidic than physiological pH, in inflammatory and tumor tissues.

Another form of endogenous trigger resides in the form of redox-sensitive liposomes through the inclusion of a redox-active group attached to the lipids of bilayer membranes. Moieties such as ferrocene have been incorporated into surfactants to create micelles that can be broken up into monomers upon addition of a reducing agent.[46] Ferrocene and chelated transition metal complexes can be incorporated into multilamellar liposomes that are destroyed upon exposure to a reducing agent.[47-49] Finally, ferrocene coupled with cationic lipids for a form of a redox-active liposome has been demonstrated as a viable method for transferring DNA across cell membranes.[50]

Aside from exploiting environmental differences to trigger liposomal destruction, other groups have demonstrated the use of antibodies and enzymes as a method to direct liposomes to a therapeutic region of the body for site-specific drug delivery. Antibodies can be directly attached to the lipid headgroup or to the terminal end of a poly(ethylene glycol) chain to create immunoliposomes that can be tuned to target antigen molecules expressed on the membranes of tumor cells.[2] Peptide sequences have also been integrated into liposome surfaces that are targeted toward blood vessels found in tumors.[2]

The overexpression or the involvement of enzymes at tumor sites has been another venue for endogenous triggering that has recently experienced interest for a number of different research groups. Elastase, an enzyme involved in the inflammatory response and tumor sites, has been used to target DOPE liposomes capped with a simple peptide sequence.[51] The peptide sequence-DOPE lipids operate in a similar manner to the light-sensitive DOPE liposomes, where the peptides are used to stabilize the DOPE lipids until removal from the lipid headgroup via enzymatic cleavage. Rather than using DOPE fusion pathways, elevated activities of

phospholipase A_2 (PLA_2) in inflammatory and tumor tissues can be used to trigger PEG-liposomes due to observations of enhanced hydrolysis of the liposomes by PLA_2.[52] PLA_2 interacts with liposomes and catalyzes the hydrolysis of the lipids at the *sn*-2 position, releasing fatty acids and non-bilayer single-tailed lysolipids, completely disrupting the liposomal bilayer by the destruction of the lipids themselves.[24,53] Other enzymes for triggering liposomal systems include alkaline phosphatase,[54] phospholipase C,[32] and matrix metalloproteinases MMP2[55] and MMP9.[56] Due to the upregulation of certain enzymes in tumor tissues and the ability of those enzymes to recognize specific substrates, they make an attractive and interesting endogenous trigger for payload delivery of liposomes.

1.2.4 Engineering Liposomes for Triggered Release

Ideally, an applied stimulus at a specific location triggers the onset of cargo unloading by either inducing a phase change in the lipids or through destabilizing the membrane bilayer. There exists a number of different systems in the literature that already exploit a number of different triggers with only a small fraction of those systems being enzyme responsive. However, one fundamental problem across most systems is the inattention to the environmental conditions that are used for the release assays. There is no single standard buffer system, pH, or temperature across the assays, making it difficult at best to compare release kinetics and abilities of each system. In the following sections, the nature of lipids and the impacts of different environmental conditions on their behavior will be discussed.

1.3 Nature of Lipids

1.3.1 Lipid Structure and Phase Behavior

Phospholipids consist of a wide range of amphiphilic compounds that consist of a nonpolar (hydrocarbon) and a polar (headgroup) region. In a membrane, phospholipids are densely packed with the polar headgroup region oriented toward the bulk aqueous layer, while

the more hydrophobic acyl hydrocarbon chains are oriented toward the interior of the bilayer. Phosphatidylcholine (PC) lipids (Scheme 1), consisting of a nitrogen headgroup with three methyl groups, are one of the most common lipids in biological membranes. This is due to the ability of PC lipids to align into planar bilayer sheets that minimize unfavorable interactions between the surrounding bulk aqueous environment and the hydrophobic hydrocarbon acyl chains.[57] In simple geometrical terms, the PC lipids are roughly cylindrical with a roughly equal head:tail volume ratio.[58] In terms of structural parameters, P, as determined by the steric effects of surfactant molecules is defined as:[59]

$$P = \frac{v}{al} \qquad \textbf{Equation 1.1}$$

Where v is the volume of the lipid, a is the cross-sectional area of the lipid headgroup and l is the length of the acyl hydrocarbon chain. When $P = 1$, lamellar bilayers are the most favored structure, whereas with values of $P > 1$ and $P < 1$, inverted hexagonal phase structures and micellular structures, respectively, are preferred.[60]

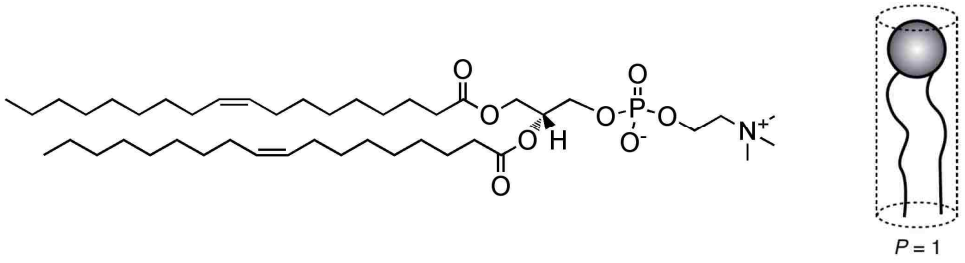

Figure 1.1: 1,2-dioleoyl-*sn*-glycero-3-phosphocholine (DOPC), otherwise known as 18:1 (Δ9-Cis) PC with estimated volume of $P = 1$, giving a cylindrical geometry with an equal head:tail volume.

Phosphatidylethanolamines (PE), Figure 1.2, at pH values greater than 9 have three protons bound to the nitrogen headgroup rather than the three methyl groups for PC lipids. The smaller headgroup, with a cross-sectional area less than the width of the acyl hydrocarbon chains, results in the observation of several different phase behaviors, differences in hydration

and hydrogen bonding, and pH-dependent charge that are not observed in PC lipids. By geometrical parameters, PE lipids can be envisioned as conical in shape, due to a low head-to-tail ratio, thus giving values for $P > 1$ and preference for inverted hexagonal phase structures.[59] PEs can make up to 40% of cellular membranes, depending on the location and function of the cell; most of the PE lipids are typically found in the interior leaflet due to packing differences in the lipids from the smaller cross-sectional area of the headgroup.[57] Changes in the amount of PE in bilayers are believed to alter the functionality of the bilayer,[61] as demonstrated with rhodopsin, a chromophoric reporter group that undergoes a conformational change that has been linked to the amount of PE in the surrounding lipid bilayer.[62] Typically referred to as non-bilayer lipids, PE lipids are believed to be a major player in the fusion process of biological cells and other membrane-bound biological systems.[63]

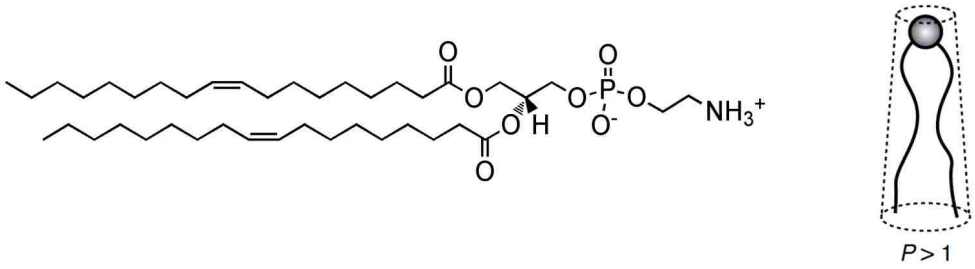

Figure 1.2: 1,2-dioleoyl-*sn*-glycero-3-phosphoethanolamine (DOPE), otherwise known as 18:1 (Δ9-Cis) PE. An estimated volume of $P > 1$, giving a conical geometry with a low head:tail volume.

In Figure 1.3 are shown the three basic phases accessible to lipids. Several other phases exist or are postulated to exist, but their role in lipid phase behavior is thought to not be significant. In the L_β gel phase, the lipid exhibits slow lateral diffusion, and the acyl chains are often referred to as "frozen", creating a rigid bilayer structure. As the temperature is increased, the acyl chains melt at a specific temperature and undergo a high enthalpy transition, T_M as the lipids undergo a phase transition to the L_α or liquid-crystalline phase.[65] The lipids in the L_α have fast lateral diffusion. This is the most common phase state of biological membranes,

serving as the initial state for liposome fusion studies. Upon further heating, only a certain subset of lipids, namely PEs and phosphatidylserine (PS), undergo a low enthalpy, higher temperature phase transition at inverted hexagonal type-II or T_H.[65] The inverted hexagonal, H_{II} is considered to be non-bilayer in water due to the inverted micellular structure having the lipid headgroups curling around a water core and the acyl hydrocarbon chains splayed outward to interact with other inverted hexagonal phase lipid tubes. The values for T_M and T_H refer to the temperature for the onset of the phase transition, as measured by calorimetry, X-Ray diffraction, or ^{31}P NMR.

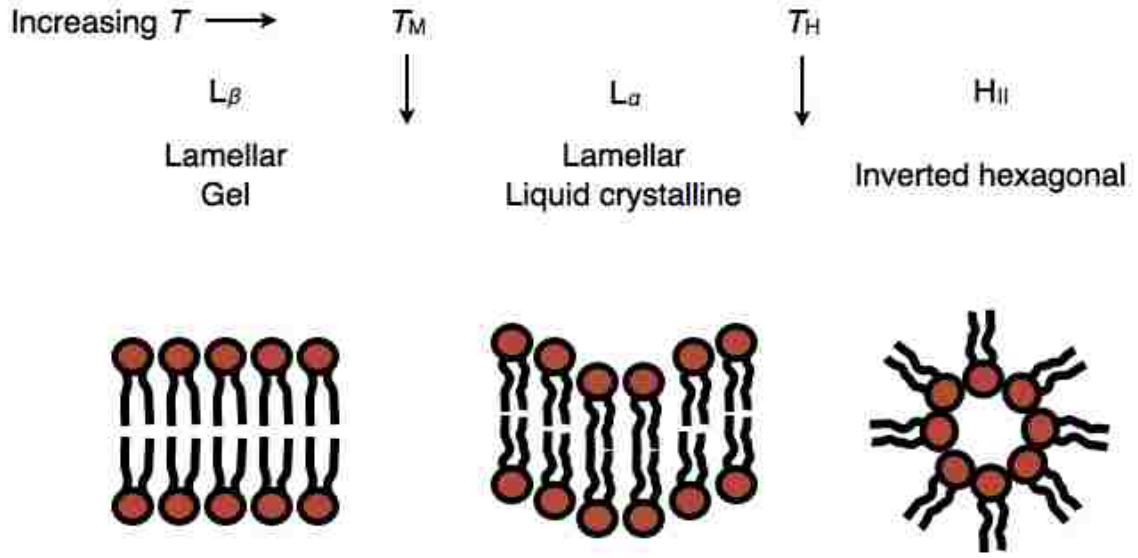

Figure 1.3: Cross-sectional schematic depicting the three basic lipid phases and the structural parameter terms used for each phase. L_β refers to the gel phase, L_α refers to the liquid-crystalline phase, and H_{II} refers to the inverted hexagonal phase. T_M is the temperature where the acyl hydrocarbon chains melt for the L_β to the L_α transition. T_H is the temperature where certain lipids will undergo an additional phase transition from L_α to H_{II}. Adapted from Bentz (1988).[64]

The polymorphic or phase preference behavior of a lipid can be estimated by the head-to-tail ratio using Equation 1. More specifically, the phase behavior of a lipid is directed by a balance between four geometry-dependent forces so as to achieve the lowest total free energy of a favored phase. Once the energy exceeds a favorable state, the lipid will undergo the phase

transition to the lower energy state, e.g. the transition of a PE bilayer from L_α to H_{II} at T_H. The four geometry-dependent forces that need to be considered are the electrostatic forces in the headgroup region, the lipid curvature (monolayer elasticity), the packing and van der Waals forces of the acyl hydrocarbon chains, and the hydration forces in both the headgroup and acyl hydrocarbon chains.[66]

Electrostatic forces in lipid assemblies have been probed through the observation of changes in the dipole moment of lipids, in addition to the surface charge of the liposomes themselves.[67] Any influence of the electrostatic forces of a lipid is limited to the headgroup region. The polarization of the headgroup has been found to shift depending on the phase state of the bilayer and whether or not ions bind or interact with the headgroups.[68] Thus, the orientation and conformation of a lipid headgroup is never constant and is easily influenced by the binding or adsorption of ions, hydrophobic ions, or by mixing with differently charged ions.[69] In PC lipids, the headgroup has a large dipole moment and measurements show that the dipole of the phosphate-choline group lies nearly parallel to the plane of the lamellar membrane.[70] However, any addition of negative surface charge decreases the size of the dipole interaction of the headgroup, resulting in the dipole being "pulled back" into the interior of the bilayer.[69] Even in PE lipids, there are further electrostatic interactions in the headgroups in the form of hydrogen bonding between the amine headgroups and the phosphate groups. Studies using deuterium-labeled hydrocarbon chains have demonstrated a very small influence on their structure as a result of electrostatics.[69]

Lipid curvature takes into consideration the geometrical arguments for the preference in the lipid phases.[71] A smaller headgroup cross sectional area lowers the head-to-tail ratio, resulting in a lipid with a negative curvature value that will energetically prefer a concave geometry and to curl around water. Lipids with a positive curvature value will bow outward into

water and adopt a convex structure such as that of a micelle. Closely related to the values and estimations of the lipid curvature is the contribution of the acyl hydrocarbon chains. Any factors that act to widen the splay of the acyl hydrocarbon chains to create a larger tail volume, such as temperature, chain length or unsaturation, will decrease the radius of curvature of a lipid due to a change in the head-to-tail ratio. Thus, as a PE lipid has its temperature move through its T_H, the acyl hydrocarbon chains splay outward and increase the volume area of the chains, thus causing changes in the packing parameters. This is also why T_H values are not observed in PC lipids, as the increase in the acyl hydrocarbon chain volume is small enough that the lipid remains in the L_α phase well above reported temperatures for similar PE lipids.

The acyl chain length, saturation, position of any points of unsaturation (double bonds) and their conformation all have an influence on the values of T_M and T_H. For example, in unsaturated PEs, decreasing the chain length tends to increase both the T_M and T_H, as going from an 18-carbon acyl chain in DOPE to a 16 carbon acyl chain in 1,2-dihexadecanoyl-*sn*-glycero-3-phosphoethanolamine (DPPE) increases the T_M from – 16 °C to 63 °C and the T_H from 10 °C to 118 °C.[72] The degree of unsaturation in PE lipids also contributes to differences in the phase transition temperatures, as the T_H of fully saturated lipids, such as 1,2-distearoyl-*sn*-glycero-3-phosphoethanolamine (DSPE), known as 18:0 PE, is 100 °C.[72] When comparing the temperature values of DSPE to DOPE, the DOPE contains a single *cis* double-bond in each of the acyl chains which lowers the T_H to a range of 8 to 16 °C. Changing the *cis*-isomer of DOPE to the *trans*-isomer (1,2-dielaidoyl-*sn*-glycero-3-phosphoethanolamine or DEPE), known as 18:1 (Δ9-Trans) PE, results in a larger acyl hydrocarbon volume that strongly influences the values of the T_H value due to the structure of the L_α phase being more commensurate with the H_{II} phase.[73] The result is an increase in both the T_M (38 °C) and T_H (64 °C) for DEPE.[72]

Finally, the hydration of a lipid can impact its phase behavior, as easily noted when discussed in the concept of lipid curvature. The hydration of lipids will be further discussed in the next section, but as related to the concept of lipid curvature for the specific case of a PE lipid, limited amounts of water at the PE headgroup tends to impede the $L_\alpha \rightarrow H_{II}$ phase transition due to the inability of the lipid cylinders to expand via repulsive forces.[71] However, increased hydration of a lipid promotes electrostatic repulsion of lipid headgroups, thus lowering the overall free energy of the phase and resulting in favoring the H_{II} over the L_α.

1.3.2 Water Structure

Lipids residing at the water interface of lipid bilayer assemblies encounter a thin aqueous layer that is subject to strong, short-range (< 50 Å) forces from the bilayer surface.[74] Any change in the lipid hydration level or the presence of ions will have a strong influence on the net free energy of the lipid, which leads to a preference for a specific phase for non-bilayer-forming lipids. The extent of hydration surrounding a lipid headgroup depends on the effective size of the headgroup and the overall lipid geometry.[75] The hydration level of the headgroup influences the packing density of the lipids, as van der Waals interactions between adjacent lipids are weakened which results in the loosening of packing parameters.[76]

The ordering of water molecules at a bilayer surface results in unfavorable entropy in the interaction between the bilayer and the aqueous phase.[77] This change in entropy may be partially off-set by the favorable chance in enthalpy, arising from the binding of water to the lipid headgroups. In fully hydrated choline headgroups, the enthalpy compensation is achieved through binding of an estimated 14–30 water molecules, with the number of bound water molecules being a function of the acyl hydrocarbon chain heterogeneity and unsaturation.[78] The majority of the water is clustered within 5 Å of the headgroup with a small number of water molecules penetrating as far into the lipid as the phosphate, according to theoretical

calculations.[74] The ordered water around the headgroup induces a conformational change in the dipole of the phosphate-choline group from one that is coplanar with respect to the bilayer plane to one that is nearly perpendicular to the bilayer plane.[69] This change in the dipole serves to decrease the mean bilayer thickness that results from expansion of the area of the acyl hydrocarbon chains.

PE headgroups bind less water than PC headgroups due to decreased surface interactions with the aqueous phase by the smaller amine headgroup[79] and because of the presence of hydrogen bonding between adjacent amine headgroups. A fully hydrated ethanolamine headgroup in the L_α phase is estimated to have between 10–12 water molecules surrounding it,[77] while there are approximately seven water molecules surrounding the headgroup for DOPE in the H_{II} phase.[80] In addition, there is significant headgroup hydrogen bonding between the ammonium, the surrounding water, and between the oxygen atoms of neighboring phosphate and ammonium groups, which serves to reduce the polarity of the headgroup and align it coplanar to the bilayer plane.[70] In PE, the enthalpy compensation from the unfavorable entropy from the ordering of water molecules is less effective than in PCs due to the fewer water molecules surrounding the headgroup.[77]

1.3.3 Altering Phase Behavior

The lamellar to inverted hexagonal phase transition ($L_\alpha \rightarrow H_{II}$) in PE lipids is a very low entropy event and can be triggered by weak energetic influences of ions, hydration, temperature, and pH. The chain length of the lipid itself has a very small contribution to the overall phase behavior; the values of enthalpy and entropy for the $L_\alpha \rightarrow H_{II}$ transition experience a very small increase with increasing chain lengths in an approximately linear fashion.[81] Various environmental conditions, such as the hydration level of the lipids, and aqueous bulk conditions, e.g. temperature, pH and salt concentration have observable effects on the phase behavior.

As discussed in Section 1.3.2, the lipid hydration level has an influence on the phase behavior of the lipid; for example by dehydrating a lipid (e.g. there is less water available to hydrate the lipid headgroup), the value of the T_M increases while decreasing the value of T_H.[81] PE lipids have been previously observed to form stable lamellar phases and liposomes at pH values above 9 resulting from protonation of the amine headgroup.[82] A significant issue in the literature concerning the study of pH effects on PE lipids is the buffers used to control the pH, as certain buffers, for example phosphate buffer, is valid over pH values of 5.7 to 8.0. Changing buffer systems to reach pHs below 5, for example from phosphate to acetate, changes the behavior of the lipids which may exhibit an altered phase behavior in one buffer compared to another buffer. Thus, it is difficult to establish the exact relationship between pH and phase behavior of PE lipids, as alterations to the components of the buffer system used to change the pH can impact both T_M and T_H values.

For salts, such as NaCl, it has been observed that increasing the salt concentration serves to increase T_M while decreasing T_H in PE lipids. The magnitude of the salt-induced transition temperature shifts depends on the acyl hydrocarbon chain lengths of the lipids, as greater increases in the T_H with changes in salt concentration are observed in lipids with shorter chain lengths.[81]

Modification of the PE headgroup also changes the phase behavior of PE lipids, previously observed in the methylation of DOPE headgroups to give DOPE-Me. The overall effect of increasing the area of the headgroup upon headgroup methylation is decreased values of T_M and increased values of T_H.[81] In general, any modifications that increase the headgroup volume area relative to the acyl hydrocarbon chains will favor the lamellar gel phase over the hexagonal phase.

1.3.4 Hofmeister Salts

The Hofmeister series, described over a 100 years ago by Franz Hofmeister, is an ordered series of salt cations and anions, whose order is dictated by their ability to significantly modify the solubility of proteins in the aqueous electrolyte solution.[83] Salt ions in this series were ordered according to their ability to precipitate proteins (salt out) or increase the solubility of the protein (salt in). The ions that encourage salting out of proteins are called kosmotropes, and the ions that increased protein solubility are referred to as chaotropes. Chloride anion is traditionally considered to be at the center of the series, acting as a dividing line between kosmotropic and chaotropic behavior, as determined by column elution and protein solutions.[84] For lipids and especially phosphatidylethanolamine lipids, the inversion point between kosmotropic and chaotropic behavior is found to occur between Br^- and I^-.[85] Hofmeister effects become important at moderate concentrations, in the range of 0.01 to 1.0 M, and tend to increase with increasing ion concentration.[84] While different measurement techniques may give slight variations in the ordering of the ions, the series typically exhibits a similar and characteristic ordering with overall behavior of the ions remaining the same.

The typical order for the anion series with a common cation is as follows:

$$CO_3^{2-} > SO_4^{2-} > S_2O_3^{2-} > H_2PO_4^- > F^- > Cl^- > Br^- \approx NO_3^- > I^- > ClO_4^- > SCN^-$$

The Hofmeister series also applies to cations with a common anion, although the effects are dominated by the anion series. The typical Hofmesiter cation series can be ordered as follows:

$$NH_4^+ > K^+ > Na^+ > Li^+ > Mg^{2+} > Ca^{2+}$$

Hofmeister effects have been observed in a variety or processes and systems, ranging from the early observations of effects on the tension of the air-water interface,[86] to later observations of effects on protein folding, enzymatic activity, protein-protein interactions, protein crystallization, bacterial growth and even stabilities of macromolecules and lipids. In

recent years, there has been an explosion of papers related to the Hofmeister series, yet a full and proper molecular-level mechanism of the actions of the Hofmeister salts in the series still remains elusive.[87]

The physical behavior of the Hofmeister series was originally attributed to the making or breaking of water structure.[84] Thus, the origin of the names for the behavior of the ions: kosmotropes are strongly hydrated ions and were believed to be 'water structure makers' by strengthening the hydrogen-bonding network of bulk water. Chaotropes are weakly hydrated ions and were believed to be 'water structure breakers' by weakening the hydrogen-bonding network of bulk water.

Recent work by Cremer,[88] Bakker,[89,90] and Pielak[91] have cast serious doubts on the notion of bulk water changes caused by Hofmeister ions. It is becoming apparent that kosmotropic and chaotropic anions function through separate mechanisms, as kosmotropes have little to no interaction with the surface of molecules whereas chaotopics demonstrate a preference for the interfacial region, especially in fatty amine films.[88] The preferred explanation is the size of the hydrated anions is directly related to the hydration free energy of the ion. Chaotropic anions have a lower hydration free energy and are able to shed their hydration shells without a significant energetic penalty to interact with binding sites on a charged surface.

Additionally, more polarizable chaotropic anions, such as SCN^-, have a stronger ability to partition into the molecule/aqueous interfacial region so as to decrease the overall surface tension and inhibit the formation of the molecular aggregate phase while stabilizing the hydrated phase. The partitioning of the chaotropic anions may also influence the ability of a molecule to form hydrogen bonds; however, this has not been observed in a study of urea with proteins, where the urea was not found to significantly influence the hydrogen bonding network. Urea, while not a typical charged anion in the Hofmeister series, is classified as a chaotrope, as it has

been observed to enlarge the interfacial area of lipids.[65] It has also been observed that chaotropic ions, especially ClO_4^- and SCN^- increase the magnitude of negative surface potential zwitterionic lipid bilayers.[92]

Kosmotropic anions, such as SO_4^{2-}, will yield the opposite effects, as they have a higher hydration free energy and are unable to shed their hydration shells without a significant energetic penalty upon their interaction with binding sites on a charged or neutral surface. As a result of the kosmotrope binding, the overall surface tension of the molecule/aqueous interface will increase, preferring the formation of the molecular aggregate phase to the hydrated phase. In recent work by O'Brien and Williams, they studied the patterning of water molecules around SO_4^{2-} surrounded by 14 water molecules, where each water near the SO_4^{2-} donates two hydrogen bonds to a sulfate ion or the oxygen atom of a neighboring water molecule.[93] As the number of water molecules surrounding the SO_4^{2-} ion increased, they observed an increase in free-OH species associated with water, indicating that water outside of the first solvation shell of the ion was influenced by the ion and actually favored, as it was observed that additional water molecules added additional structure to the hydrated ion of up to 80 waters.[93] If the observations of O'Brien and Williams hold for the entire Hofmeister series, then on the chaotropic side, it is predicted that the ions are less hydrated and influence fewer water molecules outside of their first hydration shell. This hypothesis fits with the current theory predicted by Cremer that has at its heart, the ability of the ion to partition into an interfacial region is dictated by its hydration free energy. That is, ions with low free energies of hydration tend to incorporate partially into the interfacial region with suspected facile binding to the surface. The opposite would hold for kosmotropic with high free energies of hydration.

In general, kosmotropes will favor molecular conformation having reduced surface areas, whereas chaotropes will favor molecular conformations with increased surface areas.[65] This

observation can be used to understand the phase stability of lipids, especially non-lamellar phase forming lipids such as PEs, as their phase properties are strongly influenced by the presence of kosmotropic and chaotropic salts and agents. The two main transitions observed in PE lipids consist of a high enthalpy and low temperature endotherm, T_M, that corresponds to the lamellar gel ($L\beta$) to lamellar liquid-crystalline ($L\alpha$) transition and a low enthalpy and high temperature endotherm that corresponds to the $L\alpha$ to inverted hexagonal (H_{II}) transition (T_H).[65] The presence of Hofmeister salts will favor certain phases of lipid depending on the nature of the salt. It has been shown for PEs that kosmotropic salts promote the formation of the aggregated phase of lipid (H_{II}) but destabilize the more hydrated ($L\alpha$) phase; this event for PE lipids causes a decrease in the temperature of the $L\alpha \rightarrow H_{II}$ transition (T_H) and a smaller increase for the $L\beta \rightarrow L\alpha$ transition (T_M). Chaotropic salts have the opposite effect on PE lipids, as they provide a solution enviroment that favors the $L\alpha$ phase while destabilizing the H_{II} phase, thus increasing T_H and decreasing T_M. DSC measurements have been performed on PE lipids that have demonstrated that kosmotropic salts lead to an increase in the temperature as well as an increase in the entropy and enthalpy for the $L\alpha \rightarrow H_{II}$ phase transition while chaotropic salts lower the temperature, entropy, and enthalpy for the $L\beta \rightarrow L\alpha$ phase transition.[65] The thermodynamics of the $L\alpha \rightarrow H_{II}$ phase change supports the previously discussed theory of interfacial water and ion hydration levels, as increases in the entropy and enthalpy of the H_{II} phase are greater in the presence of kosmotropes, indicating that the amount of ordered water increases around reduced interfacial area of the headgroups to balance the increase in entropy and enthalpy. In the case of PEs, the higher sensitivity of the T_H to the presence of Hofmeister anions is dominated by the decreased amount of water surrounding the phosphoethanolamine headgroup in the H_{II} phase versus the $L\alpha$ phase. There is little change in the conformational order of the acyl chains when

moving from the L_α to the H_{II} phase, and so the slight amount of thermodynamic price that is paid for this conformational change is more than offset by the energetics of the hydration change.

1.3.5 Liposome Fusion, Lipid Mixing and Contents Mixing

While membrane fusion is a vital component of biological processes and cellular function, a complete understanding of the underlying forces that are necessary to bring together and mix the lipids of two apposing lipid bilayers remains incomplete. Regardless of the mechanisms and forces driving the molecular rearrangement of the lipids in apposing bilayer membranes, the final step of the fusion process is a single unified membrane. After the fusion of two apposing membranes, the unified structure can – depending on the lipid composition of the membrane – either remain stable, become permeable to the interior cargo, or destabilize via lysis of the entire structure.

Liposome fusion occurs in bilayer membrane systems where there exists a tendency for a portion of the lipid composition to form non-bilayer inverted hexagonal phases. The tendency of the bilayer to fuse is increased by heating the system toward the lamellar/inverted hexagonal phase transition temperature (T_H), by adding lipids that lower the transition temperature, by changing the pH of the bulk solution, or by adding certain charge screening or dehydrating species to the system. Regardless of the factors present to induce fusion between two bilayer membranes, several stages from model liposomal systems have been identified in the overall process:[64]

1) Aggregation of apposing membranes to overcome electrostatic and hydration repulsion forces that prevent close approach;
2) Close approach of membranes to establish a zone of contact;
3) Interaction between apposing membranes by formation of intermediate structures;
4) Rearrangement of molecular packing of lipids to form a single, unified membrane;

5) If $T > T_H$, assembly into inverted hexagonal structures followed by rupture and leakage of contents from liposomes occurs;
6) If $T < T_H$, intermixing of membrane components and internal aqueous contents occurs with reduced content leakage.

The destabilization process of membranes is imparted by the balance between average surface forces that direct the formation of intermediate structures and eventually lysis of the two bilayers. Thus, membrane fusion of two liposomes can be considered at two levels: (1) *kinetic*, where the overall fusion process is rate limiting under a particular environmental condition and (2) *structural* where the interactions between molecular packing constraints of the lipids and the formation of intermediate structures determine the pathway of destabilization of fusion or lysis.[64]

From a kinetic point of view, the following equation can be used to describe the fusion between two similar apposing membrane bilayers:

$$V_1 + V_1 \underset{D_{11}}{\overset{C_{11}}{\rightleftharpoons}} V_2 \xrightarrow{f_{11}} F_2 \qquad \textbf{Equation 2}$$

where V_1 denotes single liposome vesicles, V_2 is an aggregated intermediate of the two single liposomes, and F_2 is the final fused structure. C_{11}, D_{11}, and f_{11} are rate constants, where C_{11} is affected by the energy of attractive interaction between the two liposome monomers, while D_{11} is controlled by the energy of repulsion of the two liposomes, and f_{11} is the rate of destabilization of the aggregated intermediate to the final fusion product.[64] The most common environmental conditions that will prevent the kinetic fusion from occurring are the ability to remove the interfacial water from the approaching, apposed bilayers, hydration layer repulsion, electrostatic interactions and van der Waals attractions. To fully establish the kinetic parameters, use of both liposome aqueous content mixing and liposome lipid mixing assays (step five from above) are

required as it is difficult to differentiate fusion from contact-mediated lysis (step six from above) solely depending on the outcome from liposome content release assays.

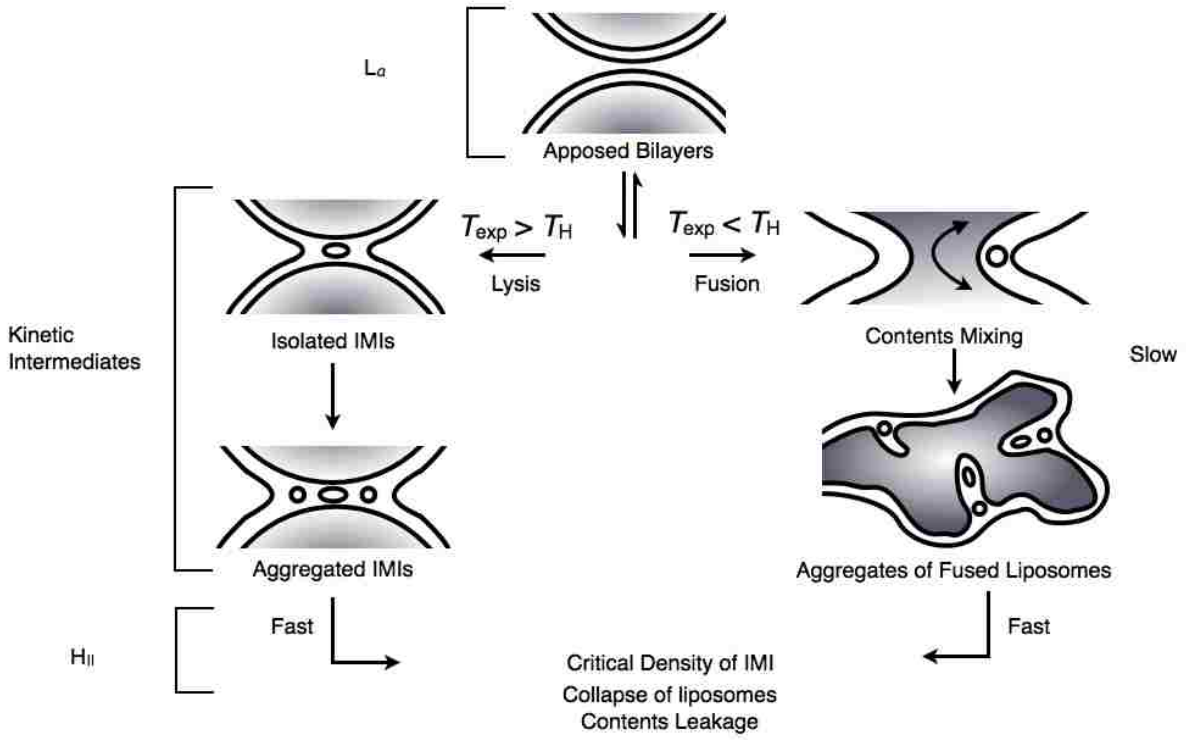

Figure 1.4: Diagram and pathways for liposome fusion and destabilization for liposomes composed of polymorphic lipids. Adapted from Bentz (1988)[64] and Siegel (1984).[94]

Determination of the structural contributions to the fusion process is significantly more difficult due to the size of interlamellar intermediates (IMIs) and the rate at which the fusion process occurs. Siegel and Epand have published a number of informative and thorough studies using time-resolved cryotransmission electron microscopy (TRC-TEM), ^{31}P NMR, and differential scanning calorimetry that have provided ample evidence to advance the theory of the formation of interlamellar intermediates known as stalks, but they have not been able to successfully provide clear microscopic evidence for the formation of stalk intermediates.[95-97] It has been proposed by others that individual connections between apposing bilayers elongate directly into structures that correspond to fragments of H_{II} phase structures that assemble sideways into full H_{II} phase tubes.[98,99]

The proposed model, as depicted in Figure 1.4, involves the close approach of two liposomes containing fusogenic lipids above their T_H, and thus they are ready to undergo conversion to the H_{II} phase. The first step is proposed to be the formation of small (~ 10 nm or less in diameter) connections referred to as interlamellar intermediates (IMIs).[95] If the area of contact between the two liposomes is large enough, further stalks will form and continue the conversion of fusogenic lipids to the H_{II} state, resulting in the leakage of any encapsulated contents and further rapid conversion of the bilayer to H_{II}. Tension will develop in the liposome bilayers, eventually becoming significant enough to rupture the liposomes and collapse the entire structure into non-bilayer structures.[96]

Thus, by exploiting the ability of PE lipids to undergo the $L\alpha \rightarrow H_{II}$ phase change when temperature is above the T_H, liposomes can be programmed to respond to various environmental conditions that determine the rate and completeness of the phase transition and ultimately the amount of the internal contents released. By attaching a cleavable headgroup that can be triggered by the presence of an endogeneous stimulus, DOPE can be forced into the $L\alpha$ phase due to the presence of a larger headgroup volume and increased hydration around the headgroup. The removal of the capping headgroup will revert the conditions around the lipid headgroup to the ones preferred by the lipid, thus creating an environment favorable for close approach of apposing bilayer surfaces with subsequent bilayer fusion, phase transition of the lipids into the H_{II}, and contents release.

1.4 Stimuli-Responsive (Redox-Active) Liposomes

1.4.1 Trimethyl-locked Quinone Headgroup

Enzyme-responsive liposomes have evolved out of research on bioactivated drugs and small-molecule prodrugs as a method to protect the drug or molecule from degradation until it reaches a specific site. The molecule or drug enters the body in a deactivated form due to the

covalent attachment of an organic protecting group that is removed via enzymatic action at a target site, rendering a therapeutically active drug.

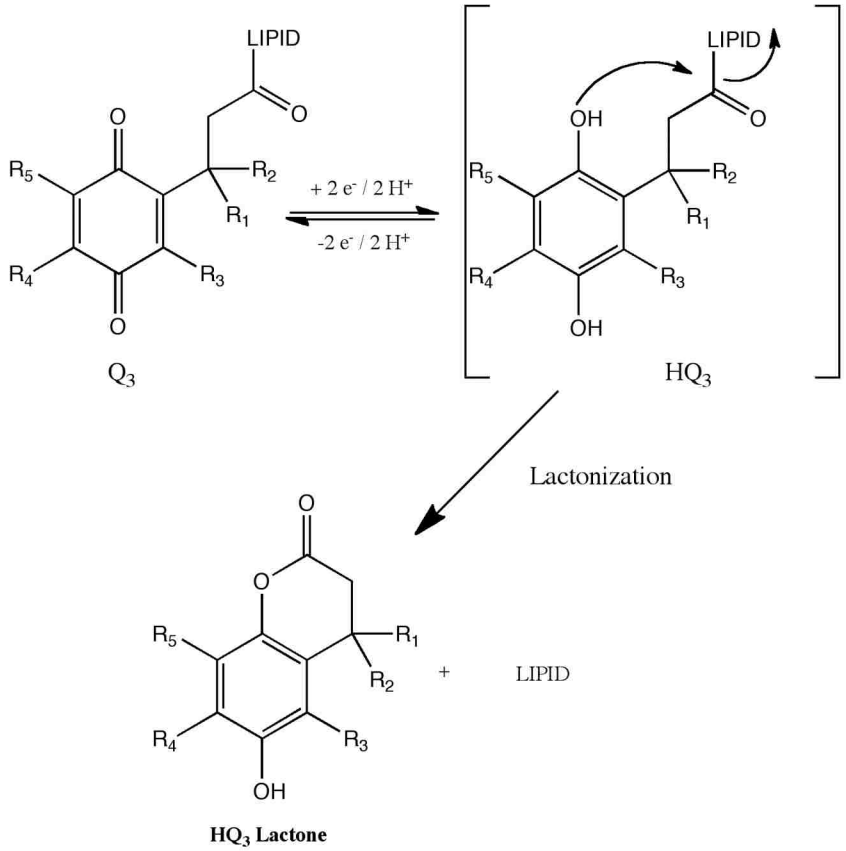

Scheme 1.1: Reductive lactonization of **1** Q_3 produces **3** HQ_3 lactone and lipid;
$R_1 = R_2 = R_3 = R_4 = R_5 = CH_3$.

In order to design a redox-sensitive organic protecting group for covalent attachment to lipids, a suitable substrate with activity toward upregulated enzymes in the specific location for delivery is required. Quinone reductases have been reported to be upregulated in many tumor and cancer tissues, making them ideal to function as a trigger group that uses the reduction of the quinone to a hydroquinone to drive the removal of the protecting group. Furthermore, quinone-propionic acid ("trimethyl-lock")[100] protecting groups have been previously attached to drugs,[101] and our group has attached them to the exterior of dendrimers[102,103] for release of payloads. The release of the quinone propionic acid capping group is driven by a two-electron reduction of the

quinone to trigger a intramolecular cyclization reaction[104] that results in a lactone that self releases from the parent molecule, as shown in Scheme 1.1.

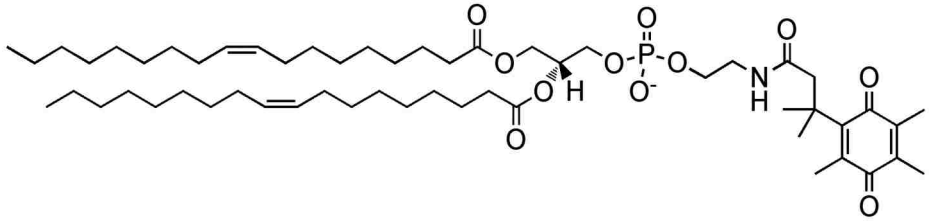

Figure 1.5 Redox-active, trimethyl-locked quione capped DOPE (Q_3-DOPE)

1.4.2 Effects of Substitution: *Gem*-methyl and Ring Substitution

The rate of lactonization of the Q_3 trimethyl lock is facilitated through the composition of the geminal groups (R_1 and R_2) on the C-5 carbon and the R_3 group on the quinone ring.[105] If all three are methyl groups, e.g. Q_3, then the "trimethyl lock" has a strong accelerating effect on the rate of lactonization, resulting in an approximate 10^3 increase in lactonization rates.[106] One hypothesis for the acceleration is that the presence of the *gem*-methyl groups serve to introduce distortional strain into the quinone ring that serves to bring the quinone carbonyl group into a more favorable angle for attack for the lactonization reaction.[107,108] Removal of the *gem*-methyls by substitution with hydrogens results in a reduction in the lactonization rate as the strain on the quinone is relived and the quinone carbonyl group is in a less favorable position for the lactonization reaction to occur. The methyls on the quinone can also be removed (for Q_0, R_1-R_5 = H on Scheme 1.1) for further adjustment of the lactonization rates, as now the electrochemical potential of the quinone is influenced by the absence of electron withdrawing or donating groups.

1.4.3 NQO1

NAD(P)H:quinone oxidoreductase type 1 (NQO1) was initially discovered in the late 1950s by Ernster[109] and is a homodimeric flavin enzyme that catalyzes the two-electron reduction of quinones and quinoid compounds via hydride transfer from the 1,5-dihydro-flavin adenine dinucleotide ($FADH_2$) site in each monomer.[110,111] NADH or NADPH are used as the

electron source for the reduction catalysis, the overall pathway following a ping-pong mechanism. Elevated levels of expressed NQO1 have been reported in a broad range of human tumors, including breast, colon, pancreatic, and lung.[112] NQO1 has previously been described for bioactivation of prodrugs[113] and other bioactivatable drugs,[114,115] yet it remains unreported for the activation of quinone-based liposomal systems.

1.4.4 Challenges of Redox Environment

The use of chemical reducing agents limits the use of certain buffers and a number of traditional fluorescence assays that have previously been used to study liposome fusion, aqueous content mixing, guest release, and lipid mixing. Sodium dithionite has a reduction potential on the order of -0.66 V vs. SCE, sufficient to reduce the various quinone headgroups studied to date in our group.[116] Due to the low reduction potential of $S_2O_4^{2-}$, careful selection of organic buffers and fluorescent probes is required; this includes any compounds containing aryl-nitro, diazo-, C- and N-nitroso, and carbonyl groups that are easily reduced by sodium dithionite.[117] The breakdown of dithionite is accelerated in solutions with pH values below 7.5, as it is estimated that dithionite breaks down at a rate of 2% per minute at pH 6.5 and this rate increases with lower pH values.[118]

Membrane fusion is traditionally monitored through the quenching of 1-aminonaphthalene-3,6,8-trisulfonic acid, ANTS, fluorescence by the collisional quencher *N*, *N'*-*p*-xylylenebis-(pyridinium bromide) (DPX). The ANTS and DPX pair can be co-encapsulated in a liposome to study the rate of content leakage, as the pair is released into the bulk aqueous media, the ANTS is released from the DPX, creating an increase in the fluorescence intensity that can be related to the amount of probe released from the liposome. Alternatively, ANTS and DPX can be encapsulated into separate liposomes and membrane fusion with content mixing will cause the two to come into contact and quench the ANTS fluorescence.[82,119] This assay, despite

its popularity and ability to determine contents mixing was avoided due to the concern over reduction of ANTS upon introduction of sodium dithionite. Another liposome contents mixing assay, terbium (Tb^{3+}) and dipicolinic acid (DPA), relies on the interaction of Tb^{3+} with DPA initially encapsulated in two separate liposome populations.[119] Upon contents mixing from membrane fusion, the Tb^{3+} complexes with the DPA, creating an increase in the fluorescence intensity. Alternatively, the Tb^{3+}/DPA complex can be co-encapsulated in a liposome and the fluorescence signal would be lost upon competitive chelation with divalent cations and EDTA in the medium. The concern over Tb^{3+}, which must be complexed with citrate to prevent interaction with the negatively charged lipids, results in the destabilization of PE liposomes via premature inverted hexagonal phase transitions.

The final contents leakage assay available is the encapsulation of carboxyfluorescein or calcein, both of which undergo self-quenching at concentrations above 25 mM.[120] Release of the calcein into the bulk aqueous medium relaxes the self-quenching and the fluorescence signal increases. Calcein, fortunately, is relatively insensitive to sodium dithionite and does not experience any reduction in fluorescence intensity upon exposure to the reducing agent.

For fusion assays studying the mixing of lipids, the most popular assays involve Forster energy transfer from 7-nitrobenz-2-oxa-1,3-diazol-4-yl (NBD) to rhodamine (Rh), which decreases as the lipids are diluted during the fusion process.[119] Both NBD and Rh are sensitive to sodium dithionite, undergoing reduction to non-fluorescencent species. NBD-labeled lipids have previously been used to study the flip-flop times of lipids in a bilayer, as the exterior NBD-labeled lipids can be reduced by sodium dithionite, leaving only the interior NBD-labeled lipids to exchange with the exterior leaflet.[121]

1.5 References

(1) Bangham, A. D.; Standish, M. M.; Watkins, J. C. Diffusion of Univalent Ions across Lamellae of Swollen Phospholipids. *J. Mol. Biol.* **1965**, *13* (1), 238-252.

(2) Torchilin, V. P. Recent Advances with Liposomes as Pharmaceutical Carriers. *Nat. Rev. Drug. Discov.* **2005**, *4* (2), 145-160.

(3) Zhang, L.; Gu, F. X.; Chan, J. M.; Wang, A. Z.; Langer, R. S.; Farokhzad, O. C. Nanoparticles in Medicine: Therapeutic Applications and Developments. *Clin. Pharmacol. Ther.* **2008**, *83* (5), 761-769.

(4) Jesorka, A.; Orwar, O. Liposomes: Technologies and Analytical Applications. *Annu. Rev. Anal. Chem.* **2008**, *1*, 801-832.

(5) Lindner, L. H.; Hossann, M. Factors Affecting Drug Release from Liposomes. *Curr. Opin. Drug Discov. Devel.* **2010**, *13* (1), 111-123.

(6) Toombes, G. E. S.; Finnefrock, A. C.; Tate, M. W.; Gruner, S. M. Determination of L-Alpha-H-II Phase Transition Temperature for 1,2-Dioleoyl-Sn-Glycero-3-Phosphatidylethanolamine. *Biophys. J.* **2002**, *82* (5), 2504-2510.

(7) Sanderson, P. W.; Williams, W. P.; Cunningham, B. A.; Wolfe, D. H.; Lis, L. J. The Effect of Ice on Membrane Lipid Phase-Behavior. *Biochim. Biophys. Acta* **1993**, *1148* (2), 278-284.

(8) Immordino, M. L.; Dosio, F.; Cattel, L. Stealth Liposomes: Review of the Basic Science, Rationale, and Clinical Applications, Existing and Potential. *Int. J. Nanomed.* **2006**, *1* (3), 297-315.

(9) Scherphof, G. L.; Dijkstra, J.; Spanjer, H. H.; Derksen, J. T. P.; Roerdink, F. H. Uptake and Intracellular Processing of Targeted and Nontargeted Liposomes by Rat Kupffer Cells Invivo and Invitro. *Ann. N.Y. Acad. Sci.* **1985**, *446*, 368-384.

(10) Maeda, H.; Sawa, T.; Konno, T. Mechanism of Tumor-Targeted Delivery of Macromolecular Drugs, Including the Epr Effect in Solid Tumor and Clinical Overview of the Prototype Polymeric Drug Smancs. *J. Controlled Release* **2001**, *74* (1-3), 47-61.

(11) Papahadjopoulos, D.; Gabizon, A. Targeting of Liposomes to Tumor-Cells Invivo. *Ann. N.Y. Acad. Sci.* **1987**, *507*, 64-74.

(12) Kong, G.; Braun, R. D.; Dewhirst, M. W. Hyperthermia Enables Tumor-Specific Nanoparticle Delivery: Effect of Particle Size. *Cancer Res.* **2000**, *60* (16), 4440-4445.

(13) Gregoriadis, G., Fate of Liposomes in Vivo and Its Control: A Historical Perspective. In *Stealth Liposomes*, Lasic, D. D.; Martin, F., Eds. CRC Press: Boca Raton, FL, 1995; pp 7-12.

(14) Lasic, D. D.; Papahadjopoulos, D. Liposomes Revisited. *Science* **1995**, *267* (5202), 1275-1276.

(15) Woodle, M. C.; Lasic, D. D. Sterically Stabilized Liposomes. *Biochim. Biophys. Acta* **1992**, *1113* (2), 171-199.

(16) Felgner, P. L.; Ringold, G. M. Cationic Liposome-Mediated Transfection. *Nature* **1989**, *337* (6205), 387-388.

(17) Sioud, M.; Sorensen, D. R. Cationic Liposome-Mediated Delivery of Sirnas in Adult Mice. *Biochem. Biophys. Res. Commun.* **2003**, *312* (4), 1220-1225.

(18) Torchilin, V. P.; Trubetskoy, V. S.; Whiteman, K. R.; Caliceti, P.; Ferruti, P.; Veronese, F. M. New Synthetic Amphiphilic Polymers for Steric Protection of Liposomes in Vivo. *J. Pharm. Sci.* **1995**, *84* (9), 1049-1053.

(19) Woodle, M. C.; Engbers, C. M.; Zalipsky, S. New Amphipatic Polymer-Lipid Conjugates Forming Long-Circulating Reticuloendothelial System-Evading Liposomes. *Bioconjug. Chem.* **1994**, *5* (6), 493-496.

(20) Metselaar, J. M.; Bruin, P.; de Boer, L. W.; de Vringer, T.; Snel, C.; Oussoren, C.; Wauben, M. H.; Crommelin, D. J.; Storm, G.; Hennink, W. E. A Novel Family of L-Amino Acid-Based Biodegradable Polymer-Lipid Conjugates for the Development of Long-Circulating Liposomes with Effective Drug-Targeting Capacity. *Bioconjug. Chem.* **2003**, *14* (6), 1156-1164.

(21) Maruyama, K. Intracellular Targeting Delivery of Liposomal Drugs to Solid Tumors Based on EPR Effects. *Adv. Drug Delivery Rev.* **2011**, *63* (3), 161-169.

(22) Charrois, G. J. R.; Allen, T. M. Multiple Injections of Pegylated Liposomal Doxorubicin: Pharmacokinetics and Therapeutic Activity. *J. Pharmacol. Exp. Ther.* **2003**, *306* (3), 1058-1067.

(23) Zamboni, W. C.; Gervais, A. C.; Egorin, M. J.; Schellens, J. H. M.; Zuhowski, E. G.; Pluim, D.; Joseph, E.; Hamburger, D. R.; Working, P. K.; Colbern, G.; Tonda, M. E.; Potter, D. M.; Eiseman, J. L. Systemic and Tumor Disposition of Platinum after Administration of Cisplatin or Stealth Liposomal-Cisplatin Formulations (Spi-077 and Spi-077b103) in a Preclinical Tumor Model of Melanoma. *Cancer Chemother. Pharmacol.* **2004**, *53* (4), 329-336.

(24) Andresen, T. L.; Jensen, S. S.; Jorgensen, K. Advanced Strategies in Liposomal Cancer Therapy: Problems and Prospects of Active and Tumor Specific Drug Release. *Prog. Lipid Res.* **2005**, *44* (1), 68-97.

(25) Kitano, H.; Maeda, Y.; Takeuchi, S.; Ieda, K.; Aizu, Y. Liposomes Containing Amphiphiles Prepared by Using a Lipophilic Chain Transfer Reagent - Responsiveness to External Stimuli. *Langmuir* **1994**, *10* (2), 403-406.

(26) Needham, D.; Dewhirst, M. W. The Development and Testing of a New Temperature Sensitive Drug Delivery System for the Treatment of Solid Tumors. *Adv. Drug Delivery Rev.* **2001**, *53*, 285-305.

(27) Chandra, B.; Mallik, S.; Srivastava, D. K. Design of Photocleavable Lipids and Their Application in Liposomal "Uncorking". *Chem. Commun.* **2005**, (24), 3021-3023.

(28) Zhang, Z. Y.; Smith, B. D. Synthesis and Characterization of NVOC-DOPE, a Caged Photoactivatable Derivative of Dioleoylphosphatidylethanolamine. *Bioconjugate Chem.* **1999**, *10* (6), 1150-1152.

(29) Guo, X.; MacKay, J. A.; Szoka, F. C. Mechanism of pH-Triggered Collapse of Phosphatidylethanolamine Liposomes Stabilized by an Ortho Ester Polyethyleneglycol Lipid. *Biophys. J.* **2003**, *84* (3), 1784-1795.

(30) Bergstrand, N.; Arfvidsson, M. C.; Kim, J. M.; Thompson, D. H.; Edwards, K. Interactions between Ph-Sensitive Liposomes and Model Membranes. *Biophys. Chem.* **2003**, *104* (1), 361-379.

(31) Davidsen, J.; Jorgensen, K.; Andresen, T. L.; Mouritsen, O. G. Secreted Phospholipase A(2) as a New Enzymatic Trigger Mechanism for Localised Liposomal Drug Release and Absorption in Diseased Tissue. *Biochim. Biophys. Acta* **2003**, *1609* (1), 95-101.

(32) Villar, A. V.; Alonso, A.; Goni, F. M. Leaky Vesicle Fusion Induced by Phosphatidylinositol-Specific Phospholipase C: Observation of Mixing of Vesicular Inner Monolayers. *Biochemistry* **2000**, *39* (46), 14012-14018.

(33) Yatvin, M. B.; Weinstein, J. N.; Dennis, W. H.; Blumenthal, R. Design of Liposomes for Enhanced Local Release of Drugs by Hyperthermia. *Science* **1978**, *202* (4374), 1290-1293.

(34) Weinstein, J. N.; Magin, R. L.; Yatvin, M. B.; Zaharko, D. S. Liposomes and Local Hyperthermia - Selective Delivery of Methotrexate to Heated Tumors. *Science* **1979**, *204* (4389), 188-191.

(35) Weinstein, J. N.; Magin, R. L.; Cysyk, R. L.; Zaharko, D. S. Treatment of Solid L1210 Murine Tumors with Local Hyperthermia and Temperature-Sensitive Liposomes Containing Methotrexate. *Cancer Res.* **1980**, *40* (5), 1388-1395.

(36) Couffin-Hoarau, A. C.; Leroux, J. C. Report on the Use of Poly(Organophosphazenes) for the Design of Stimuli-Responsive Vesicles. *Biomacromolecules* **2004**, *5* (6), 2082-2087.

(37) Lamparski, H.; Liman, U.; Barry, J. A.; Frankel, D. A.; Ramaswami, V.; Brown, M. F.; O'Brien, D. F. Photoinduced Destabilization of Liposomes. *Biochemistry* **1992**, *31* (3), 685-694.

(38) Spratt, T.; Bondurant, B.; O'Brien, D. F. Rapid Release of Liposomal Contents Upon Photoinitiated Destabilization with Uv Exposure. *Biochim. Biophys. Acta* **2003**, *1611* (1-2), 35-43.

(39) Barun, V. V.; Ivanov, A. P.; Volotovskaya, A. V.; Ulashchik, V. S. Absorption Spectra and Light Penetration Depth of Normal and Pathologically Altered Human Skin. *J. Appl. Spectrosc.* **2007**, *74* (3), 430-439.

(40) Thomas, J. L.; Tirrell, D. A. Polyelectrolyte-Sensitized Phospholipid Vesicles. *Acc. Chem. Res.* **1992**, *25* (8), 336-342.

(41) Chu, C.-J.; Szoka, F. C. Ph-Sensitive Liposomes. *J. Liposome Res.* **1994**, *4*, 361-395.

(42) Mellman, I.; Fuchs, R.; Helenius, A. Acidification of the Endocytic and Exocytic Pathways. *Annu. Rev. Biochem.* **1986**, *55*, 663-700.

(43) Gerweck, L. E.; Seetharaman, K. Cellular Ph Gradient in Tumor Versus Normal Tissue: Potential Exploitation for the Treatment of Cancer. *Cancer Res.* **1996**, *56* (6), 1194-1198.

(44) Cosse, J.-P.; Michiels, C. Tumour Hypoxia Affects the Responsiveness of Cancer Cells to Chemotherapy and Promotes Cancer Progression. *Anti-Cancer Agents Med. Chem.* **2008**, *8*, 790-797.

(45) Drummond, D. C.; Zignani, M.; Leroux, J. C. Current Status of pH-Sensitive Liposomes in Drug Delivery. *Prog. Lipid Res.* **2000**, *39* (5), 409-460.

(46) Saji, T.; Hoshino, K.; Aoyagui, S. Reversible Formation and Disruption of Micelles by Control of the Redox State of the Head Group. *J. Am. Chem. Soc.* **1985**, *107* (24), 6865-6868.

(47) Medina, J. C.; Gay, I.; Chen, Z. H.; Echegoyen, L.; Gokel, G. W. Redox-Switched Molecular Aggregates - the 1st Example of Vesicle Formation from Hydrophobic Ferrocene Derivatives. *J. Am. Chem. Soc.* **1991**, *113* (1), 365-366.

(48) Medina, J. C.; Li, C. S.; Bott, S. G.; Atwood, J. L.; Gokel, G. W. A Molecular Receptor Based on the Ferrocene System - Selective Complexation Using Atomic Ball-Bearings. *J. Am. Chem. Soc.* **1991**, *113* (1), 366-367.

(49) Munoz, S.; Gokel, G. W. Redox-Switched Vesicle Formation from Two Novel, Structurally Distinct Metalloamphiphiles. *J. Am. Chem. Soc.* **1993**, *115* (11), 4899-4900.

(50) Abbott, N. L.; Jewell, C. M.; Hays, M. E.; Kondo, Y.; Lynn, D. M. Ferrocene-Containing Cationic Lipids: Influence of Redox State on Cell Transfection. *J. Am. Chem. Soc.* **2005**, *127* (33), 11576-11577.

(51) Pak, C. C.; Ali, S.; Janoff, A. S.; Meers, P. Triggerable Liposomal Fusion by Enzyme Cleavage of a Novel Peptide-Lipid Conjugate. *Biochim. Biophys. Acta* **1998**, *1372* (1), 13-27.

(52) Jorgensen, K.; Vermehren, C.; Mouritsen, O. G. Enhancement of Phospholipase A2 Catalyzed Degradation of Polymer Grafted PEG-Liposomes: Effects of Lipopolymer-Concentration and Chain-Length. *Pharm Res* **1999**, *16* (9), 1491-1493.

(53) Jorgensen, K.; Vermehren, C.; Mouritsen, O. G. Enhancement of Phospholipase A(2) Catalyzed Degradation of Polymer Grafted PEG-Liposomes: Effects of Lipopolymer-Concentration and Chain-Length. *Pharmaceut Res* **1999**, *16* (9), 1491-1493.

(54) Davis, S. C.; Szoka, F. C. Cholesterol Phosphate Derivatives: Synthesis and Incorporation into a Phosphatase and Calcium-Sensitive Triggered Release Liposome. *Bioconjugate Chem.* **1998**, *9* (6), 783-792.

(55) Terada, T.; Iwai, M.; Kawakami, S.; Yamashita, F.; Hashida, M. Novel Peg-Matrix Metalloproteinase-2 Cleavable Peptide-Lipid Containing Galactosylated Liposomes for Hepatocellular Carcinoma-Selective Targeting. *J. Controlled Release* **2006**, *111* (3), 333-342.

(56) Sarkar, N. R.; Rosendahl, T.; Krueger, A. B.; Banerjee, A. L.; Benton, K.; Mallik, S.; Srivastava, D. K. "Uncorking" of Liposomes by Matrix Metalloproteinase-9. *Chem. Commun.* **2005**, (8), 999-1001.

(57) Siegel, D. P., Lipid Membrane Fusion. In *The Structure of Biological Membranes*, 2nd ed.; Yeagle, P. L., Ed. CRC Press: Boca Raton, 2005; pp 255-308.

(58) Hamai, C.; Yang, T. L.; Kataoka, S.; Cremer, P. S.; Musser, S. M. Effect of Average Phospholipid Curvature on Supported Bilayer Formation on Glass by Vesicle Fusion. *Biophys. J.* **2006**, *90* (4), 1241-1248.

(59) Israelachvili, J. N.; Wolfe, J. The Membrane Geometry of the Prolamellar Body. *Protoplasma* **1980**, *102* (3-4), 315-321.

(60) Marsh, D. Intrinsic Curvature in Normal and Inverted Lipid Structures and in Membranes. *Biophys. J.* **1996**, *70* (5), 2248-2255.

(61) Verkleij, A. J. Lipidic Intramembranous Particles. *Biochim. Biophys. Acta* **1984**, *779* (1), 43-63.

(62) Brown, M. F. Influence of Nonlamellar-Forming Lipids on Rhodopsin. *Curr. Top Membr.* **1997**, *44*, 285-356.

(63) Boni, L. T.; Hui, S. W. Polymorphic Phase Behaviour of Dilinoleoylphosphatidylethanolamine and Palmitoyloleoylphosphatidylcholine Mixtures. Structural Changes between Hexagonal, Cubic and Bilayer Phases. *Biochim. Biophys. Acta* **1983**, *731* (2), 177-185.

(64) Bentz, J.; Ellens, H. Membrane-Fusion - Kinetics and Mechanisms. *Colloids Surf.* **1988**, *30* (1-2), 65-112.

(65) Sanderson, P. W.; Lis, L. J.; Quinn, P. J.; Williams, W. P. The Hofmeister Effect in Relation to Membrane Lipid Phase-Stability. *Biochim. Biophys. Acta* **1991**, *1067* (1), 43-50.

(66) Hui, S. W.; Sen, A. Effects of Lipid Packing on Polymorphic Phase Behavior and Membrane Properties. *Proc. Natl. Acad. Sci. U. S. A.* **1989**, *86* (15), 5825-5829.

(67) Lairion, F.; Disalvo, E. A. Effect of Dipole Potential Variations on the Surface Charge Potential of Lipid Membranes. *J. Phys. Chem. B* **2009**, *113* (6), 1607-1614.

(68) Rydall, J. R.; Macdonald, P. M. Investigation of Anion Binding to Neutral Lipid Membranes Using ^{2}H NMR. *Biochemistry* **1992**, *31* (4), 1092-1099.

(69) Scherer, P. G.; Seelig, J. Electric Charge Effects on Phospholipid Headgroups. Phosphatidylcholine in Mixtures with Cationic and Anionic Amphiphiles. *Biochemistry* **1989**, *28* (19), 7720-7728.

(70) Langner, M.; Kubica, K. The Electrostatics of Lipid Surfaces. *Chem. Phys. Lipids* **1999**, *101* (1), 3-35.

(71) Gruner, S. M. Intrinsic Curvature Hypothesis for Biomembrane Lipid-Composition - a Role for Nonbilayer Lipids. *Proc. Natl. Acad. Sci. U.S.A.* **1985**, *82* (11), 3665-3669.

(72) Avanti Polar Lipids. http://www.avantilipids.com (accessed May 2011).

(73) Harper, P. E.; Mannock, D. A.; Lewis, R. N.; McElhaney, R. N.; Gruner, S. M. X-Ray Diffraction Structures of Some Phosphatidylethanolamine Lamellar and Inverted Hexagonal Phases. *Biophys. J.* **2001**, *81* (5), 2693-2706.

(74) Wiener, M. C.; White, S. H. Structure of a Fluid Dioleoylphosphatidylcholine Bilayer Determined by Joint Refinement of X-Ray and Neutron-Diffraction Data 3. Complete Structure. *Biophys. J.* **1992**, *61* (2), 434-447.

(75) Kinnunen, P. K. J.; Kıiv, A.; Lehtonen, J. Y. A.; Rytömaa, M.; Mustonen, P. Lipid Dynamics and Peripheral Interactions of Proteins with Membrane Surfaces. *Chem. Phys. Lipids* **1994**, *73* (1-2), 181-207.

(76) Makino, K.; Shibata, A., Chapter 2: Surface Properties of Liposomes Depending on Their Composition. In *Advances in Planar Lipid Bilayers and Liposomes*, Liu, A. L., Ed. Academic Press: 2006; Vol. Volume 4, pp 49-77.

(77) Yeagle, P. L.; Sen, A. Hydration and the Lamellar to Hexagonal(Ii) Phase-Transition of Phosphatidylethanolamine. *Biochemistry* **1986**, *25* (23), 7518-7522.

(78) Damodaran, K. V.; Merz, K. M. A Comparison of DMPC-Based and DLPE-Based Lipid Bilayers. *Biophys. J.* **1994**, *66* (4), 1076-1087.

(79) Bouchet, A. M.; Frias, M. A.; Lairion, E.; Martini, F.; Almaleck, H.; Gordillo, G.; Disalvo, E. A. Structural and Dynamical Surface Properties of Phosphatidylethanolamine Containing Membranes. *Biochim. Biophys. Acta* **2009**, *1788* (5), 918-925.

(80) Gawrisch, K.; Parsegian, V. A.; Hajduk, D. A.; Tate, M. W.; Gruner, S. M.; Fuller, N. L.; Rand, R. P. Energetics of a Hexagonal Lamellar Hexagonal-Phase Transition Sequence in Dioleoylphosphatidylethanolamine Membranes. *Biochemistry* **1992**, *31* (11), 2856-2864.

(81) Seddon, J. M.; Cevc, G.; Marsh, D. Calorimetric Studies of the Gel-Fluid (L-Beta-L-Alpha) and Lamellar-Inverted Hexagonal (L-Alpha-H-II) Phase-Transitions in Dialkyl and Diacylphosphatidylethanolamines. *Biochemistry* **1983**, *22* (5), 1280-1289.

(82) Ellens, H.; Bentz, J.; Szoka, F. C. Ph-Induced Destabilization of Phosphatidylethanolamine-Containing Liposomes - Role of Bilayer Contact. *Biochemistry* **1984**, *23* (7), 1532-1538.

(83) Kunz, W.; Henle, J.; Ninham, B. W. 'Zur Lehre Von Der Wirkung Der Salze' (About the Science of the Effect of Salts): Franz Hofmeister's Historical Papers. *Curr. Opin. Colloid Interface Sci.* **2004**, *9* (1-2), 19-37.

(84) Collins, K. D.; Washabaugh, M. W. The Hofmeister Effect and the Behaviour of Water at Interfaces. *Q. Rev. Biophys.* **1985**, *18* (4), 323-411.

(85) Koynova, R.; Brankov, J.; Tenchov, B. Modulation of Lipid Phase Behavior by Kosmotropic and Chaotropic Solutes - Experiment and Thermodynamic Theory. *Eur. Biophys. J. Biophy.* **1997**, *25* (4), 261-274.

(86) Heydweiller, A. Concerning the Physical Characteristics of Solutions in Correlation. II. Surface Tension and Electronic Conductivity of Watery Salt Solutions. *Ann. Phys.* **1910**, *33* (11), 145-185.

(87) Kunz, W.; Lo Nostro, P.; Ninham, B. W. The Present State of Affairs with Hofmeister Effects. *Curr. Opin. Colloid Interface Sci.* **2004**, *9* (1-2), 1-18.

(88) Gurau, M. C.; Lim, S. M.; Castellana, E. T.; Albertorio, F.; Kataoka, S.; Cremer, P. S. On the Mechanism of the Hofmeister Effect. *J. Am. Chem. Soc.* **2004**, *126* (34), 10522-10523.

(89) Omta, A. W.; Kropman, M. F.; Woutersen, S.; Bakker, H. J. Influence of Ions on the Hydrogen-Bond Structure in Liquid Water. *J. Chem. Phys.* **2003**, *119* (23), 12457-12461.

(90) Omta, A. W.; Kropman, M. F.; Woutersen, S.; Bakker, H. J. Negligible Effect of Ions on the Hydrogen-Bond Structure in Liquid Water. *Science* **2003**, *301* (5631), 347-349.

(91) Batchelor, J. D.; Olteanu, A.; Tripathy, A.; Pielak, G. J. Impact of Protein Denaturants and Stabilizers on Water Structure. *J. Am. Chem. Soc.* **2004**, *126* (7), 1958-1961.

(92) Mclaughlin, S.; Bruder, A.; Chen, S.; Moser, C. Chaotropic Anions and Surface-Potential of Bilayer Membranes. *Biochim. Biophys. Acta* **1975**, *394* (2), 304-313.

(93) O'Brien, J. T.; Prell, J. S.; Bush, M. F.; Williams, E. R. Sulfate Ion Patterns Water at Long Distance. *J. Am. Chem. Soc.* **2010**, *132* (24), 8248-8249.

(94) Siegel, D. P. Inverted Micellar Structures in Bilayer Membranes. Formation Rates and Half-Lives. *Biophys. J.* **1984**, *45* (2), 399-420.

(95) Siegel, D. P.; Epand, R. M. The Mechanism of Lamellar-to-Inverted Hexagonal Phase Transitions in Phosphatidylethanolamine: Implications for Membrane Fusion Mechanisms. *Biophys. J.* **1997**, *73* (6), 3089-3111.

(96) Siegel, D. P. Inverted Micellar Intermediates and the Transitions between Lamellar, Cubic, and Inverted Hexagonal Lipid Phases. I. Mechanism of the L Alpha-Hii Phase Transitions. *Biophys. J.* **1986**, *49* (6), 1155-1170.

(97) Siegel, D. P. Inverted Micellar Intermediates and the Transitions between Lamellar, Cubic, and Inverted Hexagonal Lipid Phases. II. Implications for Membrane-Membrane Interactions and Membrane Fusion. *Biophys. J.* **1986**, *49* (6), 1171-1183.

(98) Hui, S. W.; Stewart, T. P.; Boni, L. T. The Nature of Lipidic Particles and Their Roles in Polymorphic Transitions. *Chem. Phys. Lipids* **1983**, *33* (2), 113-126.

(99) Caffrey, M. Kinetics and Mechanism of the Lamellar Gel/Lamellar Liquid-Crystal and Lamellar/Inverted Hexagonal Phase Transition in Phosphatidylethanolamine: A Real-Time X-Ray Diffraction Study Using Synchrotron Radiation. *Biochemistry* **1985**, *24* (18), 4826-4844.

(100) Milstien, S.; Cohen, L. A. Stereopopulation Control .1. Rate Enhancement in Lactonizations of Ortho-Hydroxyhydrocinnamic Acids. *J. Am. Chem. Soc.* **1972**, *94* (26), 9158-9165.

(101) Weerapreeyakul, N.; Visser, P.; Brummelhuis, M.; Gharat, L.; Chikhale, P. J. Reductive and Bioreductive Activation Is Controlled by Electronic Properties of Substituents in Conformationally-Constrained Anticancer Drug Delivery Systems. *Med. Chem. Res.* **2000**, *10* (3), 149-163.

(102) Ong, W.; McCarley, R. L. Redox-Driven Shaving of Dendrimers. *Chem. Commun.* **2005**, (37), 4699-4701.

(103) Ong, W.; McCarley, R. L. Chemically and Electrochemically Mediated Release of Dendrimer End Groups. *Macromolecules* **2006**, *39* (21), 7295-7301.

(104) Carpino, L. A.; Triolo, S. A.; Berglund, R. A. Reductive Lactonization of Strategically Methylated Quinone Propionic-Acid Esters and Amides. *J. Org. Chem.* **1989**, *54* (14), 3303-3310.

(105) Jung, M. E.; Piizzi, G. Gem-Disubstituent Effect: Theoretical Basis and Synthetic Applications. *Chem. Rev.* **2005**, *105* (5), 1735-1766.

(106) King, M. M.; Cohen, L. A. Stereopopulation Control 7. Rate Enhancement in the Lactonization of 3-(Ortho-Hydroxyphenyl)Propionic Acids - Dependence on the Size of Aromatic Ring Substituents. *J. Am. Chem. Soc.* **1983**, *105* (9), 2752-2760.

(107) Wang, B.; Nicolaou, M. G.; Liu, S.; Borchardt, R. T. Structural Analysis of a Facile Lactonization System Facilitated by a "Trimethyl Lock". *Bioorg. Chem.* **1996**, *24* (1), 39-49.

(108) Winans, R. E.; Wilcox, C. F. Comparison of Stereo-Population Control with Conventional Steric Effects in Lactonization of Hydrocoumarinic Acids. *J. Am. Chem. Soc.* **1976**, *98* (14), 4281-4285.

(109) Ernster, L. DT-Diaphorase - a Historical Review. *Chem. Scr.* **1987**, *27A*, 1-13.

(110) Phillips, R. M.; Naylor, M. A.; Jaffar, M.; Doughty, S. W.; Everett, S. A.; Breen, A. G.; Choudry, G. A.; Stratford, I. J. Bioreductive Activation of a Series of Indolequinones by Human DT-Diaphorase: Structure-Activity Relationships. *J. Med. Chem.* **1999**, *42* (20), 4071-4080.

(111) Faig, M.; Bianchet, M. A.; Talalay, P.; Chen, S.; Winski, S.; Ross, D.; Amzel, L. M. Structures of Recombinant Human and Mouse NAD (P)H : Quinone Oxidoreductases: Species Comparison and Structural Changes with Substrate Binding and Release. *Proc. Natl. Acad. Sci. U.S.A.* **2000**, *97* (7), 3177-3182.

(112) Fitzsimmons, S. A.; Workman, P.; Grever, M.; Paull, K.; Camalier, R.; Lewis, A. D. Reductase Enzyme Expression across the National Cancer Institute Tumor Cell Line Panel: Correlation with Sensitivity to Mitomycin C and E09. *J. Natl. Cancer I.* **1996**, *88* (5), 259-269.

(113) Rooseboom, M.; Commandeur, J. N. M.; Vermeulen, N. P. E. Enzyme-Catalyzed Activation of Anticancer Prodrugs. *Pharmacol. Rev.* **2004**, *56* (1), 53-102.

(114) McKeown, S. R.; Cowent, R. L.; Williams, K. J. Bioreductive Drugs: From Concept to Clinic. *Clin. Oncol.* **2007**, *19* (6), 427-442.

(115) Faig, M.; Bianchet, M. A.; Winski, S.; Hargreaves, R.; Moody, C. J.; Hudnott, A. R.; Ross, D.; Amzel, L. M. Structure-Based Development of Anticancer Drugs: Complexes of NAD(P)H : Quinone Oxidoreductase 1 with Chemotherapeutic Quinones. *Structure* **2001**, *9* (8), 659-667.

(116) Mayhew, S. G. Redox Potential of Dithionite and SO_2^- from Equilibrium Reactions with Flavodoxins, Methyl Viologen and Hydrogen Plus Hydrogenase. *Eur. J. Biochem.* **1978**, *85* (2), 535-547.

(117) Devries, J. G.; Kellogg, R. M. Reduction of Aldehydes and Ketones by Sodium Dithionite. *J. Org. Chem.* **1980**, *45* (21), 4126-4129.

(118) Selmer, T., Anoxic Testing and Purification of Enzymes. In *Handbook of Clostridia*, Durre, P., Ed. CRC Press: Boca Raton, FL, 2005; pp 87-127.

(119) Duzgunes, N.; Bentz, J., Fluorescence Assas for Membrane Fusion. In *Spectroscopy Membrane Probes*, Loew, L. M., Ed. CRC Press: Boca Raton, FL, 1988; Vol. 1, pp 117-159.

(120) Memoli, A.; Palermiti, L. G.; Travagli, V.; Alhaique, F. Effects of Surfactants on the Spectral Behaviour of Calcein (II): A Method of Evaluation. *J. Pharm. Biomed. Anal.* **1999**, *19* (3-4), 627-632.

(121) McIntyre, J. C.; Sleight, R. G. Fluorescence Assay for Phospholipid Membrane Asymmetry. *Biochemistry* **1991**, *30* (51), 11819-11827.

CHAPTER 2

EXPERIMENTAL

2.1 Buffer Preparation

All buffer components were purchased from Sigma Aldrich and were of Bioultra (>99%) grade or better; they were used without further purification. All buffer salts were used with the counter ion of potassium whenever available. The standard buffer system in all experiments was composed of pH 7.4 50 mM phosphate buffer with 75 mM KCl. For higher salt measurements, the 50 mM phosphate buffer was maintained with the required concentration of the specific salt added and the solution brought up to pH 7.4 with KOH. For applications requiring non-phosphate buffers, pH 7.4 10 mM 2-[2-hydroxy-1,1-bis(hydroxymethyl)ethyl)amino] ethanesulfonic acid (TES) with the appropriate concentration of KCl was used. All buffers were filtered through a 0.1–μm pore size polycarbonate track-etched membrane prior to storage in glass bottles in a refrigerator until required for experimental use. Prior to use, all buffers were allowed to come to room temperature while under nitrogen purge to degas the buffers.

2.2 Liposome Preparation

2–3 mg of the desired lipid was dissolved in a minimal amount of $CHCl_3$ (approximately 1 mL) in a 10 mL (14/20) ground joint test tube. The $CHCl_3$ was removed under a gentle flow of ultra-high purity (UHP) argon to create a thin lipid film on the bottom of the tube. The lipid film was further dried overnight under high vacuum. Lipids were hydrated in the appropriate amount of the desired buffer to create a 1 mg mL^{-1} solution. The solution was aged for an hour on a rotary mixer and vortexed every 20 minutes for 10–15 seconds. The hydrated lipids were then cycled through six freeze-thaw cycles using a dry ice/acetone bath and a warm water bath. The solution was allowed to come into equilibrium with the ambient temperature for 20 min before it was extruded. Extrusion was performed 20 times at ambient temperature through one 100-nm

pore Whatman Nuclepore polycarbonate track-etched membrane using a Mini-Extruder (Avanti Polar Lipids, Alabaster, AL). Lipids were stored in an amber glass vial and shielded from light and used immediately for experiments.

For calcein-loaded liposomes, the same procedure as above was followed except that the buffered solution contained calcein (40 mM). Calcein (Sigma Aldrich, St. Lewis, MO) was used without further purification, and solutions were prepared fresh for each experiment in 5 mL aliquots. Briefly, a small amount of KOH (30–40 mg) was dissolved in 1 mL of buffer, followed by the addition of calcein and an additional 3.8 mL of buffer. The solution was sonicated to dissolve the calcein to yield a transparent orange-colored solution prior to titrating the pH back to 7.4 using KOH to yield an opaque reddish-brown solution. After the pH adjustment, the total volume was brought up to 5 mL and the buffered calcein solution stored in the dark. Following the extrusion, the calcein-loaded liposomes were separated from the non-encapsulated calcein through size-exclusion chromatography on a 20 cm × 10 cm Sephadex G-75 resin column. 0.5 mL of the solution was loaded onto the column each time and approximately 1 mL (12 drops) of the leading band collected in amber glass vials. No significant loss of calcein was observed after three days at ambient temperatures and conditions while liposomes stored under argon and low temperatures (8 °C) were stable for up to seven days.

2.3 Size Exclusion Chromatography

Sephadex G-75 from GE Healthsciences was used as the separation medium. The overall column length was 20 cm with an internal diameter of 10 cm. Total column volume was 20 mL according to the bed volume parameters provided by GE Healthcare (12–15 mL swelled per g dry). Sephadex G-75 was prepared according to the literature provided by GE Healthcare: 1.67 g of Sephadex into 26 mL of buffer and allowed to swell at room temperature for 24 hrs. The buffer used for the swelling of the Sephadex G-75 was always the same as the one to be used in

the calcein-loaded liposome separation, thus for different salt buffers, a new column would be prepared for that specific buffer system. After 24 hrs, any remaining buffer was decanted and an additional 35 mL of buffer was added to make a 75% suspension. The suspended Sephadex G-75 was degassed for 20 minutes in a sonicator prior to gravity packing the column. Freshly packed columns were washed several times with the buffer system prior to conditioning with non-calcein containing liposomes. Prior to the first separation, each column was conditioned by the addition of unloaded liposomes, which is believed to prevent non-specific adsorption of during the actual separation of liposomes from calcein to the Sephadex G-75 beads.[1]

2.3.1 Size Exclusion Chromatography Procedures

Approximately 0.75 mL of calcein-loaded liposomes were added dropwise to the top of the column bed, allowing each drop to be absorbed into the Sephadex G-75 before the next drop was introduced. The elution buffer was the same as the buffer used to prepare the calcein liposome solution. Once the entire fraction of calcein-loaded liposomes was added to the column, 2 mL of buffer was slowly introduced along the sides of the column to wash any remaining calcein on the sides of the column walls. The first wash was allowed to be absorbed into the column bed prior to adding a second 2 mL buffer wash to begin eluting the bands. After the second wash was absorbed into the column bed, 7 mL of buffer was slowly added to the column so as to not disturb the column bed for elution. The 7 mL of buffer was maintained during the entire separation procedure. The calcein-liposome solution splits into two distinct bands after passing through approximately 5 cm of the column with the fast moving leading band containing calcein-loaded liposomes and the slower moving second band containing only free calcein. The first band typically has a yellow-brown color that gradually becomes more yellow before eluting from the column. Twelve drops of the leading band is collected for each fraction and is stored in a 4 mL amber glass vial that is further shielded from light until the second

separation is complete. Once the calcein-loaded liposomes have eluted, the column is flushed with buffer until no discernable color from the calcein remains in the Sephadex G-75. After fully washing the column, the second fraction of the calcein and liposome solution is added and the same procedure as above repeated. After the two separation procedures, the column was maintained with 7 mL of buffer to keep the Sephadex G-75 fully hydrated during storage. The columns were capped with a rubber septum and wrapped with Parafilm. On average, a column would be suitable for regular use and multiple separations for up to a month before discoloration from excess calcein or poor separation performance required that a new column be prepared with fresh Sephadex G-75.

2.4 Calcein Release Experiments

Calcein-encapsulated liposomes were diluted with the appropriate buffer using adsorption values at λ = 265 nm and diluting to a value of 0.55, which corresponds to a 0.1 mM lipid concentration based on ε_{265} = 5500 M^{-1} cm^{-1} for the Q_3 headgroup. Alternatively, ε_{272} = 10330 M^{-1} cm^{-1} was used for the Q_1 headgroup and ε_{240} = 7030 M^{-1} cm^{-1} for the Q_0 headgroup. 3 mL of the diluted liposomes were transferred to a sealable quartz fluorescence cell (Hellma, Plainview, NY) and purged with a gentle flow of UHP argon for five min. All fluorescence experiments were performed on a PerkinElmer LS-55 luminescence spectrophotometer equipped with a PTP-1 fluorescence peltier system coupled to a PCB1500 water peltier system (PerkinElmer, Waltham, MA) capable of maintaining temperatures within ± 0.5 °C across the cell. Temperatures were maintained at 25 °C unless otherwise noted. λ_{ex} = 490 nm, slit = 2.5 mm and λ_{em} = 520 nm, slit = 3.5 mm. Time based measurements were performed with a time interval of 1 min per data point up to 1500 minutes with a 0.1 second integration time. In order to bring the fluorescence intensity level of the calcein down below the detector saturation limit of 1000 counts, the detector voltage was reduced to 770 V in addition to placing two stacked neutral

density filters (Omega Optics, Brattleboro, VT) in the emission path to reduce the total transmission to 16% of the original intensity. For samples with a higher calcein intensity, a neutral density filter reducing the total transmission intensity to 8% was used. The neutral density filters had no observable impact on the appearance of the fluorescence release traces for calcein dequenching fluorescence, only serving to reduce the overall intensity of the dequenched calcein to a level below the detector saturation level.

For chemical reduction and calcein release from the liposomes, 2–3 mg of solid $Na_2S_2O_4$ (85%, Acros, New Jersey, NJ) was measured out into a 2 mL snap-top vial and purged with a gentle flow of UHP argon. 1 mL of UHP argon purged buffer was slowly added to the vial, mixed, and immediately used for reduction experiments. $Na_2S_2O_4$ was freshly prepared for each experiment. An appropriate amount of the $Na_2S_2O_4$ buffer solution was injected into the argon-purged fluorescence cuvette with a 50 μL Gastight syringe (Hamilton, Reno, NV) for a 1:1 molar equivalent of $Na_2S_2O_4$:Q-DOPE according to the dilution equation. The fluorescence cuvette was inverted several times before being replaced in the instrument prior to the next measurement point taken. The time was noted as t_0. The reduction of the capping quinone headgroup and the subsequent release and dequenching of the calcein was allowed to proceed without interruption until the final intensity value was no longer increasing. To set the 100% calcein (F_{100}) release value, 15 μL of 15% (v/v) Triton X-100 (Sigma-Aldrich, St. Lewis, MO) was added to the cuvette to yield a 0.1% Trition concentration. After Trition addition, an additional fifteen minutes of fluorescence intensity was recorded prior to the end of the experiment.

The percentage of calcein leakage was calculated as follows:

$$\%Leakage = \frac{(F_t - F_0)}{(F_{100} - F_0)} * 100 \qquad \textbf{Equation 2.1}$$

F_0 was set as 0% leakage and was the average of the first four points prior to the $Na_2S_2O_4$ addition at t_0. F_{100} was taken as the 100% leakage and was the average of the four points after the Trition X-100 addition. F_t corresponds to the fluorescence intensity observed at the point in time.

2.5 Liposome Characterization

Dynamic light scattering measurements were obtained from back scatter intensities (173°, 633-nm red laser) obtained at 25 °C on a Zetasizer Nano ZS (Malvern Instruments, Worcestershire, UK) particle size analyzer. Both calcein-free and calcein-loaded liposomes were observed with no significant diameter differences. Zeta potentials were obtained at 25 °C in a folded capillary zeta potential cell using a Smoluchowski model with F(Ka) = 1.5.

2.6 Differential Scanning Calorimetry

A VP-DSC (Microcal, Piscataway, NJ) with 0.52-mL capillary cells was used for all thermal measurements of lipid samples. Baseline responses of all buffers were obtained by continuous scanning from 1 °C to 40 °C at 40 °C/hour for a minimum of 12 hours. Both the reference cell and the sample cell were completely filled with buffer (0.52 mL) and the top sealed to a minimum of 20 PSI. Once a repeatable baseline was achieved, the instrument was brought to 1 °C for 20 min prior to quickly loading the hydrated DOPE into the sample cell. Prior to loading, the DOPE was vortexed for 20 seconds to suspend the DOPE liposomes. The DOPE was allowed to come into thermal equilibrium at 1 °C for 20 minutes before the temperature was ramped up to a final temperature of 40 °C at 40 °C hr^{-1}.

2.6.1 DOPE Preparation for DSC

1 mL of a 10 mg mL^{-1} DOPE (Avanti Polar Lipids, Alabaster, AL) in $CHCl_3$ solution was transferred to a pre-weighed 5 mL round bottom tube. The $CHCl_3$ was removed via a gentle flow of UHP argon for one hour followed by high vacuum. The tube was weighed again and the

difference used to find the mass of dry DOPE lipid. An appropriate amount of buffer was added to bring the lipid concentration to 14 mg mL^{-1} (18.8 mM). The DOPE was allowed to age at room temperature for 20 min on a rotary shaker before being subjected to six cycles of freeze/thaw in liquid nitrogen (10 min) and 1:1 ethylene glycol:water bath at 0 °C (20 min). The lipids were vigorously vortexed between each cycle to completely suspend the lipids in the buffer. The fully hydrated lipids were stored overnight at – 1 °C.

Prior to loading the hydrated DOPE into the DSC, the 1:1 ethylene glycol:water bath was brought to – 5 °C for 30 min to bring the lipids well below the T_H. The DOPE was quickly transported to the pre-equilibrated instrument at 1.5 °C in an ice/water bath and loaded as quickly as possible to avoid warming the sample.

2.7 Q_1-DOPE Synthesis

The synthesis of Q_1-DOPE was performed following the synthesis pathway of Rohde[2] and Ong[3] with the following modifications:

2.7.1 Q_1-Lactone (a)

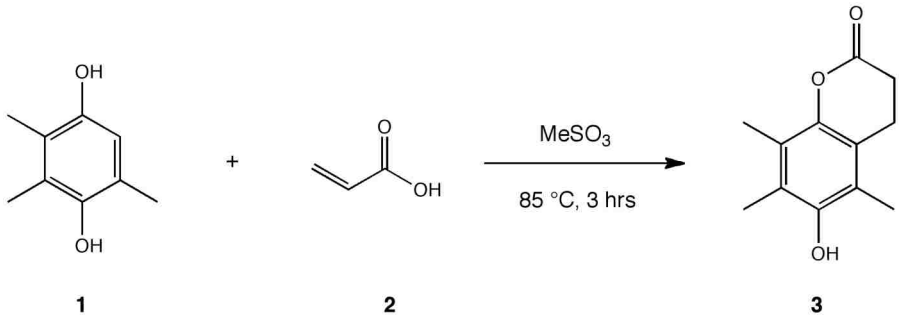

Scheme 2.1: Reaction for Q_1-lactone (**3**).

5 grams (32.8 mmol) of **(1)** 2,3,5-trimethylhydroquinone was mixed with **(2)** 2.6 grams (36.3 mmol) acrylic acid and methanesulfonic acid ($MeSO_3$) (40 mL). The mixture was stirred at 85 °C under argon for 3 hours then cooled to room temperature. 100 mL of ice water was added to the mixture with stirring, yielding a dark red precipitate. The precipitate was extracted

with four washes of 50 mL ethyl acetate. The combined organic layer was further washed with two 100 mL water washes followed by two washings with saturated $NaHCO_3$. The organic layer was dried over $MgSO_4$ and the ethyl acetate removed by rotary evaporation. Dark red-brown crystals were left to dry overnight under high vacuum. The crystals were washed with cold *n*-hexanes:chloroform (70:30 v/v) and allowed to dry under high vacuum overnight to give 1.8 g (36 %) of the desired product **(3)** as a red-brown crystals. Yield: 36%; ^{1}H NMR 400 MHz ($CDCl_3$) δ 5.33 (s, 1H), 4.59 (s, 1H), 3.65 (s, 1H), 2.40 (s, 2H), 2.31 (s, 2H), 1.82 (s, 9H).

2.7.2 Q_1-PA (b)

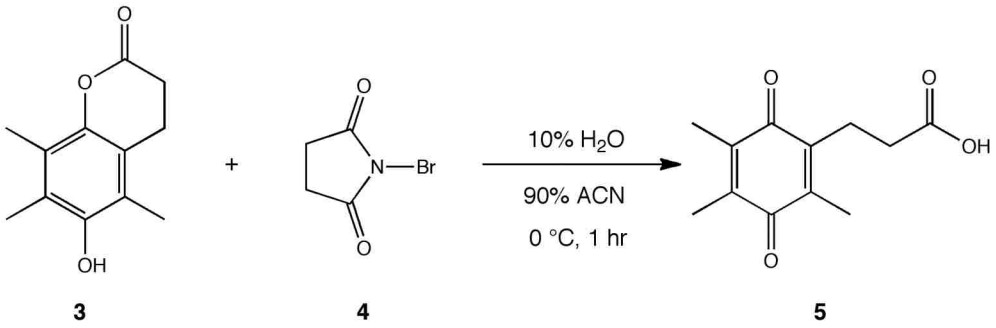

3 **4** **5**

Scheme 2.2: Reaction for Q_1-proponic acid (**5**).

Q_1-lactone **(3)** (2 g, mmol) was added to a solution of 45 mL acetonitrile and 9 mL of water. **(4)** *N*-bromosuccinimide (1.86 g, mmol) was combined with 15 mL acetonirile and added dropwise over an hour to the Q_1-lactone mixture with stirring at room temperature. The reaction was allowed to continue for 1.5 hours. Rotary evaporation was used to remove the acetonitrile before adding 40 mL of water. The solution was extracted with CH_2Cl_2 (4 x 40 mL). The combined organic layers were washed with saturated NaCl (2 x 40 mL) and dried over $MgSO_4$. The CH_2Cl_2 was removed by rotary evaporation to yield an oily yellow-brown product **(5)**. Yield: 87%; ^{1}H NMR 400 MHz ($CDCl_3$) δ 2.80 (t, 2H), 2.53 (t, 2H), 2.05 (s, 3H), 2.02 (s, 6H).

2.7.3 Q_1-NHS (c)

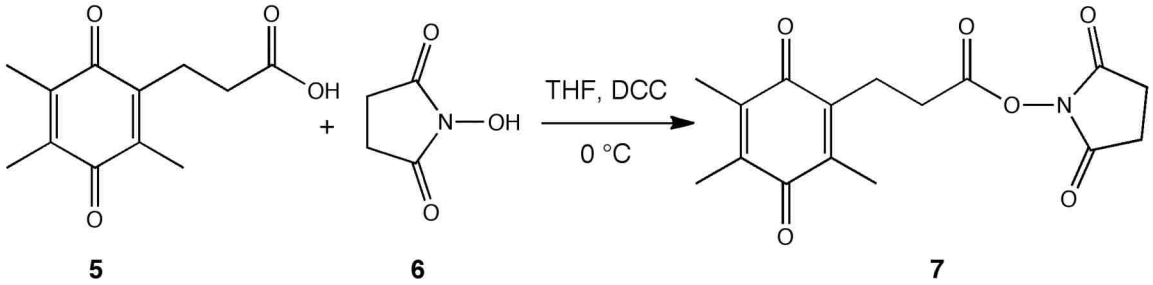

5 6 7

Scheme 2.3: Reaction for Q_1-NHS (**7**).

Q_1-PA **(5)** (0.5g, mmol) was added to **(6)** NHS (0.25g, mmol) and 20 mL dry THF with stirring, under argon, and cooled to 0 °C. Only after the mixture was at 0 °C, *N*,*N*'-dicyclohexylcarbodiimide (DCC) (0.5g, mmol) was added and the reaction was allowed to proceed for 20 hours. The products were filtered to remove urea and washed with ethyl acetate (3 x 5 mL), yielding a yellow filtrate. Ethyl acetate was removed from the filtrate by rotary evaporation to yield a yellow solid. The product was recrystallized in hot ether and stored in the freezer overnight. Pure yellow crystals of the product **(7)** were collected and dried. Yield: 72% ^{1}H NMR 400 MHz ($CDCl_3$) δ 2.90 (m, 2H), 2.82 (m, 6H), 2.50 (t, 2H), 2.07 (s, 3H), 2.02 (s, 6H).

2.7.4 Q_1-DOPE (d)

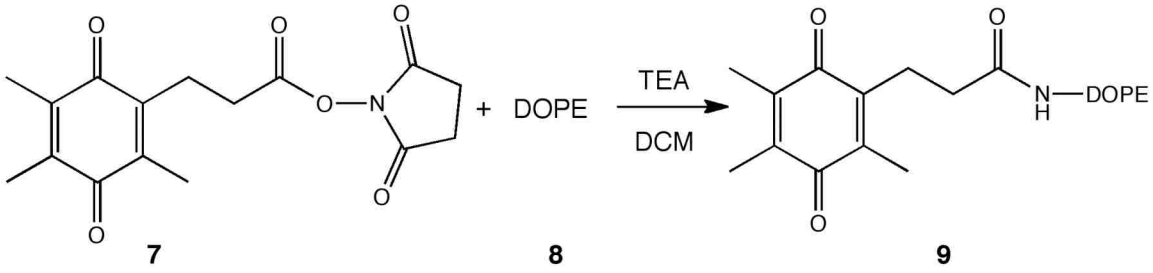

7 8 9

Scheme 2.4: Reaction for Q_1-DOPE (**9**).

Fresh **(8)** DOPE in powder form was weighed in the vial, dissolved in minimal dry CH_2Cl_2, transferred to a 100 mL three-neck round bottom flash. An additional 5 mL of dry

CH_2Cl_2 was added to the round bottom and the mixture cooled to 0 °C while under Ar. The DOPE was used to calculate the desired ratio of components: Q_1-NHS:DOPE:TEA (1.06:1:5). Once the lipid mixture reached 0°C, the appropriate amount of TEA was added with stirring. Following the TEA addition, the appropriate amount of **(7)** Q_1-NHS was added and the mixture was covered and allowed to react for two hours in the ice bath. After 2 hrs, the ice bath was removed and the reaction allowed to continue for an additional 2 hrs, covered, at room temperature. The reaction was stopped by the addition of 50 mL CH_2Cl_2. A 50 mL 5% sodium bicarbonate extraction was performed and the CH_2Cl_2 layer collected. The CH_2Cl_2 products mixture was dried over Na_2SO_4, and the CH_2Cl_2 was removed via rotary evaporation. Remaining solvent was further removed by high vacuum for several hours to yield a waxy yellow film. Purification of the products was performed using a 10 gram column on a Flashmaster. The column was prepared with CH_2Cl_2:ethyl acetate (1:1) and the products were introduced onto the column with the same solvent mixture. CH_2Cl_2:ethyl acetate (1:1) was used to remove the pale yellow band of unreacted materials. CH_2Cl_2:MeOH:*n*-hexanes (3:1:2) was used to move the Q_1-DOPE band through the column and was collected into a 100 mL round bottom flask. The CH_2Cl_2:MeOH:*n*-hexanes was removed by rotary evaporation to yield a thin yellow waxy film. The pure **(9)** Q_1-DOPE was transferred to a 15 mL round bottom flask via a minimal amount of $CHCl_3$, which was removed by a gentle argon flow followed by high vacuum. Yield: 88%; ^{1}H NMR ($CDCl_3$, 400 MHz) δ 7.40 (bs, 1H), 5.32 (m, 4H), 5.21 (m, 1H), 4.37 (m, 1H), 4.16 (m, 1H), 3.96 (m, 4H), 3.48 (m, 2H), 2.76 (t, 2H), 2.31 (t, 2H), 2.27 (m, 4H), 2.02-1.94 (m, 17H), 1.55 (m, 4H), 1.24 (m, 4OH), 0.89 (t, 6H).

2.8 References

(1) Lasch, J.; Weissig, V.; Brandl, M., Preparation of Liposomes. In *Liposomes*, 2nd ed.; Torchilin, V. P.; Weissig, V., Eds. Oxford University Press: 2003; pp 3-30.

(2) Rohde, R. D.; Agnew, H. D.; Yeo, W. S.; Bailey, R. C.; Heath, J. R. A Non-Oxidative Approach toward Chemically and Electrochemically Functionalizing Si(111). *J. Am. Chem. Soc.* **2006**, *128* (29), 9518-9525.

(3) Ong, W.; Yang, Y. M.; Cruciano, A. C.; McCarley, R. L. Redox-Triggered Contents Release from Liposomes. *J. Am. Chem. Soc.* **2008**, *130* (44), 14739-14744.

CHAPTER 3

MODULATION OF DOPE PHASE BEHAVIOR WITH HOFMEISTER SALTS

3.1 Introduction

Liposomes as delivery containers continue to attract considerable interest, especially in the realm of drug and reagent delivery. The presence of endogenous triggers at a desired site of delivery has driven research to develop stimuli-responsive liposomes that exploit the site-specific phenomena to remotely activate liposomes to unload encapsulated cargo. The ability to exert control over the location of release brings to fruition the ability to influence the rates of unloading from the liposomes as to match drug efficacy profiles for increased therapeutic impact.

Q_3-DOPE was developed as a redox-active lipid that can be reduced upon exposure to reductive chemicals or quinone reductase enzymes.[1] Initial stability and release studies demonstrated the ability of this novel system to encapsulate and release contents upon demand. Like many stimuli-responsive liposomes, DOPE was used as the base lipid due to its preference to form non-lamellar phases at room or physiological temperatures. However, upon careful examination of the Q_3-DOPE system, it was discovered that the rates of release could be influenced by buffer composition. The buffer influence was traced to the rich and interesting chemistry of DOPE that allows for tuning of the rates of content release from the system through manipulation of the phase transition process. The effects of temperature, salt concentration and salt type are well described in the literature for lipid behavior and liposome fusion, but their impact on contents release were largely unknown or unreported prior to the work described here. Thus, it should be possible to exert an additional level of control over the rate of content release by manipulating the kinetic and thermodynamic parameters that govern the phase transition of DOPE lipids.

Here I report on efforts to unravel how the rate of contents release, from Q_3-DOPE liposomes relates to the modulation of the phase transition temperature of DOPE lipids by the presence of Hofmeister salts. To the best of our knowledge, this is the first time that the graded response of lipid $L_\alpha \rightarrow H_{II}$ transition temperature, T_H, to Hofmeister salts has been observed and conducted with contents release rates. The ability of Q_3-DOPE to adopt stable lamellar liposome structures opens the possibility of performing rapid changes in the headgroup chemistry through reductive action. Once the capping quinone headgroup is removed, liposomes composed of lamellar phase DOPE lipids are able to readily approach and aggregate with an apposing DOPE-rich liposome that converts the apposing liposomes into non-bilayer structures and releases any encapsulated contents. DOPE was selected as the lipid due to its reported T_H values of approximately 10 °C, thus at room temperature and under neutral pH conditions, it has a preference for the non-bilayer phase. By carefully manipulating the ambient temperature and buffer composition, I demonstrate that the rates of release observed in calcein unloading experiments correlate inversely with the values of T_H obtained from DSC measurements. A discussion of Hofmeister salt interactions with lipid bilayers and its effects on lipid phase behavior is presented as a possible explanation for the observed rate changes for contents release in Q_3-DOPE liposomes.

3.2 Experimental Section

3.2.1 Materials

Q_3-DOPE liposomes were prepared as described in Chapter 2, Section 2.2. Unless otherwise noted, a standard pH 7.4 buffer composed of 50 mM phosphate and 75 mM KCl at 25 °C was used. For the Hofmeister salt series, at pH 7.4 50 mM phosphate buffer was used for the various salts.

3.2.2 UV-Vis Measurements and Reduction of Q_3 Headgroup

The molar coefficient for Q_3-DOPE was determined by a standard series of dilutions from a known stock solution of the lipid in 0.5 mM phosphate buffer with 75 mM KCl at pH 7.4. To determine the reduction behavior of and times for reduction of the Q_3 headgroup, a solution of 0.1 mM Q_3-DOPE was introduced into a septum sealed quartz cuvette and then purged with argon. A 21 mM solution of sodium dithionite ($Na_2S_2O_4$) was prepared in argon-purged buffer and stored in a sealed vial prior to its being injected (14 μL) into the Q_3-DOPE solution so as to yield a 1:1 molar ratio of Q_3-DOPE:$Na_2S_2O_4$. The low concentration of $Na_2S_2O_4$ was required to prevent a large absorbance peak at 315 nm from the $Na_2S_2O_4$ that obscures all lower absorbance peaks.

3.2.3 Q_3-DOPE

Q_3-DOPE was prepared as previously described.[1] Q_3-DOPE liposomes, calcein-loaded Q_3-DOPE liposomes, and buffers were all prepared as described in Chapter 2. For fluorescence dye-dequenching studies, 40 mM calcein was encapsulated inside Q_3-DOPE liposomes, and the final liposome concentration was set to 0.1 mM based on UV-vis absorbance measurements using $\varepsilon_{265\ nm} = 5500\ cm^{-1}$ for the quinone headgroup. $Na_2S_2O_4$ solutions were always prepared using argon purged buffers, maintained under argon in septum-sealed vials, and used immediately upon preparation. A 1:1 molar ratio of $Na_2S_2O_4$:Q_3-DOPE was used to reduce the quinone headgroup and drive the lactonization reaction. A 0.1% (v/v) solution of Triton X-100 was used to lyse the liposomes and fully liberate any remaining encapsulated calcein; the observed fluorescence value was used as that for 100% liposome contents release. The values of % calcein release were calculated as described in Chapter 2.4

3.2.4 Q_3-DLiPE

Q_3-DLiPE (Q_3-capped 1,2-dilinoleoyl-*sn*-glycero-3-phosphoethanolamine, 18:2 PE, DLiPE) was prepared by Nichole Hollabaugh Carrier.[2] The same procedures for calcein encapsulation and fluorescence studies were followed as described for Q_3-DOPE.

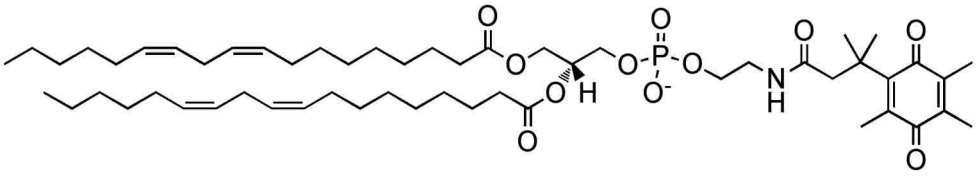

Figure 3.1. Redox-active, trimethyl-locked, quinone-capped 1,2-dilinoleoyl-*sn*-glycero-3-phosphoethanolamine (Q_3-DLiPE) with two *cis*-double bonds per hydrocarbon chain (18:2) PE.

3.3 Results

3.3.1 UV-Vis Observation of Q_3 Headgroup Reduction

In Figure 3.2 is shown a typical absorbance spectrum of Q_3-DOPE liposomes in pH 7.4 50 mM phosphate buffer with 75 mM KCl. The $\pi \rightarrow \pi^*$ peak of the quinone at λ = 265 nm can clearly be seen, providing a spectroscopic handle for which the concentration of Q_3-DOPE liposomes can be calculated. In Figure 3.3 is shown the reduction of the Q_3 headgroup upon introduction of one molar equivalent of $Na_2S_2O_4$ with each line representing successive one-minute scan of the process. $Na_2S_2O_4$ has an absorbance peak at 315 nm, thus requiring careful addition of the reducing agent so as to create interference with the near-by Q_3 absorbance peak. According to the absorbance measurements, the majority of the reduction of the Q_3 headgroup is complete within 15 min, however, this may not be an accurate measure of the actual reduction time, as the lactone has an absorbance peak around 280 nm that begins to appear within 2 min as the reduction proceeds. In order to properly observe the reduction of the Q_3 headgroup, a reducing agent that does not have an absorbance peak near the peak of interest or the product needs to be used. The lactone product near the peak for the Q_3 headgroup also provides an issue with properly observing the complete reduction and conversion between the two peaks.

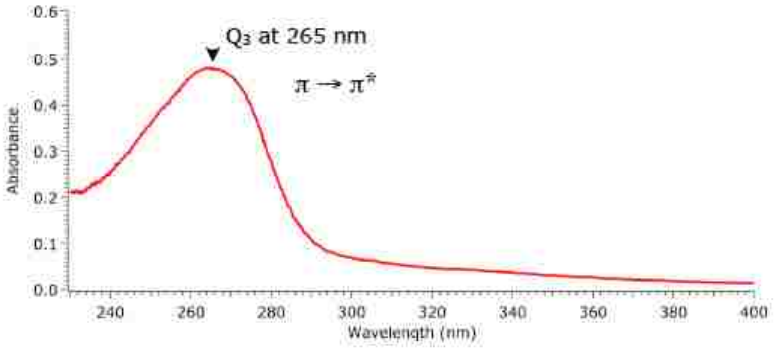

Figure 3.2. UV-vis absorbance of Q_3-DOPE liposomes in pH 7.4 50 mM phosphate buffer with 75 mM KCl at 25 °C showing λ_{max} = 265 nm.

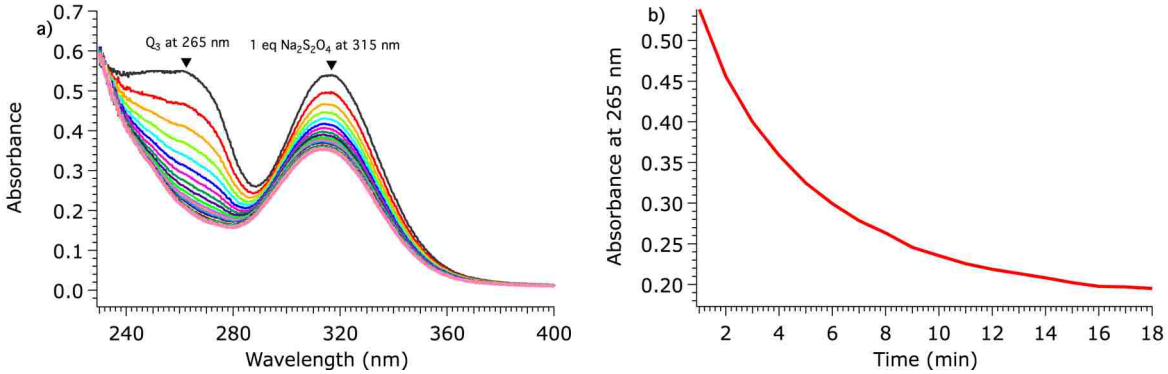

Figure 3.3. UV-vis absorbance traces for the reduction of Q_3-DOPE upon the introduction of 1 molar equivalent $Na_2S_2O_4$. In a) the absorbance contributions of both the Q_3 headgroup and the $Na_2S_2O_4$ are shown, with each trace obtained at one minute subsequent to the after introduction of the reducing agent while b) shows the decreasing absorbance values of the Q_3 headgroup as it is reduced as the lactone.

3.3.2 Calcein Release from Q_3-DOPE Upon Chemical Reduction

In Figure 3.4 is shown the stability over a period of 20 hrs of 0.1 mM Q_3-DOPE liposomes with 40 mM calcein encapsulated in pH 7.4 50 mM phosphate buffer with 75 mM KCl at 25 °C. The Q_3-DOPE liposomes are stable, as fluorescence emission of the calcein is essentially unchanged over long time periods, indicating that little to no leakage from the liposomes occurs. Addition of 0.1 % (v/v) Triton X-100 at 1223 minutes to lyse the liposomes and liberate the calcein into the bulk aqueous medium, resuls in a rapid increase in fluorescence emission. The percent calcein release was calculated as discussed in Chapter 2. The slow

decline in the calcein fluorescence intensity after the addition of Triton X-100 is presumed to be due to the presence of the surfactant itself, which causes slight quenching of the calcein fluorescence.[3]

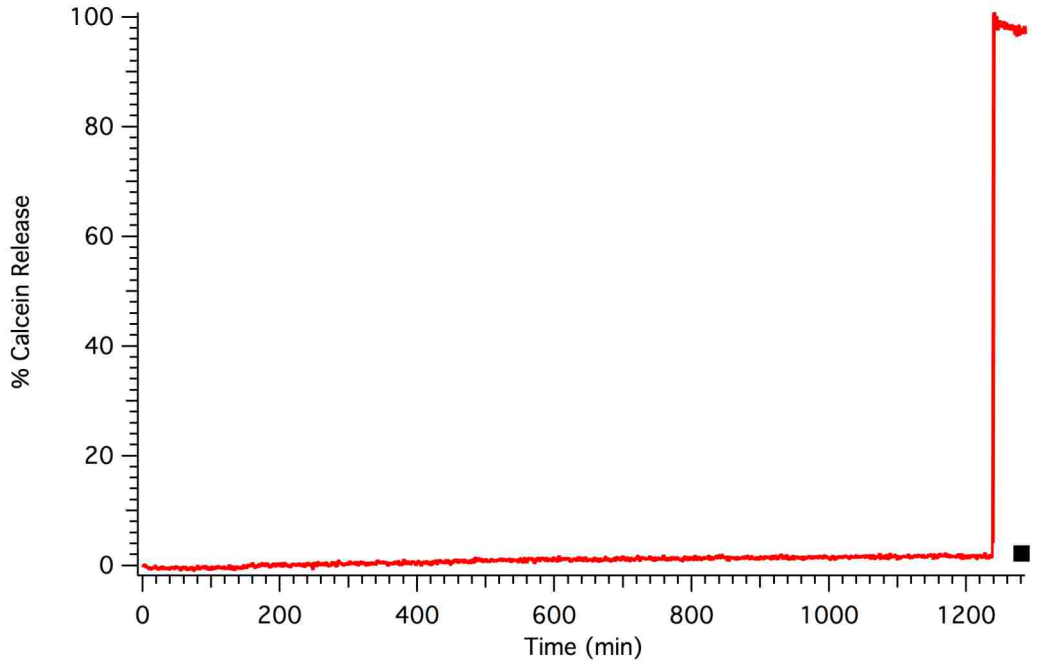

Figure 3.4. Stability of Q_3-DOPE liposomes with 40 mM calcein encapsulated. No leakage of the calcein was observed as noted by the lack of increase in fluorescence intensity with time. 0.1% (v/v) of Triton X-100 was added at 1223 minutes (■) to lyse the liposomes and liberate the calcein, accounting for the sudden increase in fluorescence intensity of the free and unquenched calcein.

Previous stability studies indicated that the Q_3-DOPE liposomes are stable for three days when stored on the bench open to the air and exposed to light. Storage under Ar, shielded from light, and at 4 °C extends the lifetime of the calcein-encapsulated liposomes to at least seven days.

Dynamic light scattering has yielded, on average, Q_3-DOPE liposomes with diameters between 100 and 120 nm and PDIs less than 0.1, indicating monodisperse samples. Zeta potentials have been measured to be – 55 mV in pH 7.4 50 mM phosphate buffer with 75 mM KCl at 25 °C.

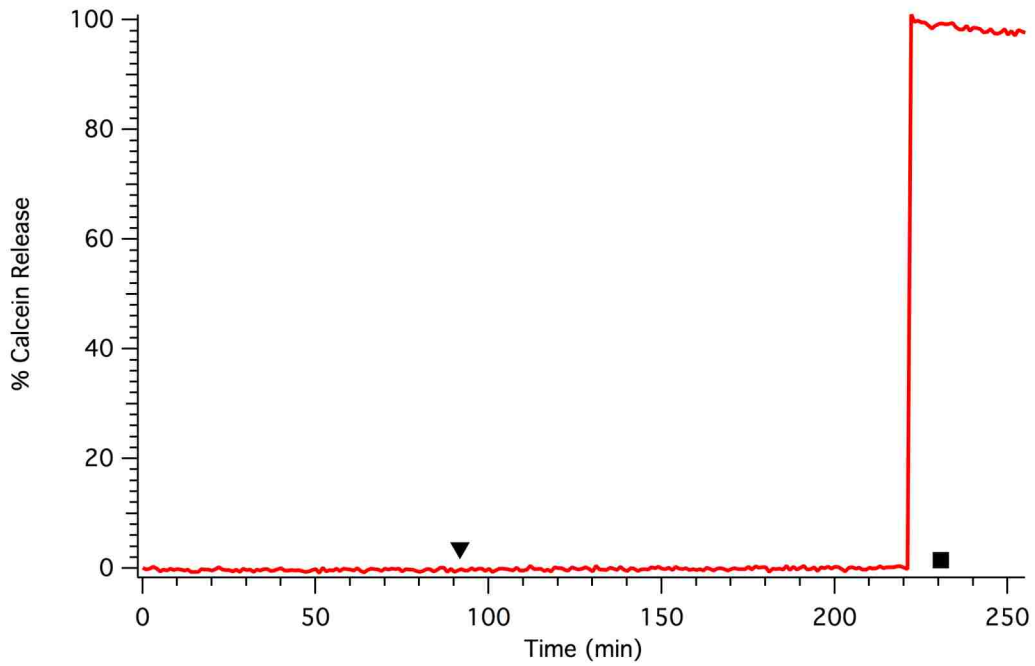

Figure 3.5. Demonstration that the addition of a non-redox active salt, $NaHSO_3$ at the addition of 1:1 molar ratio of $NaHSO_3$:Q_3-DOPE has no effect on the liposome stability, noted by the black triangle (▼). The Q_3-DOPE liposomes were lysed with an aliquot of 0.1 % (v/v) Triton X-100 at 271 minutes (■), dequenching the encapsulated calcein and causing a rapid increase in fluorescence intensity.

Figure 3.5 establishes that the addition of a 1:1 molar ratio (salt:Q_3-DOPE) of a non-redox active salt, the same ratio used in the addition of the chemical reducing agent $Na_2S_2O_4$, has no appreciable effect on the stability of Q_3-DOPE liposomes. Had an ionic shock event occurred, there would have been a change in the fluorescence emission intensity of the calcein caused by perturbation of the liposome bilayer after 92 min. The liposomes were lysed by an addition of 0.1 % (v/v) Triton X-100 at 271 min, completely releasing the encapsulated calcein from the liposomes.

A standard calcein release curve is shown in Figure 3.6 after introduction of $Na_2S_2O_4$. Several features can be observed in the release trace: a "lag" phase where the Q_3 headgroup is reduced and released from the DOPE during the first 18 minutes. Following the lag phase, the fluorescence intensity decreases in a contraction phase where it is believed that the liposomes are

contracting due to water transport as the bilayer settles into the L_α configuration that is free of the capping quinone headgroup.[4] The contraction phase reaches a minimum at 22 minutes where the liposomes begin to approach, aggregate, and then fuse so as to form H_{II} phase DOPE that results in the release and dequenching of the encapsulated calcein. At 47 minutes, 50% of the calcein is released followed by a final 94% release at 67 minutes.

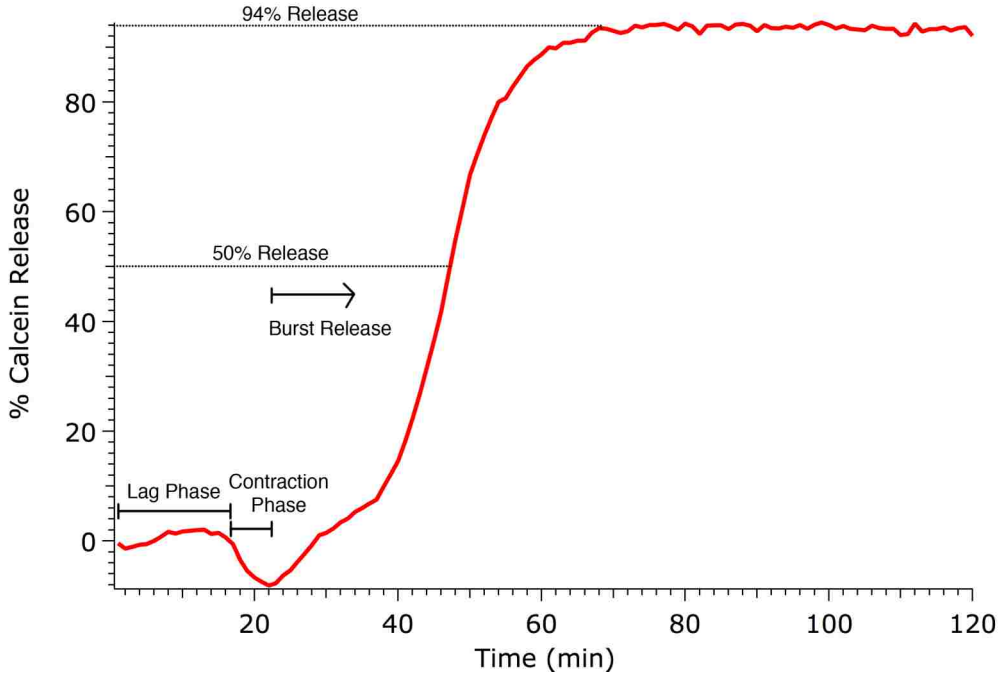

Figure 3.6. A standard calcein release curve from Q_3-DOPE in pH 7.4 50 mM phosphate buffer with 75 mM KCl at 25 °C. 40 mM calcein was encapsulated in the liposomes and released via addition of a 1:1 molar ratio of $Na_2S_2O_4$:Q_3-DOPE at $t = 0$.

3.3.3 Mass Action Kinetics

The rate of contents release from a liposome can be used to determine the type of leakage occurring in the system, such as if individual liposomes are leaking their contents or that the contents release depends on contact between liposomes. It is possible to study this by observing the kinetics of liposome aggregation or mass action kinetics.[5,6] Briefly, the initial steps of liposome contact and aggregation involve the close approach of two apposing liposomes that results in liposome aggregation. Next, the two liposome bilayers, if under favorable conditions,

will fuse and cause local bilayer destabilization that can further result in release of aqueous contents or mixing of the aqueous contents. The mass action model employed is represented by:

$$V_1 + V_1 \underset{D_{11}}{\overset{C_{11}}{\rightleftharpoons}} V_2 \xrightarrow{f_{11}} F_2 \qquad \textbf{Equation 3.1}$$

The approach and aggregation of two liposomes, V_1, is governed by the kinetic rate constant for dimerization, C_{11}. It is possible for the liposomes to dissociate, e.g. if close approach and dimerization are not energetically favorable, represented by the dissociation constant D_{11}. In the case of dissociation, contents leakage from aggregation will not occur; any absent contents would indicate release from individual liposomes that experience self-destabilization and leakage. If leakage does not depend on liposome contact and aggregation, then the contents release curves will be independent of liposome concentration:

$$V_1 \xrightarrow{l_1} F_1 \qquad \textbf{Equation 3.2}$$

Where V_1 is an isolated liposome experiencing a rate of contents leakage, l_1, as it converts to the leaky or open liposome F_1. In the case of individual liposomes leaking, then as the concentration of the liposomes is increased, there will be no observed change in the rate of release.

In Figure 3.7, it is observed that as Q_3-DOPE liposome concentration is decreased from 0.2 mM to 0.02 mM, the rate of contents release declines. This observation suggests that in order to release the internal aqueous contents, the DOPE liposomes must come into contact and aggregate after reduction of Q_3-DOPE liposomes and release of the capping quinone headgroup by lactonization. Even at low concentrations, the liposomes must come into close approach and aggregate in order for content release to occur and there is no to minimal lone leakage of individual liposomes. If individual liposomes were leaking, then increasing the concentration of liposomes would not change the rate of content release and each concentration of liposome would lie on the same line. The data in Figure 3.7 combined with the initial stability studies in

Figure 3.4 and results in Chapter 4 show that in order for content release from the Q_3-DOPE liposomes to occur, they must a) be reduced, b) release their quinone capping trimethyl-locked quinone headgroup as a lactone to reveal the DOPE lipids, and c) approach each other so as to allow for bilayer contact between DOPE liposomes.

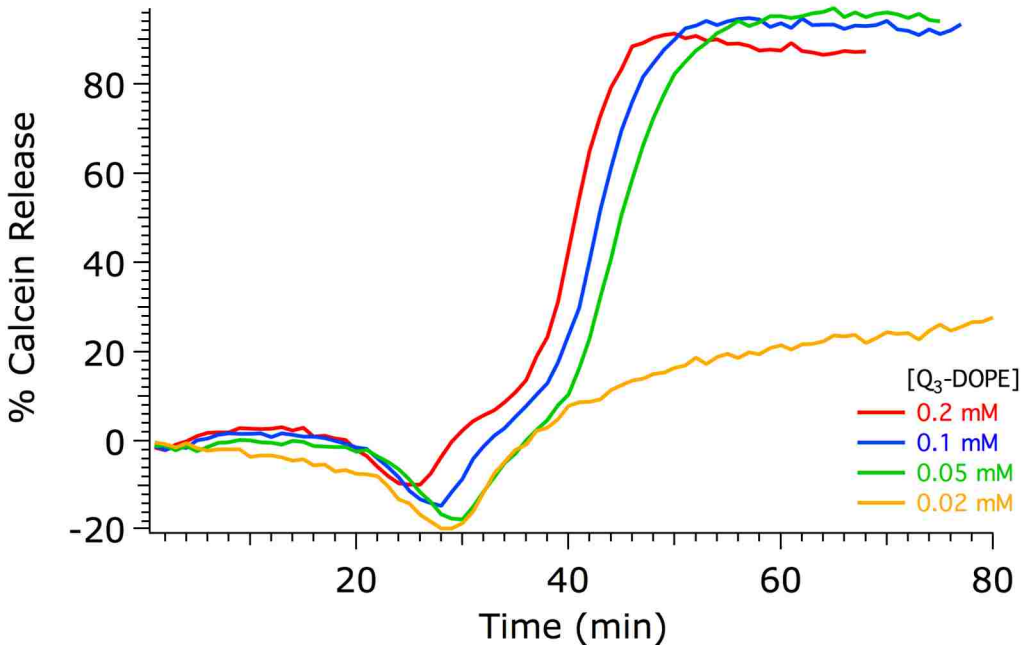

Figure 3.7. Fluorescence release traces for Q_3-DOPE liposomes as a function of liposome concentration. Increasing concentrations of Q_3-DOPE were used with the same buffer of 50 mM phosphate with 75 mM KCl, pH 7.5 and 25 °C. As the concentration of the liposomes was increased, so was the rate of fusion, suggesting that bilayer contact and liposome aggregation are required in order to release any encapsulated contents.

3.3.4 Variation of Buffer Components

The rationale for initially studying the effects of salt concentration calcein release rate was that the Q_3-DOPE system was originally studied in 0.1 M phosphate buffer with 0.1 M KCl.[1] The reason behind this was from observations from papers by Amsberry[7] and Milstien,[8] both of whom noted phosophate buffer catalysis of the lactionization of their simple trimethyl-lock systems. Thus, the initial hypothesis of this work was based on probing the effects of phosphate buffer concentration on the rate of calcein release for Q_3-DOPE liposomes. For this initial study,

two different sets of buffer were prepared: one phosphate based with KCl and one 2-[(2-hydroxy-1,1-bis(hydroxymethyl)ethyl)amino]ethanesulfonic acid (TES) based with KCl.

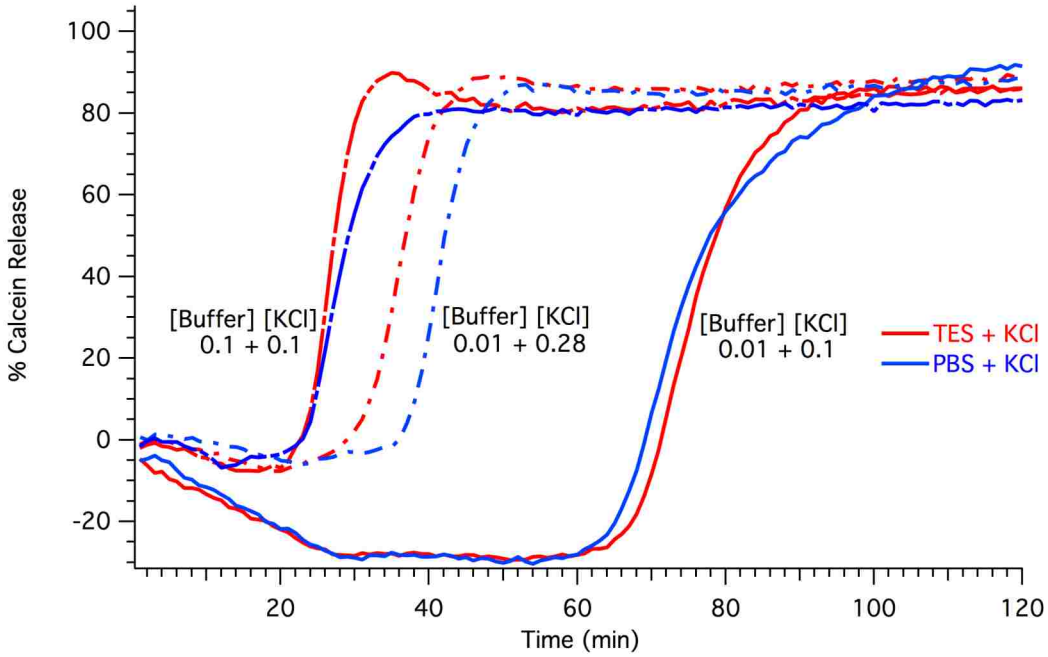

Figure 3.8. Comparison of release using two buffer systems; red traces represent TES buffer at 0.01 and 0.1 M concentrations and various KCl concentrations. Blue traces represent phosphate buffer at 0.01 and 0.1 M concentrations with various KCl concentrations. The greatest change in release rate is from the increase in salt concentration, from 0.1 M to 0.28 M with maintaining 0.01 M buffer. 0.1 mM Q_3-DOPE liposomes were used in each experiment.

The combined results are shown in Figure 3.8. Comparing the release rates of the phosphate buffer versus the TES buffer, there appears to be little difference in the times and rates for the two buffers. However, the more interesting observation from Figure 3.8 is that the concentration of salt has a significant influence on the rate of calcein release. As the buffer concentration is held constant at 0.01 M and the salt varied from 0.1 M to 0.28 M, the four parameters for the lag phase, the burst phase, the 50% release point, and completion of the calcein release times all decrease. Increasing the buffer concentration to 0.1 M serves to further decrease the time in which the calcein is released from the system. These observations pointed

to a relation between salt concentration and calcein content release rather than the concentration of the buffer having an influence on calcein release.

3.3.5 Variation of KCl Concentration

Differences in rates of Q_3-DOPE contents release due to the concentration of salt present were observed in the previous section as noted in the experiments with variations in KCl concentration. To further probe this effect, calcein release studies were undertaken wherein the phoshpahte buffer concentration was held at a constant 50 mM while the concentration of the salt was varied. 50 mM phosphate buffer was selected as a concentration between the two previous phosphate concentrations used in the previous section as it would be capable of providing ample buffering capacity. With a constant lipid concentration of 0.1 mM, the salt concentration was increased from 75 mM to 0.5 M, as shown in Figure 3.9.

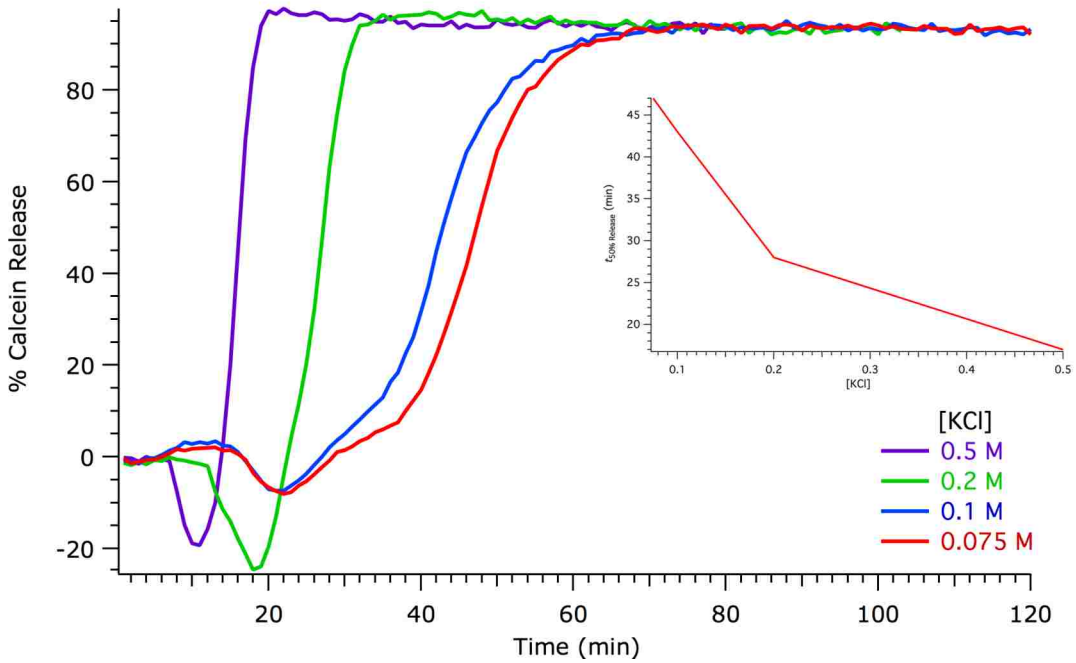

Figure 3.9. Calcein release curves for Q_3-DOPE liposomes as a function of KCl concentration. 50 mM phosphate buffer with increasing KCl concentrations, pH 7.5 and 25 °C. Q_3-DOPE liposome concentrations were maintained at 0.1 mM and a 1:1 $Na_2S_2O_4$:Q_3-DOPE injection was maintained for each salt concentration. Insert shows the $t_{50\%\ release}$ for each concentration of KCl.

Table 3.1. Summary of the four events: end of the lag phase, end of the contraction phase, 50% calcein release, and completion of release for increasing concentrations of KCl in Figure 3.9.

KCl (M)	Lag Phase End (min)	Contraction End (min)	50% Opening (min)	Max. Release (min)
0.5	6	11	16	20
0.2	12	18	27	35
0.1	15	21	43	68
0.075	16	21	47	68

As summarized in Table 3.1, increasing the salt concentration has a significant influence on calcein release kinetics. With a constant lipid concentration at 0.1 mM, there should be no difference in approach and fusion rates of the liposomes. Observations from UV-vis spectroscopy, as shown in Figure 3.10, allows one to conclude that the concentration of the salt has no significant influence on the reduction of the Q_3 headgroup. With increasing salt concentration, it is expected to decrease the T_H of DOPE and an observed increase in phase conversion from L_α to H_{II}.[9]

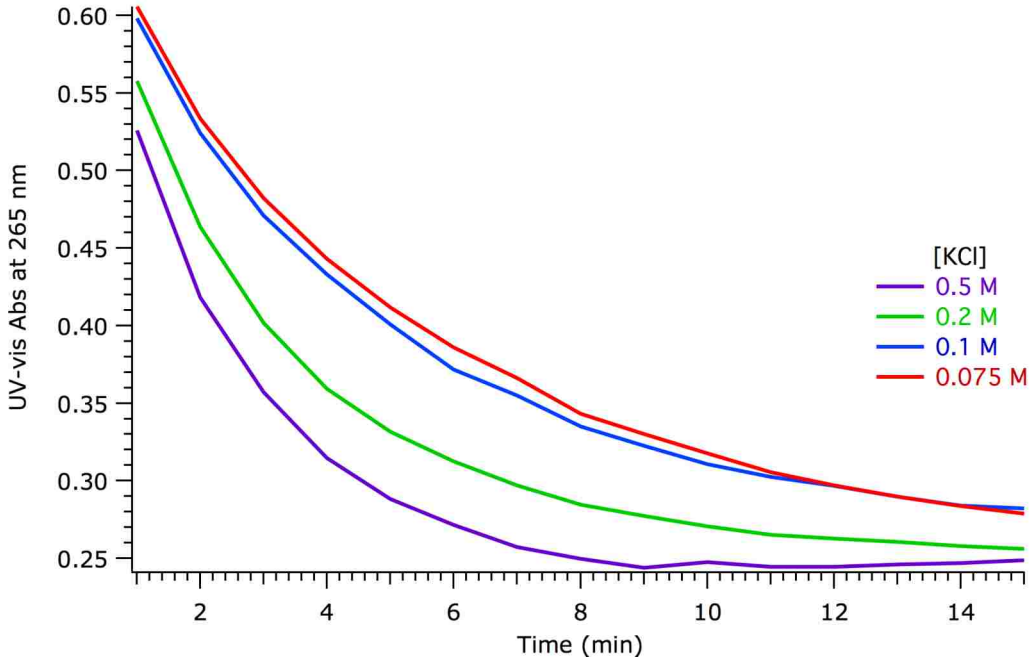

Figure 3.10. Absorbance traces at $\lambda_{265\ nm}$ for the reduction of the Q_3 headgroup in Q_3-DOPE liposomes as a function of KCl concentration. 0.1 mM Q_3-DOPE from the same preparations as in Figure 3.9 were used. pH 7.4 50 mM phosphate buffer with 75 mM KCl, 25 °C. Reduction performed by addition of 1:1 molar ratio of $Na_2S_2O_4$ in a argon-purged, septum-sealed quartz cuvette.

3.3.6 Variation of Salt Cation

Another concern that arose during the optimization process for the study of Q_3-DOPE was the composition of the buffer components. Previous experiments with Q_3-DOPE were performed with phosphate-buffered sodium salts and KCl.[1] Once the entire system was switched to K^+, the rates of calcein release were observed to have changed in appearance (data not shown). Two separate 50 mM phosphate buffers with 75 mM salt were prepared, each one containing only Na^+ or K^+ counter ions.

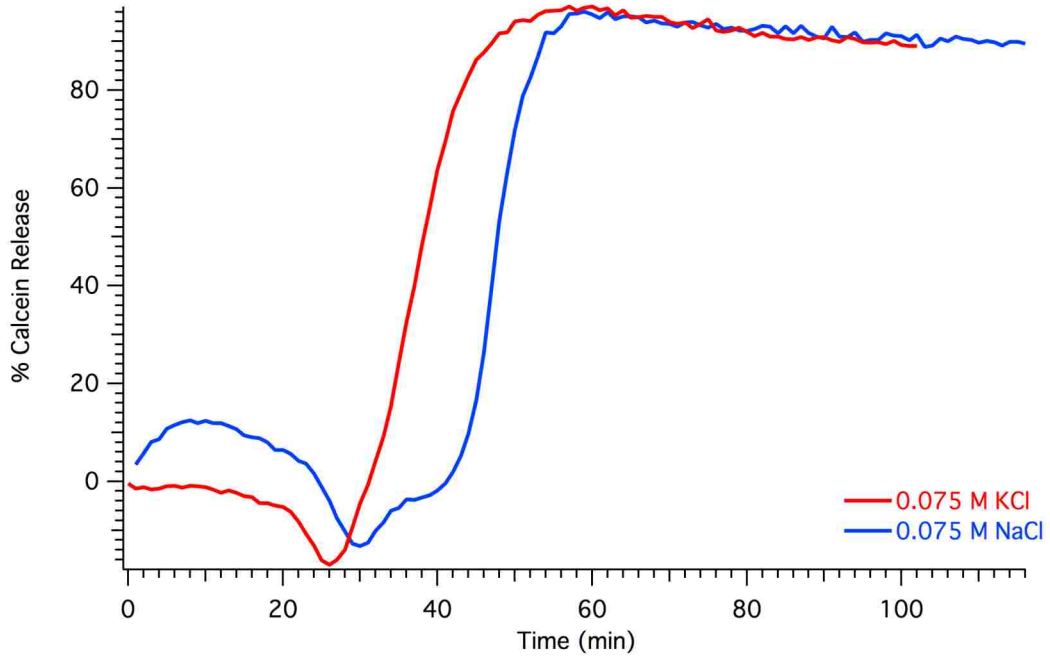

Figure 3.11. Calcein release curves for 0.1 mM Q_3-DOPE liposomesin two different salt solutions. The blue curve represents all phosphate components with Na^+ cations and 75 mM NaCl. The red curve represents all phosphate components K^+ cations and 75 mM KCl. Both buffers were at pH 7.4, and the experiments were performed at 25 °C.

Table 3.2. Comparison of Na^+ and K^+ salts on the rate of calcein release after reduction of Q_3-DOPE liposomes.

75 mM Cation	Lag Phase End (min)	Contraction End (min)	50% Opening (min)	Max. Release (min)
K^+	18	26	38	54
Na^+	23	30	48	58

In Figure 3.11 are shown the effects counter cations have on the rate of calcein release from Q_3-DOPE liposomes upon reduction. K^+ experiences both the end of the contraction phase at 26 min and 50% opening at 38 min sooner than compared to Na^+. Na^+ requires an additional 4 minutes before the contraction phase ends at 30 minutes and the content release enters the burst phase, releasing 50% of the liposomal contents at 48 min.

The difference between the Na^+ and K^+ buffers demonstrates that careful selection of the buffer components is required, as mixing Na^+ phosphate buffer with KCl will influence the rate of content release. The explanation for the observed differences between the two cations comes from Chapter 1, Section 1.3.4 where Hofmeister salts are discussed. While the emphasis of the section was on the anion series, cations have been demonstrated to have a weaker Hofmesiter effect on protein and lipid phases from kosmotropic cations and chaotropic cations. Hofmeister cations have an influence on the phase preference of PE lipids, although the effect not as strong as the anion series, it is worth taking note in the Q_3-DOPE system. According to the order presented in Chapter 1, Section 1.3.4:

$$NH_4^+ > K^+ > Na^+ > Li^+ > Mg^{2+} > Ca^{2+}$$

Where K^+ will have more kosmotropic character than Na^+, which serves to favor the H_{II} phase at the expense of the $L\alpha$, resulting in a faster rate of phase conversion of the DOPE lipids and a faster rate of calcein release from the liposomes. Other cations in the series were unavailable for study due to pH (NH_4^+), availability (Li^+, only Li_3PO_4 and LiH_2PO_4 are available) or being divalent (Mg^{2+}, Ca^{2+}) and disruptive to the $L\alpha$ DOPE liposomes. Divalent cations have been used to drive destabilization of PE by rapid aggregate formation aggregation and contents release, even at pH 9.5.[10,11]

Another possible impact centered on alkali metal cations can have on lipids is their interactions and possible binding with lipid bilayers.[12] Gurtovenko and Vattulainen observed

through force field simulations that in PC bilayers, Na^+ has the strongest interaction with the carbonyl region of the lipid, resulting in compression of the membrane bilayer.[12] K^+ was found to have a much weaker influence on the PC bilayers due to the size and the hypothesis that it experiences a very weak binding with the surface. In PE bilayers, it was found that there was less influence by the monovalent salts, with an observed weak binding of Na^+ and almost no binding for K^+. The lesser influence in PE bilayers was associated with the presence of the intramolecular hydrogen bonds between lipids that assist in preventing cation binding with the surface.

3.3.7 Temperature Studies

In addition to its relevance with regards to liposome opening in the human body at 37 °C, it was important to study how temperature affected the $L\alpha \rightarrow H_{II}$ transition. All previous calcein release traces were recorded at a constant value 25 °C during the course of the experiment. With reported values of T_H for DOPE phase transition from $L\alpha \rightarrow H_{II}$ ranging between – 4 °C and 16 °C, 25 °C was estimated to be a suitable starting temperature for the initial studies of content release behavior from Q_3-DOPE liposomes.

At 25 °C, the typical behavior of the Q_3-DOPE reduction and calcein dequenching is observed, achieving maximum contents release after 60 minutes. Increasing the temperature of the cuvette to 35 °C results in an increased rate of release of the calcein and fusion rates of the liposomes; maximum contents release was achieved in 31 minutes, significantly ahead of the 50% opening of the same liposome 25 °C. The increased rates of release are expected at higher temperature values for two reasons – Arrhenius behavior for the lactonization reaction and the temperature dependent $L\alpha \rightarrow H_{II}$ transition.[13] In an activated process, the rate of a reaction will increase with increased temperature. For the lactonization reaction, it has been shown or can be calculated, that the rate constant increases by approximately 7x for the 25 °C to 35 °C increase in

temperature. Thus, it is anticipated that the 10 °C increase from 25 °C to 35 °C would decrease the time for calcein release by 85%. Furthermore, it has been shown that the $L\alpha \rightarrow H_{II}$ transition rates follows $|T_{exp} - T_H|$;[13] the increased experimental temperature will impact the rate of the $L\alpha \rightarrow H_{II}$ phase transition. The further the experimental temperature is increased above T_H, the faster the phase conversion will occur.

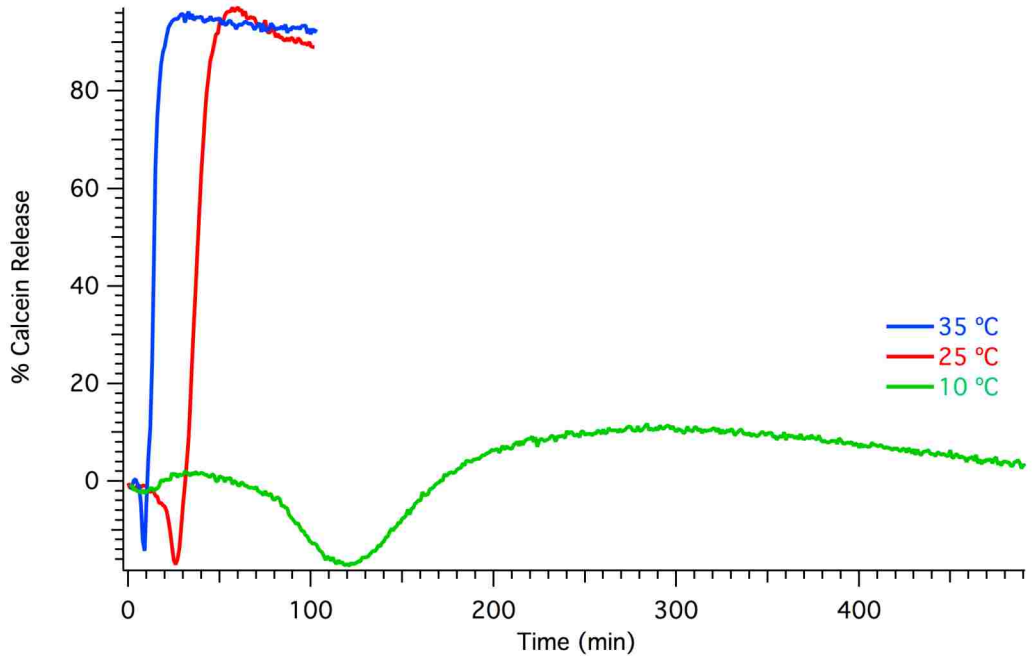

Figure 3.12. Temperature effect on calcein release rates from Q_3-DOPE liposomes. Conditions: 0.1 mM Q_3-DOPE in 50 mM phosphate buffer with 75 mM KCl, pH 7.4.

Table 3.3. Summary of temperature on the rate of release from Q_3-DOPE liposomes

Temperature	Lag Phase End (min)	Contraction End (min)	50% Opening (min)	Max. Release (min)
10 °C	60	120	Not observed	Not observed
25 °C	15	26	40	60
35 °C	7	9	12	31

Lowering the temperature to values approaching the T_H of the lipid serves to decrease the rate of lactonization and the $L\alpha \rightarrow H_{II}$ phase transition. The lower trace in Figure 3.12 at 10 °C demonstrates the slowing of the calcein release rates; at 10 °C the $L\alpha$ will be favored over the H_{II}

phase. Such slowing of the $L_\alpha \rightarrow H_{II}$ transition has been previously observed in temperature jump experiments, where lipids held very close to their T_H value experienced a very slow phase conversion that took up to several weeks to go to completion.[14]

At 10 °C, the lag phase takes 60 minutes before the release enters the contraction region. The contraction is over at 120 minutes and a very slow release of calcein begins to occur, reaching a maximum release of 12% at 272 minutes. As explained in Chapter 1, Figure 1.4, the pathway of liposome destabilization has changed, as T_{exp} is now on the order of T_H, placing the pathway on the right side of the figure. Q_3-DOPE liposomes will still aggregate at 10 °C; however, instead of a rapid collapse into the H_{II} phase through interlamellar intermediate formation, a much slower process of liposome fusion and contents mixing occurs with a slow release of encapsulated contents over long periods of time. Another interesting feature on the 10 °C release curve is that the lag and contraction phases are still present. The width of the contraction region has increased, supporting the hypothesis of slower lactonization rate due to the low experimental temperature.

3.3.8 Q_3-DLiPE

Initial directions of how the value of the T_H affects the rate of liposomal contents release was investigated with Q_3-DLiPE, as DLiPE has a reported T_H between −10 °C and − 16 °C.[15] The rationale was that the lower T_H value versus DOPE with a T_H of ~ 10 °C would result in an increase in the rate of contents release at 25 °C, similar to the observed increase in the rate of release with Q_3-DOPE at 35 °C versus 25 °C as in Figure 3.12.

In Figure 3.13 are shown the calcein release curves for Q_3-DLiPE and Q_3-DOPE liposomes at 25 °C upon reductive activation by a molar equivalent of $Na_2S_2O_4$. One major feature to note is the slower and less complete calcein release with Q_3-DLiPE liposomes versus that for Q_3-DOPE liposomes. Upon introduction of $Na_2S_2O_4$, both lipids experience a 21-minute

"lag" phase; however the conclusion of the contraction region and the onset of the burst phase for the DLiPE begins at 24 minutes. The contraction for DLiPE is smaller in magnitude at – 4% and the rate of release was observed to slow after 50 minutes. Q_3-DOPE experiences a larger contraction at –15%, reaching the minima of the process at 26 minutes, afterwards the burst phase of the release begins. 52 minutes are required to achieve 50% contents release for Q_3-DLiPE, whereas Q_3-DOPE liposomes release 50% of their contents in 36 minutes. After 50% release, Q_3-DLiPE never fully achieves the level of release observed for Q_3-DOPE liposomes (≥ 85%), even after an extended period of time of up to four hours (data not shown).

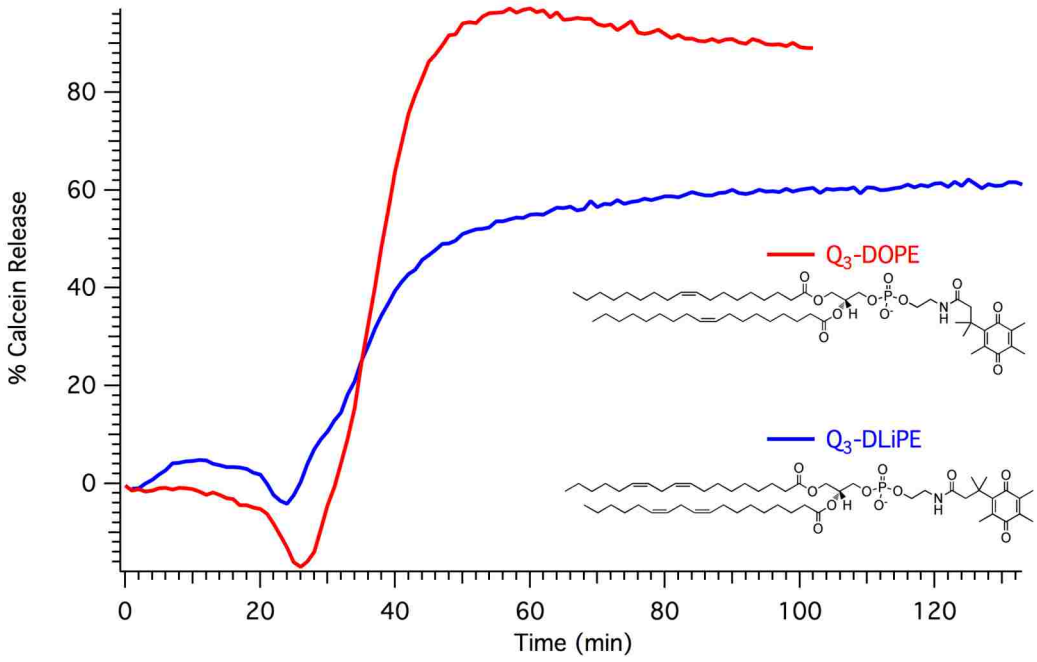

Figure 3.13. Comparison of release rates from 0.1 mM Q_3-DOPE and 0.01 mM Q_3-DLiPE liposomes in 50 mM phosphate buffer with 75 mM KCl, pH 7.4 at 25 °C.

The slower release rates observed in Q_3-DLiPE appear to result from a slower transition of the DLiPE lipids from the $L\alpha$ phase to the H_{II} phase. The rationale behind this is two-fold: one addresses the volume differences that acyl hydrocarbon chains have when they contain more than one double bond and the second addresses the crystal structure differences between the $L\alpha$ and the H_{II} phases. The presence of two double bonds in the acyl hydrocarbon chain will cause

the chains to occupy a larger volume, preventing the chains from packing as densely as in an acyl hydrocarbon chain containing a single double bond giving rise to a splaying of the acyl chains in the DLiPE lipid.[16] With the splaying of the acyl hydrocarbon chains, the rate of conversion from the L_α phase to the H_{II} phase is slowed due to the non-commensurate nature of the two phases.[14] The closer L_α and the H_{II} structures are to being commensurate, the faster the transition will occur, whereas deviations in the structures – such as increased swelling by hydration – will slow the rate of conversion between the phases. Similar behavior has been observed in lipids containing *cis*-(DOPE) and *trans*-(DEPE) isomers of a single double bond.[14] The L_α and H_{II} phase structures of DEPE are more commensurate, whereas DOPE is not as commensurate compared to DEPE, as it has small deviations in lattice structures in its L_α and H_{II} phases due to the kink introduced in the acyl hydrocarbon chain from the *cis*-isomer of the double bond. The difference in the conformation and occupied volume of acyl hydrocarbon chains in DOPE is enough to slow both the rate of transition and the degree of completion of the transition, as small shoulders of residual L_α phase DOPE lipids have been reported in X-Ray diffraction patterns in temperature jump experiments after the majority of the lipids have converted to H_{II}.[14]

3.3.9 Hofmester Anion Series

The noted differences between in calcein release from Q_3-DOPE liposomes with Na^+ and K^+ phosphate buffers led me to further study the effects of salt anions on the release rates. Initial studies were performed with the standard pH 7.4 50 mM phosphate buffer while the concentration of the various salts were at 75 mM, using KCl as the initial point to establish trends in rates of calcein release from the liposomes. Following the Hofmeister series with K^+ as the common cation, the following anions were studied, starting with the kosmotropes on the left and moving to the chaotropes on the right:

$$SO_4^{2-} > Cl^- > NO_3^- > ClO_4^- > SCN^-$$

In Figure 3.14 are shown the calcein release curves for the different Hofmeister salt anions at 75 mM. In general, the kosmotropes cause an increase in the rates of release, while the chaotropes cause a decrease in the rate of release. The differences in rates of release are, in general, expected to be due to the stabilization of the L_α phase at the expense of the H_{II} phase of DOPE in the case of the chaotropes, while the opposite is true for the kosmotropes.[9] Thus, this will lead to a faster rate of release in the presence of kosmotropic salts due to faster conversion of the DOPE lipids to the H_{II} phase, while the chaotropes will slow the rate of conversion to the H_{II} phase. However, due to the low salt concentrations at 75 mM, the expected order of the kosmotropes is not strictly followed, as SO_4^{2-} has the earliest times for the beginning of each point in the calcein release. Unexpectedly, NO_3^- leads to release curves with behavior very close to that for SO_4^{2-}, followed by Cl^-. Based on the Hofmeister series, the Cl^- should, in general, be more kosmotropic than NO_3^-; the difference in the 75 mM salts may be a function of the salt concentration not being sufficiently high to fully separate and sort the series into the proper order. Sanderson and Williams have observed decreased Hofmeister activity previously in their studies of POPE lipids, requiring at least 0.5 M salt for the effects to become observable.[9]

ClO_4^- and SCN^- both significantly slowed the rates of calcein release, requiring roughly 28 minutes to reach the end of the contraction phase before the occurrence of liposome fusion. The contraction regions of the chaotropic salts were vastly different from the regions of the kosmotropes, requiring a longer time to reach the inflection point and begin the burst phase of liposome fusion and rapid rates of release of calcein unloading. By the appearances of the calcein release traces, the rates for the two chaotropic ions were significantly slowed, the SCN^- to the point where it never achieved complete release, even after six hrs. It was not possible to study the effects of ClO_4^- at higher concentrations than 0.1 M due to limited solubility of $KClO_4$ in water at 25 °C.

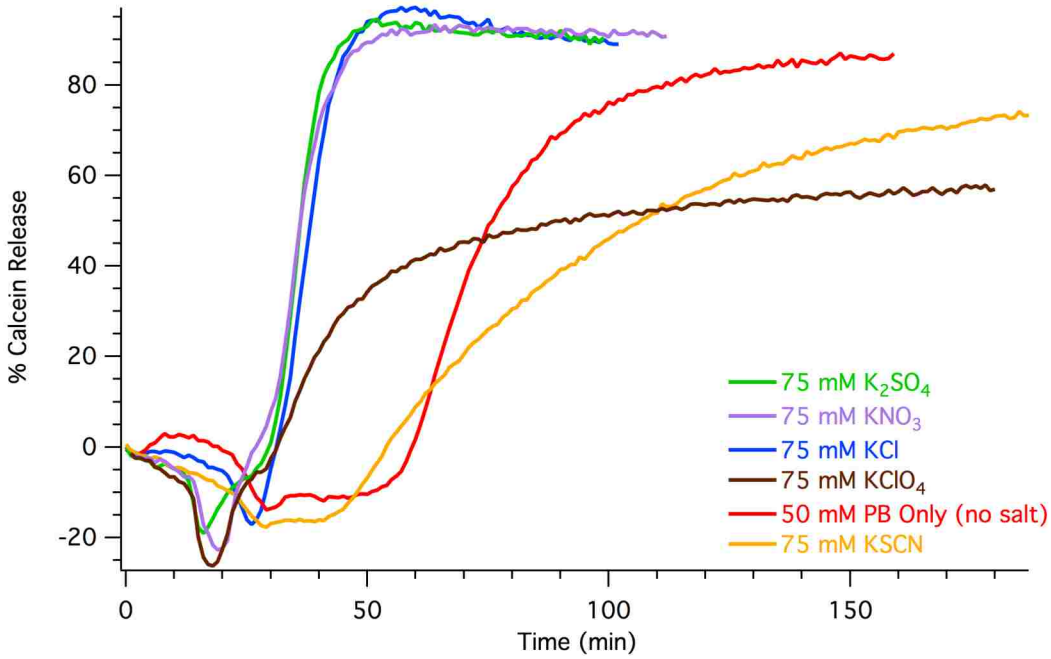

Figure 3.14. Calcein dequenching release curves from reduced Q_3-DOPE liposomes in response to the presence of the different K^+ Hofmeister salt anions. pH 7.4 50 mM phosphate buffer with 75 mM Hofmeister salt and 0.1 mM Q_3-DOPE liposomes, 25 °C.

Table 3.4. Summary of the time of release events after the reductive activation of Q_3-DOPE liposomes in response to the presence of 0.075 M Hofmeister salts.

Salt (75 mM)	Lag Phase End (min)	Contraction End (min)	50% Opening (min)	Max. Release (min)	Initial Rate of Release (min %C^{-1})
K_2SO_4	12	15	36	53	9.4
KNO_3	13	19	36	58	8.0
KCl	22	26	42	60	8.0
$KClO_4$	12	17	83	Not observed	1.8
KSCN	24	28	104	Not observed	1.1
No Salt	22	30	76	~ 142	3.3

The differences in rates of calcein release due to changing the values of T_H for DOPE from the presence of Hofmeister ions has, to the best of our knowledge, never been observed or reported before. All previous studies have been concerned solely with studying the effects of Hofmeister salts on the values of T_M and T_H for various PE lipids or the effects on the value of T_M for PC lipids with all of those studies utilizing DSC, X-Ray diffraction, or NMR to obtain the transition temperatures with the various salt anions of the Hofmeister series being present.

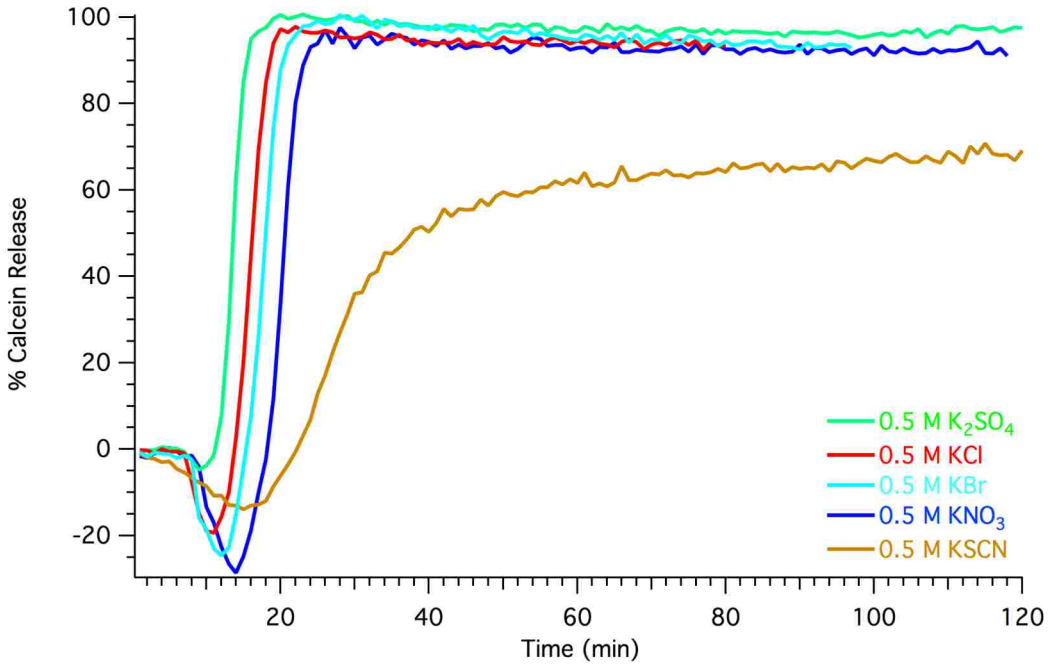

Figure 3.15. Calcein release curves from reduced Q_3-DOPE liposomes in response to the presence of 0.5 M Hofmeister salts. [Q_3-DOPE] = 0.1 mM in 50 mM phosphate buffer with 0.5 M Hofmeister salt at pH 7.4, 25 °C.

Table 3.5. Summary of the time of release events after the reductive activation of Q_3-DOPE liposomes in response to the presence of 0.5 M Hofmeister salts.

Salt (0.5 M)	Lag Phase End (min)	Contraction End (min)	50% Opening (min)	Max. Release (min)	Initial Rate of Release (min $\%C^{-1}$)
K_2SO_4	7	9	14	19	26.5
KCl	7	11	16	20	22.5
KBr	8	12	18	25	22.5
KNO_3	9	14	20	26	23.2
KSCN	10	15	37	Not observed	4.6

The impact of 0.5 M Hofmeister salts on the calcein release rate from the DOPE liposomes clearly demonstrates the kosmotropic and chaotropic nature of the salt used for Figure 3.15. 75 mM salt concentrations were enough to establish that there is indeed an effect on the rates of calcein release from the presence of Hofmeister salts. However, with certain salt anions that have small differences in their effects, such as the Cl^- and NO_3^-, higher concentrations are required for the Hofmeister effects to be clearly defined in the lipid behaviors. In Figure 3.15 are shown calcein release curves for the 0.5 M Hofmeister salt series. Further increases in salt

concentrations will serve to further increase or decrease the rates of release. However, higher salt concentrations, as in the case of Cl^- can have effects such as suppressing the T_M,[17] which can result in unknown changes to the behavior of the Q_3-DOPE lipids upon reductive activation.

Comparing the calcein release behavior for Cl^-, Br^-, and NO_3^-, it is clear they all fall within the suggested Hofmeister series, showing increasing chaotropic character as the salts move to the right of the series. The contraction region of each salt also increases as expected with the hypothesis of hydration levels surrounding the headgroups. As the ions become less hydrated, more water will be available to interact with the headgroups, which in turn results in more water to be removed before the close approach and fusion of apposing liposomes can occur. As the salts become more chaotropic, they will begin to favor the $L\alpha$ phase at the expense of the H_{II} phase. This can be estimated with the values of T_H for DOPE, as with more chaotropic ions, the T_H is expected to increase, pushing it closer to the experimental temperature of 25 °C, which results in a slowing of the phase transition. With increasing chaotropic behavior, the chance of interacting with the bilayer surface also increases, due to smaller energetic penalties for the ions to shed their hydration shells. There have been no reports of any of these three ions interacting with bilayer surfaces, but a closer approach is possible when compared to the SO_4^{2-} due to size considerations alone.

SCN^- is the most chaotropic ion studied in the 0.5 M Hofmeister anion series. As expected, there is a significant change not only in the contraction region but also in the calcein release rate, as well as the observation that the system never achieves complete release even after 6 hrs. The stabilization of the $L\alpha$ phase is reflected in this slow release, as the H_{II} is no longer as favored for formation. Additionally, the hydration of the SCN^- is low and the energetic penalties for shedding its hydration layer are also low.[19] There are several studies that provide evidence for the approach and interaction of SCN^- with the lipid bilayers. There is no evidence for this in

the calcein release experiments, but it is plausible that the SCN^- is able to interact with the DOPE bilayer in such a way as to insert itself between the headgroups, providing some hydrogen bonding interaction with the amine headgroups, which will provide a small increase in the effective area of each headgroup. This small increase in headgroup area may be enough to provide some stabilization for the $L\alpha$ phase, accounting for the slow rates of calcein release from the liposomes.

3.3.10 DSC of DOPE with Hofmeister Salts

The hypothesis regarding the effects of salts on calcein release rate for Q_3-DOPE liposomes required additional studies to provide evidence that the rate changes were a result of changes in the T_H of DOPE lipids. Changes in the T_H, as previously observed in the temperature studies, tend to affect the rates of phase conversion in DOPE lipids.[14] Additionally, it must be taken into consideration that the presence of the Hofmeister salts may affect the rate of $L\alpha \rightarrow H_{II}$ phase conversion because of differences in their impact on lipid hydration.

By symmetry arguments, the $L\alpha \rightarrow H_{II}$ transition in DOPE lipids is expected to be first order.[13] The value of T_H, therefore, is expected to be well-defined when measured under constant pressure. This, however, is not the case in reported literature T_H values for DOPE, ranging from – 4 to 16 °C. In Table 3.6 are summarized the reported T_H values and the instrumental technique, and the solvent used to determine the T_H. The large range of reported T_H values is a result of the kinetically hindered nature of the phase transition, as the conversion is influenced by rate-limiting processes such as nucleation, intermediate formation, domain growth, or hindrance in bulk water transport.[13] For example with DSC, even slow temperature scan rates will contribute to variability in T_H. In addition, fast scan rates of over 100 °C hr^{-1} will cause a shift in the T_H to artificially higher values.[20]

Table 3.6. Summary of reported literature values for the T_H of DOPE with the solvent type and the instrumental method used to determine the value.

Reference	Solvent/Buffer	Method	T_H (°C)
Epand, 1985[20]	20 mM PIPES + 150 mM NaCl	DSC ($\Delta T/\Delta t$ = 44 °C hr^{-1})	14
		DSC (11 °C hr^{-1})	8
Wistrom, 1989[21]	water	DSC (20 °C hr^{-1})	8
Sanderson, 1993[15]	water	DSC (± 300 °C hr^{-1})	– 4 to 16
Kirk, 1985[22]	water	XRD	7.5
Gruner, 1988[23]	water	XRD	7.5
Toombes, 2002[13]	water	XRD	3.3
Fenske, 1992	water	NMR	11.5
Gawrisch, 1992[24]	D_2O	NMR	– 1.5 to 6
Osman, 1994[25]	water	^{31}P NMR	0.5 to 6.5

In order to determine an appropriate scan rate for the DSC experiments on hydrated DOPE bilayers, two different scan rates were used, as shown in Figure 3.16. The scan rates were chosen based on previous work by Epand.[20] DOPE was hydrated and prepared according to the procedures outlined in Chapter 2, Section 2.6. The slower scan rate of 15 °C hr^{-1} was thought to yield a result that is closer to the true T_H for the DOPE in the buffer system used; however, the two peaks in the DSC may be from a slow conversion between the L_α and the H_{II} phase. The higher temperature shoulder is still present, but not as pronounced, when the scan rate was increased to 40 °C hr^{-1}. It was decided that the T_H value obtained at a scan rate of 40 °C hr^{-1} would be suitable for further study of the effects of Hofmeister salts on the T_H of DOPE. The results of the two scan rates are summarized in Figure 3.16 and Table 3.7.

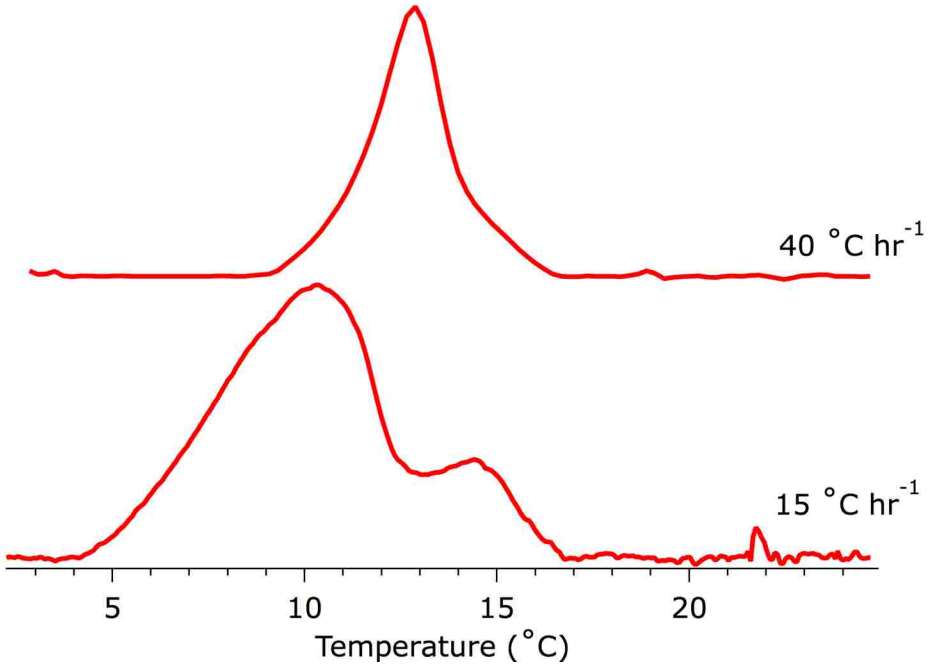

Figure 3.16. Differential scanning calorimetry traces of 14 mg mL^{-1} DOPE in pH 7.4 50 mM phosphate buffer with 75 mM KCl, pH 7.4. Upper trace, scan rate 40 °C hr^{-1}, lower trace, 15 40 °C hr^{-1}.

Table 3.7. Summary of the effect of scan rate on the value of T_H for DOPE in 50 mM phosphate buffer with 75 mM KCl, pH 7.4.

Scan Rate (°C Hr^{-1})	T_H (°C)
15	10.3/14.4
40	12.8

In Figure 3.17 is shown how the T_H of DOPE is influenced by the addition of increasing concentrations of KCl. To begin, a reference T_H value for DOPE was established using 50 mM phosphate buffer only (no added salt), yielding a T_H of 13.1 °C. The value of T_H begins to decrease with increasing salt concentrations. As with previous studies into the effects of Hofmeister salts and the values of T_H, this result was not unexpected, as with other PE lipids, changes in the values of T_H have been reported to increase or decrease at low salt concentrations depending on the Hofmeister character of the salt.[17] The response of the T_H of DOPE to KCl also demonstrates that Cl^-, in the case of DOPE, is not the center of the Hofmeister series as it does have some kosmotropic behavior. The center point is likely to be between Br^- and I^-, as

suggested by Koynova and Tenchov.[17] In Figure 3.18 is shown a similar trend of decreased T_H with increased concentrations of salt, in this case K_2SO_4.

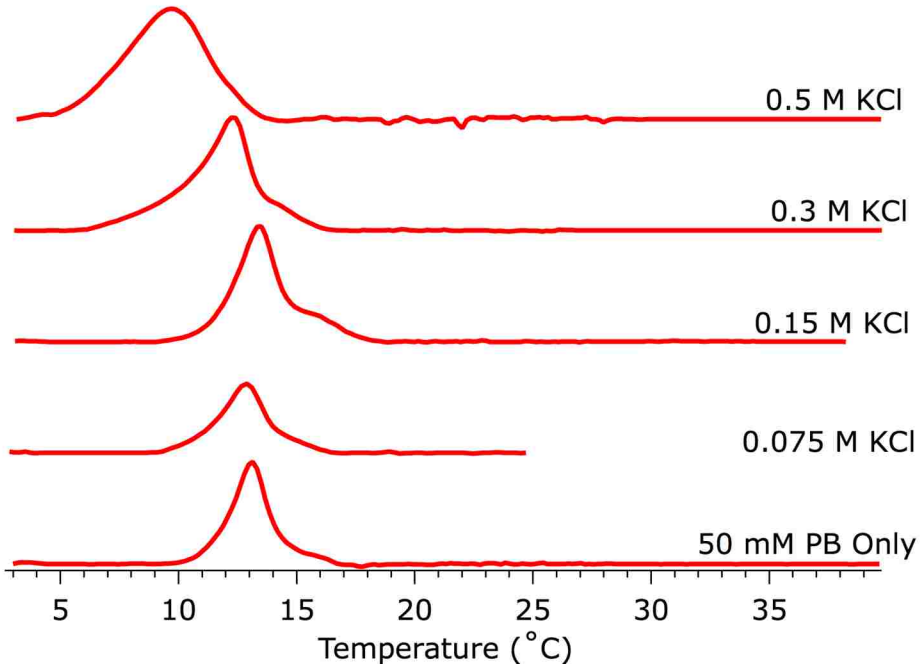

Figure 3.17. Differential scanning calorimetry traces of 14 mg mL^{-1} DOPE in pH 7.4 50 mM phosphate buffer with increasing KCl concentration. Scan rates of 40 °C hr^{-1} were used for all traces.

Table 3.8. Summary of KCl concentration on the value of T_H of DOPE.

Salt Type (M)	T_H (°C)
KCl (0.5)	9.8
KCl (0.3)	12.2
KCl (0.15)	13.4
KCl (0.075)	12.8
PB Only (No Salt)	13.1

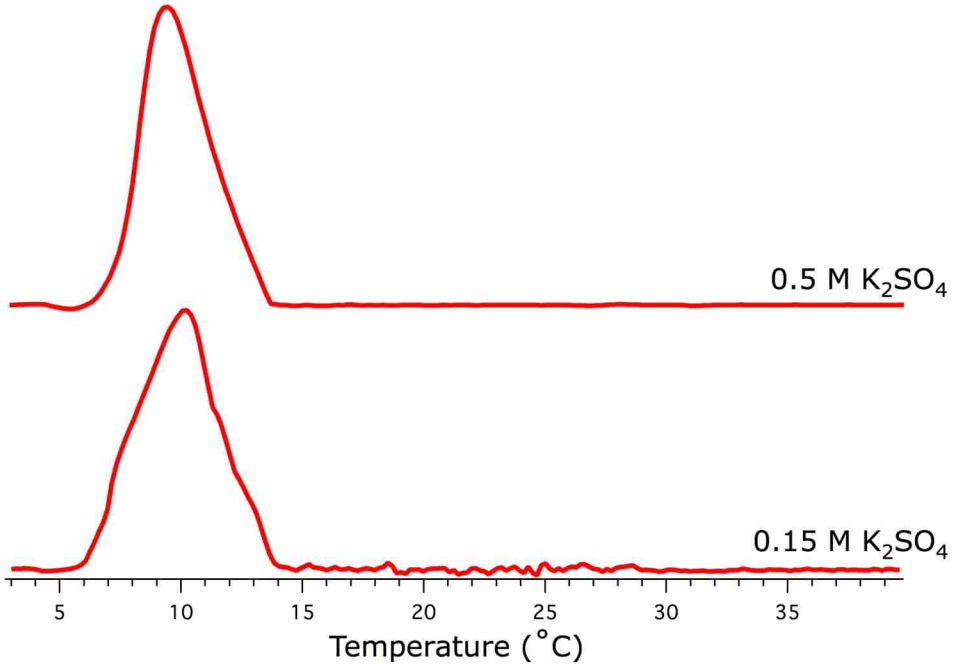

Figure 3.18. Differential scanning calorimetry traces of 14 mg mL^{-1} DOPE in pH 7.4 50 mM phosphate buffer with (upper curve) 0.5 M K_2SO_4 and (lower curve) 0.15 M K_2SO_4. Scan rates of 40 °C hr^{-1} were used for all experiments.

Table 3.9. Summary of the concentration effects from K_2SO_4 on the value of T_H for DOPE.

K_2SO_4 (M)	T_H (°C)
0.15	10.2
0.5	9.4

The T_H of DOPE is clearly affected by the type of Hofmeister salt anion present as noted in the DSC traces for a variety of potassium salts in Figure 3.19. As anticipated, based on previous T_H salt studies of other PE lipids and from the fluorescence studies on calcein release rates in this dissertation, at 0.5 M concentrations, the values of the T_H for DOPE trend with the nature of the Hofmeister salt used. For kosmotropes, the T_H is lower than the value of 13.1 °C recorded in 50 mM phosphate buffer only. With more chaotropic salts, the T_H is increased, as shown for KNO_3 and KSCN. The observed T_H for the most chaotropic ion, SCN^-, was a surprising 36.7 °C, which supports the slow calcein release rate from the reduced Q_3-DOPE liposomes in Figure 3.15 and Table 3.5.

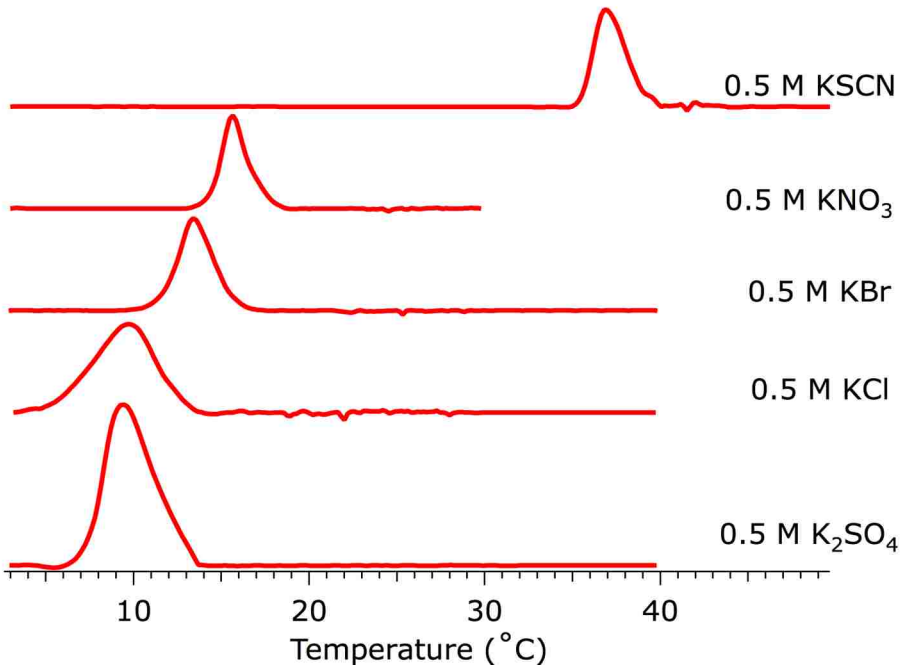

Figure 3.19. Differential scanning calorimetry traces of 14 mg mL^{-1}. DOPE in pH 7.4 50 mM phosphate buffer with 0.5 M Hofmeister salts. Scan rates of 40 °C hr^{-1} were used for all experiments.

Table 3.10. Summary of T_H values for DOPE in response to a 0.5 M Hofmeister salt series. The kosmotropic anions lowers T_H while chaotropic anions increase T_H.

Salt Type (0.5 M)	**T_H (°C)**
K_2SO_4	8.8
KCl	9.8
KBr	13.3
KNO_3	15.6
KSCN	36.7
PB Only (No Salt)	13.1

From the DSC measurements on the T_H of DOPE in various Hofmeister salts, it can be clearly seen that the type of salt present has an effect on the value of the phase transition. As expected, kosmotropic salts will decrease the T_H by favoring the H_{II} over the $L\alpha$ phase while chaotropic salts increase the T_H by favoring the $L\alpha$ over the H_{II}.

3.4 Discussion

3.4.1 Q_3-DOPE Reduction, Contents Release, and Phase Transition Behavior

The presence of the quinone trimethyl lock capping headgroup serves to increase the cross-sectional area of the DOPE lipid headgroup and increases the level of hydration surrounding the headgroup, resulting in lipid phase behavior that favors the $L\alpha$ phase at the expense of the H_{II} phase. This is evident by cryo-TEM images of lamellar vesicles of Q_3-DOPE[1] and the stability of Q_3-DOPE liposomes from Figures 3.4 and 3.5. Similar observations have been made with single methylated DOPE (DOPE-Me), in that the single methyl substitution on the amine headgroup is sufficient enough to change not only the lipid cross-sectional area[26] but also the hydration level of the headgroup; the latter has been measured to be on the order of 24 water molecules, similar to DOPC hydration levels.[27] DOPE has a hydration level of the headgroup of 7-9 waters in the H_{II} phase[28] and 14 waters in the $L\alpha$ phase.[29] The increased headgroup size and hydration of Q_3-DOPE serves to favor the $L\alpha$ phase.

Upon reduction, the cross-sectional area of the headgroup will rapidly change due to the cleavage of the lactone to yield DOPE. As a result, the hydration level of the lipid will change. Loss of the quinone and movement of water out of the headgroup region both result in decreased lipid size and thus packing, this is expected to cause a contraction in the liposome diameter that occurs as the DOPE lipid establishes an $L\alpha$ phase. During this process, intramolecular hydrogen bonding between the amine headgroups must be established and will cause additional rearrangement of the lipids within the bilayer. With the concentration of calcein at 40 mM, where it is not fully quenched, the change in liposome diameter can be observed as a decrease in the fluorescence emission of the calcein. Control experiments with Q_x-DOPE lipids whose capping quinone groups do not readily lactonize do not exhibit such a phenomenon upon reduction by $Na_2S_2O_4$, see Chapter 4. Dynamic light scattering measurements were carried out

(data not shown) in an attempt to observe this possible contraction of the liposomes; small changes in the hydrodynamic diameter of the liposomes were noted, but the instrumentation is such that it may not be sensitive to the changes in liposome diameter. This is most likely the result of the commercial DLS instrument recording a bulk average of liposome diameters, rendering it blind to the initial contraction of the liposomes, as the methods the instrument employs are biased toward larger liposomes.

3.4.2 Hofmeister Salt Effects on Kinetics of Contents Release from Liposomes

There are two main contributions for the observed differences in the rates of content release from DOPE liposomes while in the presence of a Hofmeister salt series: 1) *driving force* (thermodynamic), where the change in the energy between phase states is a result of changes in the T_H with regards to the experimental temperature, T_{exp} and 2) *kinetic behavior*, where alterations of the energy barrier between the two phases changes is the result of lipid structural changes. Both of these lead to changes in the rate of $L\alpha \rightarrow H_{II}$ transition.

In general for driving force arguments, the observed changes in T_H and rates of release in the presence of Hofmeister salts are based on the stabilization or destabilization of a lipid phase as a result of salt presence. With kosmotropics anion, the H_{II} phase will be favored over the $L\alpha$ due to destabilization in the $L\alpha$, which results in a decrease in the T_H of DOPE. Alternatively, in the presence of a chaotropic anion, the $L\alpha$ phase will be favored over the H_{II}, leading to an increase in the T_H. Thus, the main driving force for the phase transition is based on ΔT between the fixed experimental temperature, T_{exp}, and the variable $L\alpha \rightarrow H_{II}$ transition temperature, T_H. The relationship between driving force and release rate was observed when then value of T_{exp} was increased from 25 °C to 35 °C, Figure 3.12. As expected, increasing ΔT to larger values provides a higher driving force for the phase transition that results in a faster rate of contents release. The opposite occurs as ΔT is decreased, as in the case of T_{exp} of 10 °C, which has a

lower driving force and a slower rate of content release; however, at 10 °C, there is also most likely a change in the mechanism from fusion and contents release to fusion with contents mixing and contents release, vide infra. The same driving force influence (ΔT) is evident in the rate of contents release with the 0.5 M Hofmeister salt series and can be attributed to different T_H values as demonstrated by the DSC experiments, Figure 3.17. The presence of a kosmotropic salt will decrease the T_H for DOPE, which will result in an increased ΔT and a faster transition while a chaotopic salt will increase the T_H for DOPE, lowering the ΔT and causing a slower transition.

However, if $T_{exp} \leq T_H$, the nature of the liposome contents release is different than when $T_{exp} > T_H$. When T_{exp} is T_H or below, the mechanism of liposome destabilization will be significantly different than when $T_{exp} > T_H$, as described in Figure 1.4 from Chapter 1. When T_{exp} is above T_H, intermediate structures as a result of lipid mixing that leads to high stress in the bilayer, thereby leading to contents release without contents mixing. Lowering the temperature below T_H causes the liposome destabilization process to slow and requires contents mixing to occur before the liposome aggregate structures form a critical density and eventually collapse, thereby releasing their contents. Considering that the $L\alpha \rightarrow H_{II}$ phase transition is not in equilibrium during the conversion process, it is possible to have a coexistence of two phases at temperatures below T_H and it might be possible to observe some contents mixing between fusing liposomes.[14,30] Due to the concerns regarding the traditional contents mixing assays being sensitive to reducing agents, these experiments were not performed.

How can the presence of Hofmeister salts provide stabilization or destabilization of either $L\alpha$ or H_{II} phase? That is, how is the T_H influenced by the presence of the salts? The hypothesis posed here is the amount of water available to the PE lipid headgroup dictates its T_H, and that available water content is controlled by the nature of the ions in solution. Kosmotropic ions bind

water tightly, providing high solvation entropy, while chaotropic ions are less hydrated and provide low hydration entropy;[19] thus, the amount of water available to a PE lipid will be determined by the nature of the ions present and their concentration, in a manner similar to that for lipids in the presence of poly(ethylene glycol).

The free energy of a PE lipid in a given phase state, L_α or H_{II} , is significantly influenced by the amount of water available to the lipid.[31] From the study by Kirk *et al.*, it is known that at low water concentrations for PE lipids, such as DOPE, the H_{II} phase is energetically favored while at higher water concentrations, the L_α is preferred. This is demonstrated by the water-content-dependent T_H values observed in didodecylphatidylethanolamine (DDPE) in a study by Seddon *et al.*; they demonstrated that the T_H value was extremely sensitive to the number of water molecules per lipid molecule, with the T_H changing roughly 7 °C for every water molecule added or removed per lipid molecule (40 °C decrease in T_H when moving from 9 waters to 3 waters)![32] Thus, removal of lipid interfacial water by kosmotropic ions will cause a decrease in T_H while chaotropic ions that are not highly solvated will yield higher T_H values.

I now turn to the second contribution to the observed differences in rate of contents release from the liposomes in the presence of different salt ions, namely energy barrier effects. It is posited here that the presence of the different Hofmeister anions causes changes in the DOPE intermediate structures in the $L\alpha \rightarrow H_{II}$ transition such that the activation barrier is either raised or lowered. This hypothesis is supported by literature reports concerning the structural rearrangements that occur during the $L\alpha \rightarrow H_{II}$ transition in PE systems, and X-ray data on the *d*-spacings of PE lipids in their lamellar liquid crystal (L_α) and inverted micelle (H_{II}) states in the presence of Hofmeister salts.

It has been proposed by Gruner that the $L_\alpha \rightarrow H_{II}$ phase transition of PE lipids occurs by a commensurate mechanism wherein the H_{II} phase forms with the PE lipids adopting an

interlipid spacing that is identical to that of the precursor L_α phase, followed by H_{II} lattice "correction" to the equilibrium state as the result of water transport into and out of the water tubes of the H_{II} phase.[14] Thus, he proposed that there are two kinetic barriers to the $L_\alpha \rightarrow H_{II}$ phase transition, namely the high energetic cost of exposing the lipid hydrocarbon chains to the aqueous milieu as the interface undergoes the conversion, and that for the rearrangement of the lipids and lattice transport of water so as to achieve equilibrium crystallographic scenario of the H_{II} phase. Gruner and coworkers supported this hypothesis by their observations that DOPE, with a larger mismatch in the equilibrium lattice parameters between the L_α and H_{II} phases, exhibits a much slower $L_\alpha \rightarrow H_{II}$ phase transition than does 1,2-dielaidoyl-*sn*-glycero-3-phosphoethanolamine (DEPE), a 18:1 *trans*-PE lipid possessing a more commensurate L_α and H_{II} lattice parameter.[14] I first address the kinetic barrier associated with the rearrangement of lipids and transport of water so as to achieve the equilibrium H_{II} phase structure.

Based on work by Sanderson[9] and that of Gruner,[14] I hypothesize that as the lattice spacing (*d*-spacing) of the two phases become more or less equal with added Hofmeister salts, the kinetic barrier is altered for the process of PE lipid rearrangement so as to achieve the equilibrium crystallographic scenario of the H_{II} phase. Sanderson *et al*. have shown that the X-ray parameters of POPE lipids in the L_α and H_{II} phase states are sensitive to the presence and concentration of Hofmeister anions.[9] In that work, the effects of NaCl and NaI on the *d*-spacing of POPE phases in aqueous media were briefly mentioned, but their work did not focus on the possible relationship between the kinetics of the $L_\alpha \rightarrow H_{II}$ phase transition and the *d*-spacing of the two phases. Increasing the concentration of NaCl in aqueous media containing POPE lipids caused the lattice *d*-spacing of the H_{II} phase to decrease somewhat (~6 nm to 5.6 nm for [NaCl] change of 0 to 5 M) and that of the L_α phase to increased (~5.2 nm to 6 nm). Near 3 M NaCl, the lattice spacing was found to be virtually identical for the two phases. Thus, based on

Sanderson's work and that of Gruner concerning the commensurate $L_\alpha \rightarrow H_{II}$ phase transition mechanism, I hypothesize that as the lattice spacing of the two phases become more equal, the kinetic barrier is decreased for the rearrangement of PE lipids so as to achieve the equilibrium crystallographic scenario of the H_{II} phase. This should then cause the kinetics of the transition to occur more quickly. The opposite kinetic effect is predicted for chaotropes, as Sanderson found that the *d*-spacing of POPE in the L_α phase increased in the presence of higher concentrations of the chaotrope NaI.

Now I turn to the second kinetic barrier to the $L_\alpha \rightarrow H_{II}$ phase transition, namely that associated with the higher energetic cost of exposing the lipid hydrocarbon chains to the aqueous milieu as the interface undergoes the $L_\alpha \rightarrow H_{II}$ phase conversion. During the phase transition, the interamolecular forces operating within the lamellae must be interrupted and in the process of transforming the bilayer into an inverted micelle hexagonal tube, some of the hydrocarbon chains will be exposed to water.[14] Any momentary exposure of the hydrophobic lipid chains to the water is expected to produce a sudden increase in the energy barrier between the phases. This is why a cooperative transition model has been proposed with the formation of high-energy intermediate structures or interlamellar intermediates (IMIs) that form bridges between the apposing bilayers and act as regions in which the phase change can occur.[14,29] The height of the energy barrier for the intermediates depends on the magnitude of the $|T_{exp} - T_H|$ barrier height changes with ΔT in addition to the volume that the hydrocarbon chains occupy. In the case of the Q_3-DLiPE, the hydrocarbon chains occupy a larger volume compared to the hydrocarbon chains of DOPE. Thus, a slower transition to the H_{II} phase is observed, even though the ΔT is in an energetically favorable position, as the T_H is between – 10 and – 16 °C. If a lipid, such as the *trans*-isomer of DOPE, DEPE, were used that had an even smaller hydrocarbon volume, then the transition to the H_{II} will occur at a faster rate.[14]

As the L_α PE transitions to the H_{II}, it must transport water away from the headgroup as 7–9 waters per lipid headgroup have been observed.[32] If bulk transport of water does not occur, as observed by Kirk and co-workers,[31] then the free energy per lipid molecule in the H_{II} phase begins to increase while the free energy per lipid molecule in the L_α begins to decrease; thus, water transport and dehydration of the PE lipid headgroups must take place in order for the phase transition to become favorable. The propensity of the L_α phase of PEs to dehydrate increases with increasing temperature and also the amount of water surrounding the lipids can be controlled through temperature such that a specific phase can be given stability preference due to the energetics associated with the water content.[33]

Thus, in the presence of a kosmotropic anion, less water will be available to the interfacial region of the lipid hydration layer due to the formation of large hydration shells around the kosmotrope. It is conceivable that as two apposing bilayers approach while in the presence of a kosmotrope, the highly hydrated ions are excluded from the interfacial region as the lipid surfaces approach each other. However, in the case of chaotropes, the ions have a smaller hydration shell and can interact with the lipid bilayer by inserting themselves into the headgroup region of the bilayer as suggested by recent reports.[34] This action would slow the $L_\alpha \rightarrow H_{II}$ transition due to the high amount of interfacial water between the apposing lipid bilayers and the increased headgroup spacing, both of which will slow the transition. An additional barrier to slow the $L_\alpha \rightarrow H_{II}$ phase transition may come from the association of the chaotropic ions with the bilayer surface, as the ions themselves may need to be removed from the lipid headgroup regions in order for the phase transition to occur. There is no evidence for the association of chaotropic anions with H_{II} phase PE lipids, therefore it is unknown whether or not the anions are present in the headgroup regions of the H_{II} phase. The association of SCN^- with

lamellar bilayer surfaces has been previously observed, and the ion has a tendency to insert itself into the headgroup region of lipid bilayers.[34]

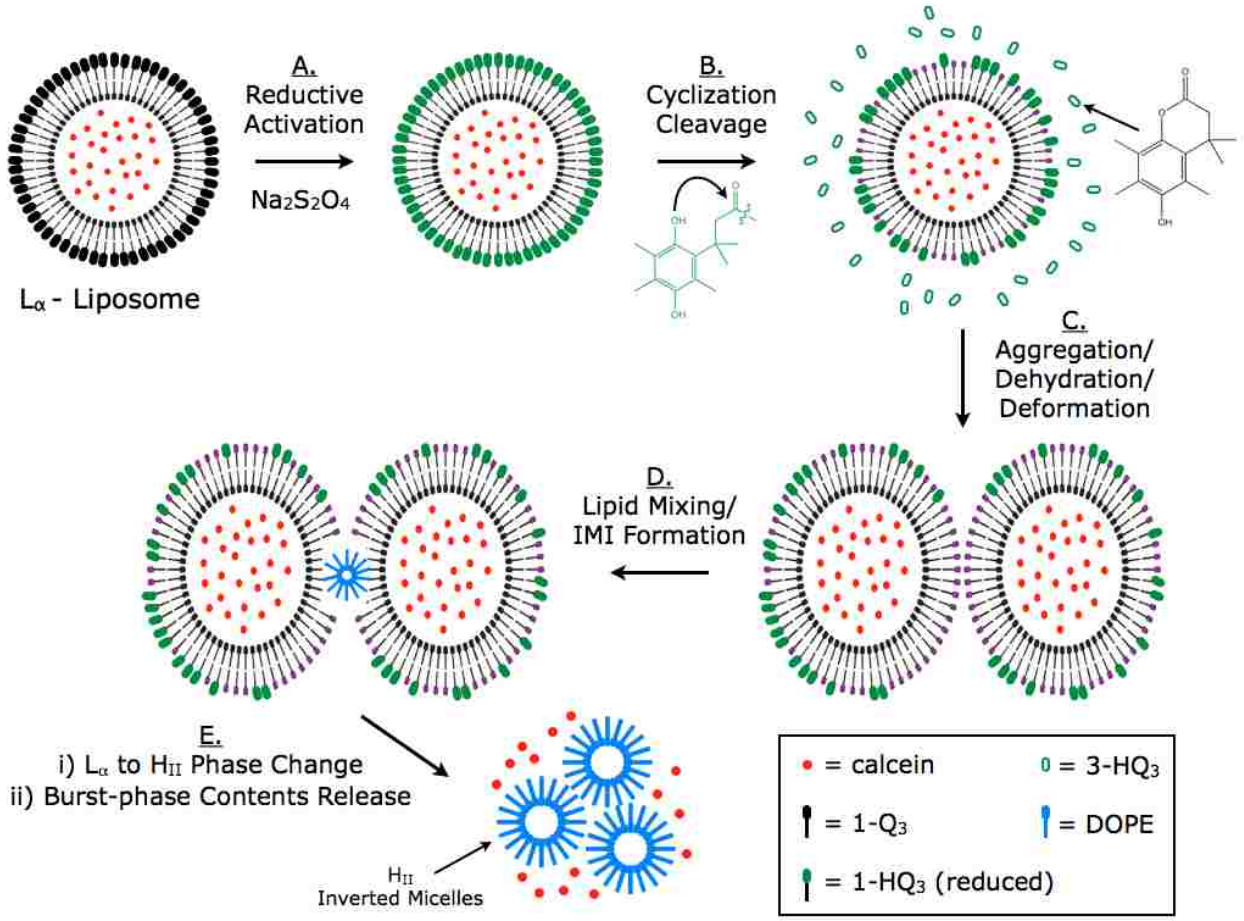

Figure 3.20. The overall proposed pathway for the reduction and contents release from Q_3-DOPE liposomes. Step **A** involves the reductive activation of the $L\alpha$ Q_3-DOPE liposomes by the chemical reducing agent, $Na_2S_2O_4$. Step **B** involves the cyclization and closure of the trimethyl-(Figure 3.20 cont'd) lock that leads to the release of the capping headgroup via formation of the lactone. The reduced liposomes now contain mostly uncapped DOPE lipids and therefore are able to undergo close approach with an apposing DOPE-rich liposome, as seen in step **C**. Upon favorable approach conditions, the DOPE lipids undergo fusion and phase conversion from $L\alpha$ to H_{II} through the formation of interlamellar intermediates (IMI)s, step **D**. Finally, step **E** shows that the H_{II} phase DOPE will reach a critical concentration and the remaining liposome will burst, rapidly releasing the majority of the encapsulated contents as the conversion of the DOPE into the H_{II} phase goes to near completion.

3.5 Conclusions

The rate of contents release from Q_3-DOPE liposomes depends on the experimental temperature, the concentration of salt and the type of salt used. Applying salts from the

Hofmeister series results in a graded response of release rates due to changes in T_H for DOPE. This behavior was found in both content release rates and in DSC measurements of T_H. Kosmotropic anions lower the T_H, increasing the contents release rate whereas chaotropic anions raise the T_H, slowing the contents release rate. The Hofmeister salts are hypothesized to work through a combination of changing the kinetic and thermodynamic properties that influence the phase preference for DOPE lipids. As a consequence, the value of T_H for the lipid appears to be influenced through the hydration level of the lipid headgroup. As demonstrated in the release rates of Q_3-DLiPE, the volume and saturation of the hydrocarbon chains needs to be taken into consideration, as altering the T_H alone is not sufficient to accelerate the content release rates. The results presented here demonstrate that careful selection and consideration needs to be made when selecting buffer components for use in future liposome release studies, as salt concentration and composition can have a significant influence on rates of release and can create difficulty in comparing different DOPE-liposome based systems. The results also demonstrate that with careful selection of the non-bilayer lipid, liposomal delivery systems can be made with graded rates of contents release. While the salt concentration, typically NaCl and KCl in cancer and tumor regions is elevated, on the order of 0.3 M for Na^+, 0.2 M for Cl^- and 0.01 M for K^+ that will have some influence on the contents release rate.[35]

3.6 References

(1) Ong, W.; Yang, Y. M.; Cruciano, A. C.; McCarley, R. L. Redox-Triggered Contents Release from Liposomes. *J. Am. Chem. Soc.* **2008**, *130* (44), 14739-14744.

(2) Carrier, N. H. Redox-Active Liposome Delivery Agents with Highly Controllable Stimuli-Responsive Behavior. Ph.D., Louisiana State University, Baton Rouge, 2011.

(3) Memoli, A.; Palermiti, L. G.; Travagli, V.; Alhaique, F. Effects of Surfactants on the Spectral Behaviour of Calcein. *J. Pharm. Biomed. Anal.* **1994**, *12* (3), 307-312.

(4) Yeagle, P. L.; Sen, A. Hydration and the Lamellar to Hexagonal-Ii Phase-Transition of Phosphatidylethanolamine. *Biochemistry* **1986**, *25* (23), 7518-7522.

(5) Bentz, J.; Nir, S.; Wilschut, J. Mass-Action Kinetics of Phospholipid Vesicle Fusion and Aggregation. *Biophys. J.* **1982**, *37* (2), A25-A25.

(6) Bentz, J.; Nir, S.; Wilschut, J. Mass-Action Kinetics of Vesicle Aggregation and Fusion. *Colloids Surf.* **1983**, *6* (4), 333-363.

(7) Amsberry, K. L.; Borchardt, R. T. The Lactonization of 2'-Hydroxyhydrocinnamic Acid Amides: A Potential Prodrug for Amines. *The Journal of Organic Chemistry* **1990**, *55* (23), 5867-5877.

(8) Milstien, S.; Cohen, L. A. Stereopopulation Control. I. Rate Enhancement in the Lactonizations of 0-Hydroxyhydrocinnamic Acids. *J. Am. Chem. Soc.* **1972**, *94* (26), 9158-9165.

(9) Sanderson, P. W.; Lis, L. J.; Quinn, P. J.; Williams, W. P. The Hofmeister Effect in Relation to Membrane Lipid Phase-Stability. *Biochim. Biophys. Acta* **1991**, *1067* (1), 43-50.

(10) Ellens, H.; Bentz, J.; Szoka, F. C. Destabilization of Phosphatidylethanolamine Liposomes at the Hexagonal Phase-Transition Temperature. *Biochemistry* **1986**, *25* (2), 285-294.

(11) Bentz, J.; Ellens, H.; Szoka, F. C. Destabilization of Phosphatidylethanolamine-Containing Liposomes - Hexagonal Phase and Asymmetric Membranes. *Biochemistry* **1987**, *26* (8), 2105-2116.

(12) Gurtovenko, A. A.; Vattulainen, I. Effect of Nacl and Kcl on Phosphatidylcholine and Phosphatidylethanolamine Lipid Membranes: Insight from Atomic-Scale Simulations for Understanding Salt-Induced Effects in the Plasma Membrane. *J. Phys. Chem. B* **2008**, *112* (7), 1953-1962.

(13) Toombes, G. E. S.; Finnefrock, A. C.; Tate, M. W.; Gruner, S. M. Determination of L-Alpha-H-II Phase Transition Temperature for 1,2-Dioleoyl-Sn-Glycero-3-Phosphatidylethanolamine. *Biophys. J.* **2002**, *82* (5), 2504-2510.

(14) Tate, M. W.; Shyamsunder, E.; Gruner, S. M.; Damico, K. L. Kinetics of the Lamellar Inverse Hexagonal Phase-Transition Determined by Time-Resolved X-Ray-Diffraction. *Biochemistry* **1992**, *31* (4), 1081-1092.

(15) Sanderson, P. W.; Williams, W. P.; Cunningham, B. A.; Wolfe, D. H.; Lis, L. J. The Effect of Ice on Membrane Lipid Phase-Behavior. *Biochim. Biophys. Acta* **1993**, *1148* (2), 278-284.

(16) Kanicky, J. R.; Shah, D. O. Effect of Degree, Type, and Position of Unsaturation on the pKa of Long-Chain Fatty Acids. *J. Colloid Interface Sci.* **2002**, *256* (1), 201-207.

(17) Koynova, R.; Brankov, J.; Tenchov, B. Modulation of Lipid Phase Behavior by Kosmotropic and Chaotropic Solutes - Experiment and Thermodynamic Theory. *Eur. Biophys. J. Biophy.* **1997**, *25* (4), 261-274.

(18) O'Brien, J. T.; Prell, J. S.; Bush, M. F.; Williams, E. R. Sulfate Ion Patterns Water at Long Distance. *J. Am. Chem. Soc.* **2010**, *132* (24), 8248-8249.

(19) Gurau, M. C.; Lim, S. M.; Castellana, E. T.; Albertorio, F.; Kataoka, S.; Cremer, P. S. On the Mechanism of the Hofmeister Effect. *J. Am. Chem. Soc.* **2004**, *126* (34), 10522-10523.

(20) Epand, R. M. High-Sensitivity Differential Scanning Calorimetry of the Bilayer to Hexagonal Phase-Transitions of Diacylphosphatidylethanolamines. *Chem. Phys. Lipids* **1985**, *36* (4), 387-393.

(21) Aurell Wistrom, C.; Rand, R. P.; Growe, L. M.; Spargo, B. J.; Crowe, J. H. Direct Transition of Dioleoylphosphatidylethanolamine from Lamellar Gel to Inverted Hexagonal Phase Caused by Trehalose. *Biochim. Biophys. Acta* **1989**, *984* (2), 238-242.

(22) Kirk, G. L.; Gruner, S. M. Lyotropic Effects of Alkanes and Headgroup Composition on the L-Alpha-H-II Lipid Liquid-Crystal Phase-Transition - Hydrocarbon Packing Versus Intrinsic Curvature. *J. Phys.* **1985**, *46* (5), 761-769.

(23) Gruner, S. M.; Tate, M. W.; Kirk, G. L.; So, P. T.; Turner, D. C.; Keane, D. T.; Tilcock, C. P.; Cullis, P. R. X-Ray Diffraction Study of the Polymorphic Behavior of N-Methylated Dioleoylphosphatidylethanolamine. *Biochemistry* **1988**, *27* (8), 2853-2866.

(24) Gawrisch, K.; Parsegian, V. A.; Hajduk, D. A.; Tate, M. W.; Gruner, S. M.; Fuller, N. L.; Rand, R. P. Energetics of a Hexagonal-Lamellar-Hexagonal-Phase Transition Sequence in Dioleoylphosphatidylethanolamine Membranes. *Biochemistry* **1992**, *31* (11), 2856-2864.

(25) Osman, P.; Cornell, B. The Effect of Pulsed Electric Fields on the Phosphorus-31 Spectra of Lipid Bilayers. *Biochim. Biophys. Acta* **1994**, *1195* (2), 197-204.

(26) Hamai, C.; Yang, T. L.; Kataoka, S.; Cremer, P. S.; Musser, S. M. Effect of Average Phospholipid Curvature on Supported Bilayer Formation on Glass by Vesicle Fusion. *Biophys. J.* **2006**, *90* (4), 1241-1248.

(27) Gruner, S. M.; Tate, M. W.; Kirk, G. L.; So, P. T. C.; Turner, D. C.; Keane, D. T.; Tilcock, C. P. S.; Cullis, P. R. X-Ray-Diffraction Study of the Polymorphic Behavior of N-Methylated Dioleoylphosphatidylethanolamine. *Biochemistry* **1988**, *27* (8), 2853-2866.

(28) Sen, A.; Hui, S. W.; Yeagle, P. L. Membrane Hydration and Its Influence on Membrane-Properties. *Biophys. J.* **1986**, *49* (2), A434-A434.

(29) Rappolt, M.; Hickel, A.; Bringezu, F.; Lohner, K. Mechanism of the Lamellar/Inverse Hexagonal Phase Transition Examined by High Resolution X-Ray Diffraction. *Biophys. J.* **2003**, *84* (5), 3111-3122.

(30) Bentz, J.; Ellens, H. Membrane-Fusion - Kinetics and Mechanisms. *Colloids Surf.* **1988**, *30* (1-2), 65-112.

(31) Kirk, G. L.; Gruner, S. M.; Stein, D. L. A Thermodynamic Model of the Lamellar to Inverse Hexagonal Phase-Transition of Lipid-Membrane Water-Systems. *Biochemistry* **1984**, *23* (6), 1093-1102.

(32) Seddon, J. M.; Cevc, G.; Marsh, D. Calorimetric Studies of the Gel-Fluid (L-Beta-L-Alpha) and Lamellar-Inverted Hexagonal (L-Alpha-H-II) Phase-Transitions in Dialkyl and Diacylphosphatidylethanolamines. *Biochemistry* **1983**, *22* (5), 1280-1289.

(33) Katsaras, J.; Jeffrey, K. R.; Yang, D. S. C.; Epand, R. M. Direct Evidence for the Partial Dehydration of Phosphatidylethanolamine Bilayers on Approaching the Hexagonal Phase. *Biochemistry* **1993**, *32* (40), 10700-10707.

(34) Aroti, A.; Leontidis, E.; Maltseva, E.; Brezesinski, G. Effects of Hofmeister Anions on DPPC Langmuir Monolayers at the Air-Water Interface. *J. Phys. Chem. B* **2004**, *108* (39), 15238-15245.

(35) Gullino, P. M.; Clark, S. H.; Grantham, F. H. The Interstitial Fluid of Solid Tumors. *Cancer Res* **1964**, *24*, 780-794.

CHAPTER 4

HEADGROUP MODIFICATIONS TO STUDY LAMELLAR STABILITY

4.1 Introduction

Accessing the effects of headgroup reduction on lamellar stability of redox-active liposomes can be made through variations in the capping quinone headgroup. Modifications of the trimethyl-lock in the Q_3 headgroup can be made that alter the cyclization rates of the lactone through *gem*-disubstituent effects[1] and conformational restriction of the quinone ring.[2] Removing the geminal methyl groups of the trimethyl-lock side-chain serves to relieve distortion of the quinone ring,[3] which leads to a significantly slower (order of 10^3 times) lactonization rate.[4] Thus, the non-geminal methyl configuration of the lock on the propionic acid side chain, is referred to as Q_1 due to the presence of the single remaining methyl on the quinone ring, as shown in Figure 4.1. Q_1 capping headgroups do not meet the requirements for fast lactonization and headgroup release from DOPE within the experimental time frame of dye-liberation experiments,[5] thus providing a method to examine the effects of reduction on the stability of the lamellar structure of the liposome.

Virtually all lactonization activity of the capping quinone can be removed by substituting the remaining methyls on the quinone with hydrogen to give a headgroup configuration referred to as Q_0. With Q_0 as the headgroup, the quinone can be reduced, but the lactonization rate is so slow that the release of the Q_0 capping headgroup from the lipid monomer effectively does not occur. Figure 4.1 summarizes the structural differences between Q_1 and Q_0 headgroups.

Combining the observations of Q_1- and Q_0-DOPE with those from Q_3-DOPE will provide the opportunity to probe the stability of the lamellar structure of the liposomes after reduction. Upon exposure of Q_3-DOPE liposomes to $Na_2S_2O_4$ several events are triggered that are observable in dye-dequenching experiments from minimal initial release, regions of contraction,

and regions where rapid uploading of the liposomes occurs. However, it is difficult to determine the initial actions that the reduction has on the stability of the lamellar structure of the liposome due to the rapid influx of protons that may lead to a large local flux in the pH surrounding the headgroups. This sudden protonation to H_2Q may create instability in the lamellar bilayer that can result in observable release or contractions in the fluorescence emission of the encapsulated calcein.

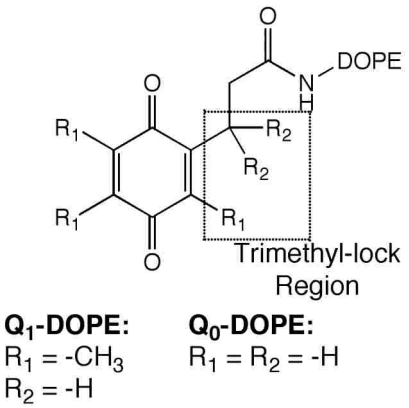

Figure 4.1. The structure of the two redox-active quinone capping headgroups for DOPE. Q_1-DOPE has a single methyl present in the lock region, which relieves the ring contortion and slows the rate of lactonization by a factor of 10^3. Removing all methyl groups from the capping headgroup gives Q_0-DOPE, a species that is readily reduced but does not lead to any significant release from the DOPE lipid monomer.

4.2 Experimental Section

4.2.1 Materials

50 mM phosphate buffer with 75 mM KCl at pH 7.4, 25 °C was used for all experiments. Liposome concentrations were to set to 0.1 mM and contained 40 mM calcein as the self-quenched encapsulated probe. All cuvettes and $Na_2S_2O_4$ solutions were purged with argon. Reduction of the headgroup was initiated by the injection of 1:1 $Na_2S_2O_4$:Q_x-DOPE.

4.2.2 Preparation of Q_1-DOPE Liposomes

Q_1-DOPE was synthetically prepared as described in Chapter 2. Liposomes of Q_1-DOPE were prepared following the procedure for Q_3-DOPE with the modification of using $\varepsilon_{272\ nm}$ = 10300 M^{-1} cm^{-1} to set the liposome concentrations to 0.1 mM via absorbance measurements.

4.2.3 Preparation of Q_0-DOPE Liposomes

Q_0-DOPE was prepared by Rasika Ranatunga Nawimanage of the McCarley research group; all characterizations provided satisfactory results. Q_0-DOPE liposomes were prepared as described in Chapter 2 following the procedure for Q_3-DOPE with the modification of using $\varepsilon_{240\ nm}$ = 7000 M^{-1} cm^{-1} to set the liposome concentrations to 0.1 mM via absorbance measurements.

4.3 Results and Discussion

4.3.1 Q_1-DOPE

Q_1-DOPE liposomes were triggered by the addition of 1:1 molar ratio of $Na_2S_2O_4$ at the triangle marker in Figure 4.2. As expected, the Q_1-DOPE liposomes were reduced, but there was no release of the capping quinone headgroup due to the absence of the trimethyl-lock requirement. After 1297 minutes, only 3% of the calcein was observed to have been released from Q_1-DOPE liposomes, which is on order of observed calcein release from stability studies of Q_3-DOPE liposomes that involved no reduction, as shown in the blue trace in Figure 4.2. The gradual release is attributed to the slow closure of the monomethyl-lock compared to the timeframe of the experiment. Significantly longer experiment times, up to a week or more, are likely to be required in order to observe any additional calcein releases. However, within such an experimental timeframe, the calcein itself would eventually become photobleached due to constant measurements along with the lipids themselves slowly oxidizing due to exposure to temperatures above lipid T_H, oxygen, and light. To further investigate the effects of the

reduction on the stability of the liposome system, a system devoid of lactone formation is required.

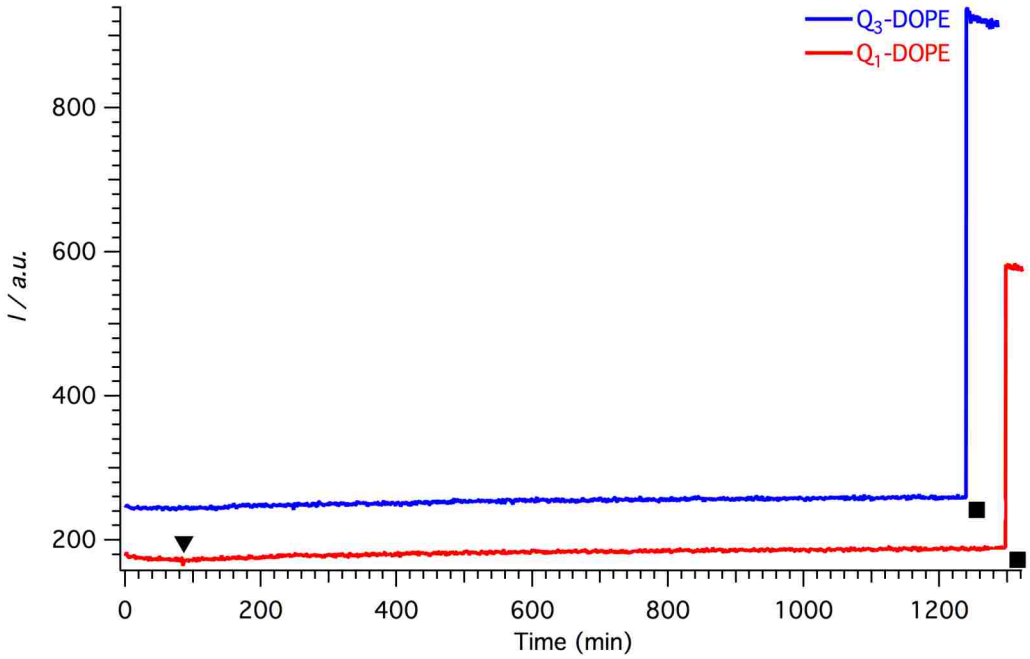

Figure 4.2. Comparison of Q_1-DOPE with Q_3-DOPE. Emission intensities (*I*) of calcein loaded liposomes at 520 nm with λ_{ex} = 490 nm under argon and 25 °C. 0.1 mM liposome concentrations used in both examples. The lower red as for the reductive activation of Q_1-DOPE at the black triangle marker by 1:1 $Na_2S_2O_4$:Q_1-DOPE. The upper blue trance is a representative stability emission observation of Q_3-DOPE with no $Na_2S_2O_4$ added. Both liposome systems were lysed with 0.1 % (v/v) Trition X-100 at the black square, resulting in the release and dequenching of calcein.

4.3.2 Q_0-DOPE

Q_0-DOPE serves to completely remove any influence of a slow closure of the monomethyl-lock that Q_1-DOPE posseses. With no lock present, the effects of quinone headgroup reduction on the stability of the liposomes can be easily observed. It is possible that upon reduction, the buffer capacity could be exceeded, thus leading to a local pH changes in the headgroup region that may cause changes in the bilayer stability or influence the diameter of the liposome. The latter issue is important in assessing the proposed contraction of the Q_3-DOPE liposomes after reduction.

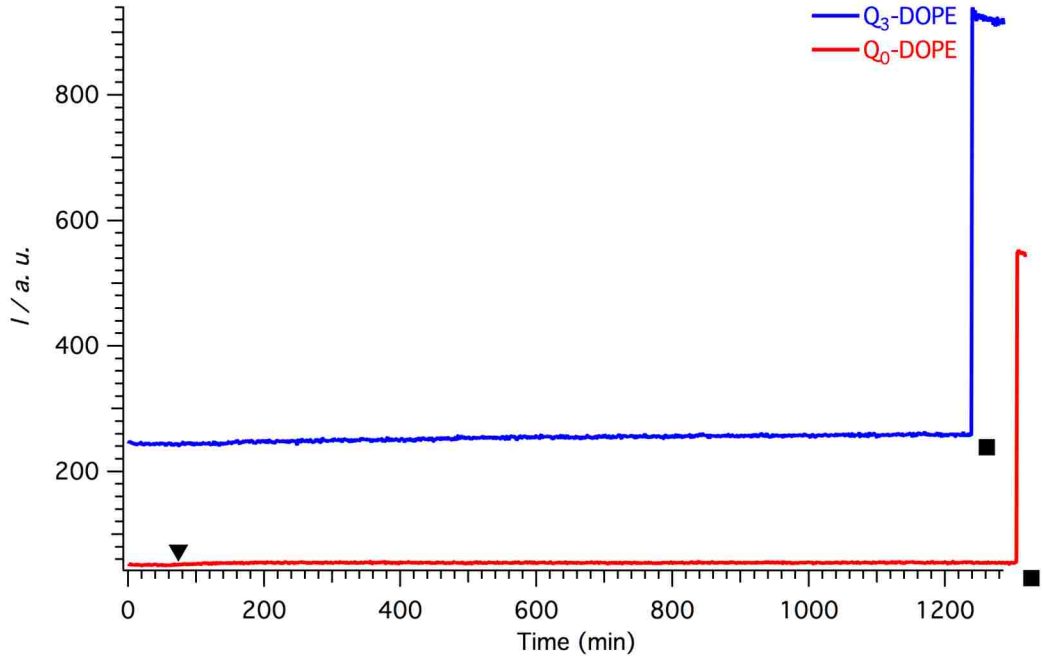

Figure 4.3. Comparison of Q_0-DOPE with Q_3-DOPE. Emission intensities (*I*) of calcein loaded liposomes at 520 nm with λ_{ex} = 490 nm under argon and 25 °C. 0.1 mM liposome concentrations were used in both liposomes. The lower red trace is for the reductive activation of Q_0-DOPE at the black triangle marker by 1:1 $Na_2S_2O_4$:Q_0-DOPE. The upper blue trance is a representative stability emission observation of Q_3-DOPE with no $Na_2S_2O_4$ added. Both liposomes systems were lysed with 0.1 % (v/v) Trition X-100 at the black square, resulting in the release and dequenching of calcein.

The reduction of both Q_1- and Q_0- headgroups on DOPE lipids demonstrates that there is no significant impact on the stability of the liposome structure from the formation of the reduced H_2Q. For example, if the rapid influx of protons to the reduced quinone had a significant influence on the local pH, then that instability would be observed in the leakage of calcein from the liposome interior. Additionally, as previously observed with the Q_3 headgroup, a decrease in the liposome diameter would also be apparent due to regions where a decrease in the emission intensity of calcein would be observable.

These results, combined with the observations of $NaHSO_3$ addition to Q_3-DOPE in the discussion of Figure 3.5, demonstrate that the addition of $Na_2S_2O_4$ does not cause a sudden shock to the system that would have result in non-fusion-related contents release. In addition, the

proposed contraction of Q_3-DOPE liposomes must certinaly occur and is due to the loss of the lactone headgroup. Thus, as confirmed with the mass action kinetic experiments with varying concentrations of Q_3-DOPE liposomes, contact between apposing lipid bilayers is required for the liposomes to release any contents.

4.4 Conclusions

By removing the strain induced on the quinone by the presence of the trimethyl-lock, the rate of lock closure and headgroup release from DOPE can be adjusted. In Q_1-DOPE, the two geminal methyls responsible for the main operation of the lock are replaced with hydrogen, causing a rate of lock closure and lactonization on the order of 10^3 times slower.[4] In the time frame of the experiments, this creates a situation where the quinone is reduced but is still attached to the lipid headgroup. From this, any fluctuations in the fluorescence intensity attributed to instability induced by rapid protonation of the quinone or pH changes that would affect the stability of the lipid bilayer would be observable. With Q_0-DOPE, the ability of the headgroup to undergo lactonization is completely removed by the substitution of hydrogens surrounding the quinone ring.

In both Q_1- and Q_0-DOPE, the addition of $Na_2S_2O_4$ to reduce the headgroups has no effect on the stability of the liposomes. These conclusions are inferred through observations of no changes in the fluorescence emission intensity of the encapsulated calcein immediately following the addition of $Na_2S_2O_4$. Q_1-DOPE is found to experience a gradual leakage due to the reduced rate of lactone formation; however, the total leakage is not observable on the experimental time frame. These results indicate that the initial changes in emission intensities in Q_3-DOPE liposomes are a direct consequence of the formation and release of the lactone.

4.5 References

(1) Jung, M. E.; Piizzi, G. Gem-Disubstituent Effect: Theoretical Basis and Synthetic Applications. *Chem. Rev.* **2005**, *105* (5), 1735-1766.

(2) Wang, B.; Nicolaou, M. G.; Liu, S.; Borchardt, R. T. Structural Analysis of a Facile Lactonization System Facilitated by a "Trimethyl Lock". *Bioorg. Chem.* **1996**, *24* (1), 39-49.

(3) Winans, R. E.; Wilcox, C. F. Comparison of Stereo-Population Control with Conventional Steric Effects in Lactonization of Hydrocoumarinic Acids. *J. Am. Chem. Soc.* **1976**, *98* (14), 4281-4285.

(4) King, M. M.; Cohen, L. A. Stereopopulation Control .7. Rate Enhancement in the Lactonization of 3-(Ortho-Hydroxyphenyl)Propionic Acids - Dependence on the Size of Aromatic Ring Substituents. *J. Am. Chem. Soc.* **1983**, *105* (9), 2752-2760.

(5) Ong, W.; Yang, Y. M.; Cruciano, A. C.; McCarley, R. L. Redox-Triggered Contents Release from Liposomes. *J. Am. Chem. Soc.* **2008**, *130* (44), 14739-14744.

CHAPTER 5

CONCLUSIONS AND OUTLOOK

5.1 Summary

The main goal of the research is to investigate the kinetics of content release following the simuli-responsive reduction of a redox-active liposomal system. Of particular interest is to demonstrate the ability to exert control over the temporal and spatial guest release through the manipulation of the phase transition behavior of phosphatidylethanolamine (PE) lipids. The effects of temperature, salt concentration, and anions of the Hofmeister series were investigated to determine the influence on the rate of encapsulated dye release from redox-active liposomes.

From dye-dequenching fluorescence experiments, it was found that after reduction, the Q_3-DOPE liposomes must come into contact and aggregate with apposing liposomes in order for content release to occur. The apposing contact and aggregation results in L_α DOPE lipids to undergo phase conversion to non-bilayer H_{II} phase, thereby disrupting the lamellar structures of the liposomes and releasing any encapsulated contents. In pH 7.4 50 mM phosphate buffer with 75 mM KCland at 25 °C, it was found that on average, 94% of the calcein could be released from the liposomes within 70 minutes after reduction by $Na_2S_2O_4$. Increasing the experimental temperature created a favorable condition for faster release, as the ΔT between T_{exp} and T_H was larger and therefore more energetically favorable for the conversion of DOPE lipids into H_{II}. Lowering T_{exp} to near T_H resulted in the rate of release slowing to the point where no significant content release was occurring over an extended period of time due to energetic differences between phases that favored the stability of the L_α phase and encouraged a different destabilization pathway involving contents mixing and slow contents leakage.

Differences in the buffer composition were investigated, as initial speculation into the acceleration into the rate of lactonization could occur through catalysis by phosphate buffers.

Comparing TES and phosphate buffer, no differences between the two components were observed. However, the variation of KCl concentration appeared to have a stronger effect on the rates of release. Further investigation revealed that concentration of KCl had similar effects as the temperature on the rate of content release, as higher salt concentrations increased the rate of calcein release.

To further investigate the salt effects, the Hofmeister series was observed to determine changes in the rate of release and to elucidate an explanation for the differences in rates of release. In dye dequenching experiments, 75 mM Hofmesiter salt concentrations were found to have an effect on the rates of release, especially in the chaotropic salts. The kosmotropic salts had a smaller response when compared to the chaotropes and the order of the salts was difficult to determine. Increasing the salt concentrations to 0.5 M revealed a marked response to the type of salt anion present, with kosmotropic salts generating a faster rate of release while chaotropes salts generated a slower rate of release. In an effort to correlate the observe changes in release rate, the T_H of DOPE was measured with DSC against 50 mM phosphate buffer containing 0.5 M Hofmesiter salts. The value of T_H was observed to increase, in accordance with the expected effects of the Hofmesiter salts and through the observed changes in rates of release in dye-dequenching experiments. Based on careful literature evaluation, the Hofmeister salts work on the phase conversion of PE lipids via both kinetic and thermodynamic pathways, creating stability and instability in the phase structures according to the type of salt present.

To address some of the kinetic differences related to the phase transition, the type of PE lipid was varied, with the selection DLiPE that has a lower T_H value than DOPE. DLiPE possesses two *cis*-double bonds in its acyl hydrocarbon chain structure, resulting in a lower value of T_H bur a larger volume occupied by the chains. Comparing the rates of release from Q_3-DOPE and Q_3-DLiPE at 25 °C demonstrated that the Q_3-DLiPE had a significantly slower

release rate, despite a favorable ΔT. The differences were attributed to the commensurate nature of the lattice structures between the L_α and H_{II} phases of each lipid. The closer to commensurate lattices in the phases, the faster the transition will occur. Thus, T_H alone cannot predict accelerations or decelerations in content release rates without consideration of the lattice structures of each phase of the lipid.

Finally, comparing different Q_x headgroups demonstrated that the reduction and rapid protonation of the H_2Q does not have any observable effect on the stability of the liposome or on the local pH. Q_1-DOPE has the requirement of the trimethyl-lock removed and showed a very slow content release rate in the experimental timeframe. Q_0-DOPE contains no lock structure and the only action on the local chemistry is through the reduction of the quinone. Within the time frame of the experiment, no release of detectable calcein was observed in Q_0-DOPE liposomes.

5.2 Conclusions

The results presented here demonstrate that changes in T_H of DOPE lipids can be observed through both DSC and dye-dequenching studies due to the presence of the redox-active capping quinone headgroup. By increasing the area of the PE headgroup with the quinone, the lipid can be effectively trapped in an L_α phase until the headgroup is removed through chemical or enzymatic reduction. After the headgroup is cleaved from the lipid headgroup, the lipids are then able to undergo phase transition to H_{II} through the aggregation and fusion of apposing PE bilayers. The rate of conversion between the two phases can be influenced by the experimental temperature, salt concentration and salt type, thus providing a unique opportunity to further study rates of phase conversions in PE lipids without X-ray diffraction.

Additionally, the results demonstrate that liposomal systems based on the fusion of DOPE lipids to generate content release require careful consideration of the buffer system used

in experiments. Many of the stimuli-responsive liposomes described in literature are based around the concept of trapping DOPE in the L_α through various means and using its phase transition into the H_{II} to create the instability to drive unloading of the liposomes. However, each system has its own experimental temperature, pHs and buffer compositions, each of which creates a unique rate of content release for the described system. The inconsistency in buffer and pH selection make it difficult to compare the effectiveness of various systems, especially in the realm of content release.

5.3 Outlook

Liposmal-based delivery systems will continue to have considerable interest and applications in drug and reagent delivery. It is therefore highly desirable to carefully consider the experimental conditions that can influence the rate of content release from the liposomal systems. By exploiting present conditions at a delivery site, a stimuli-responsive liposome can have another degree of control over the rate of drug release in order to match the drug efficacy profile, generating a more effective and less toxic treatment.

Aside from the drug delivery aspect of the redox-active liposomes describe here, the other interesting result comes in the form of the Hofmeister salt effects on the phase transition of PE lipids. While the literature remains sparse, offering few details and several hints as to possible mechanisms, Q_3-DOPE liposomes offer a very unique way to study this effect through the hydration differences of the lipid bilayers. With Q_3-DOPE and other lipid variants, such as the *trans*-isomer of DOPE, DEPE, it will be possible to further study the hydrocarbon volume differences in the lipids and the effects on the rates of content release. Further study of the phase behavior of pure DOPE is also required to ascertain the full hydration effects of the Hofmeister series. Such experiments can be performed with careful X-ray scattering to measure the *d*-spacing between lamellar bilayers in the presence of various salts and concentrations of salts to

determine the changes in the water layer. Vibrational sum frequency spectroscopy, as described by Cremer[1] also has potential for measuring the water content of the lipid bilayers, which may provide additional evidence when coupled with the X-ray data, as described by Tate and Gruner[2], as to the nature of the Hofmeister effects on the phase transitions of PE lipids.

5.4 References

(1) Gurau, M. C.; Lim, S. M.; Castellana, E. T.; Albertorio, F.; Kataoka, S.; Cremer, P. S. On the Mechanism of the Hofmeister Effect. *J. Am. Chem. Soc.* **2004**, *126* (34), 10522-10523.

(2) Tate, M. W.; Shyamsunder, E.; Gruner, S. M.; Damico, K. L. Kinetics of the Lamellar Inverse Hexagonal Phase-Transition Determined by Time-Resolved X-Ray-Diffraction. *Biochemistry* **1992**, *31* (4), 1081-1092.

APPENDIX: LIPID NAMES, STRUCTURES, AND THERMODYNAMIC DATA

All values for T_M and T_H from Avanti Polar Lipids.[1]

DOPC 18:1 (Δ9-Cis) PC 1,2-dioleoyl-*sn*-glycero-3-phosphocholine

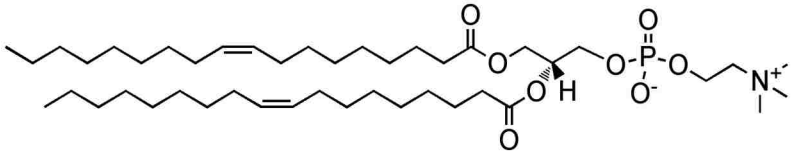

T_M = – 20 °C
T_H = not observed

DOPE 18:1 (Δ9-Cis) PE 1,2-dioleoyl-*sn*-glycero-3-phosphoethanolamine

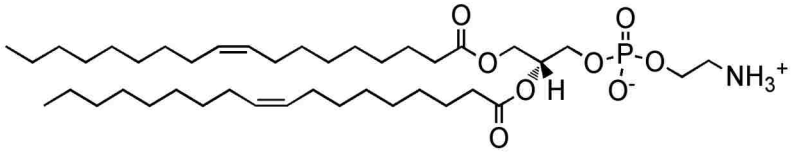

T_M = – 16 °C
T_H = 10 °C

DSPE 18:0 PE 1,2-distearoyl-*sn*-glycero-3-phosphoethanolamine

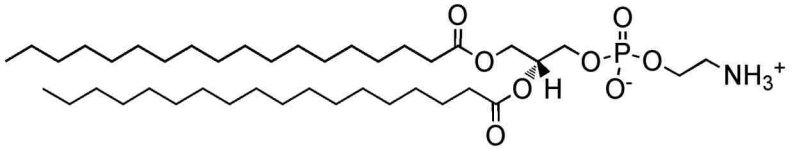

T_M = 74 °C
T_H = 100 °C

DPPE 16:0 PE 1,2-dipalmitoyl-*sn*-glycero-3-phosphoethanolamine

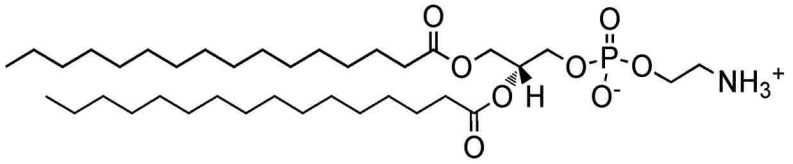

T_M = 63 °C
T_H = 118 °C

DEPE 18:1 (Δ9-Trans) PE 1,2-dielaidoyl-*sn*-glycero-3-phosphoethanolamine

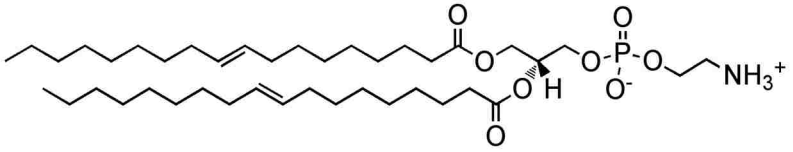

T_M = 38 °C
T_H = 64 °C

DLiPE 18:2 PE 1,2-dilinoleoyl-*sn*-glycero-3-phosphoethanolamine

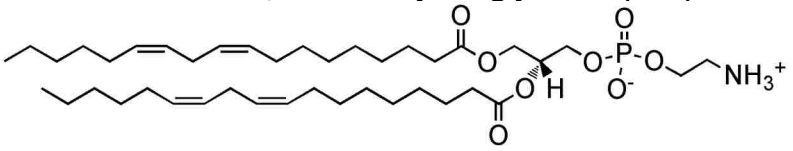

T_M = – 40 °C
T_H = – 15 °C

DOPE-Me 18:1 Monomethyl PE 1,2-dioleoyl-*sn*-glycero-3-phosphoethanolamine-N-methyl

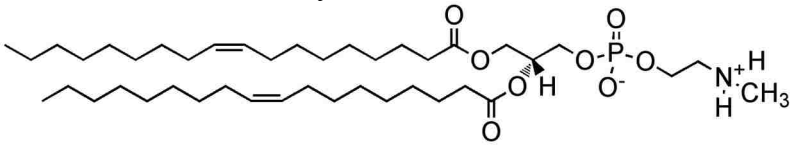

Q_3-DOPE trimethyl-locked, quinone capped, DOPE

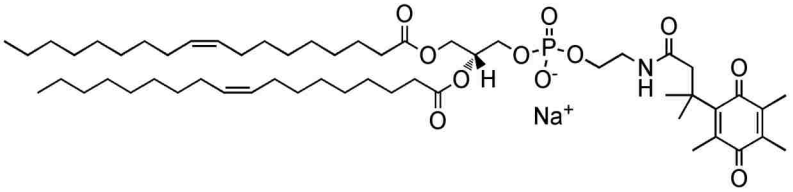

Q_3-DLiPE trimethyl-locked, quinone capped, DLiPE

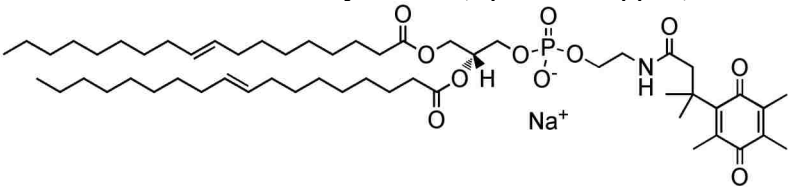

Q_1-DOPE monomethyl-locked, quinone capped, DOPE

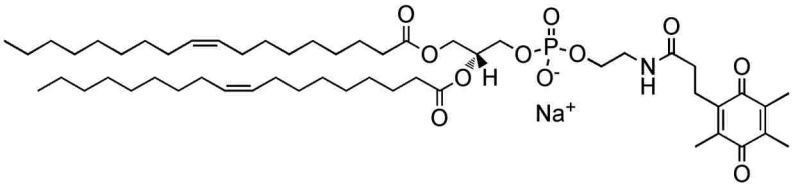

Q_0-DOPE quinone capped DOPE

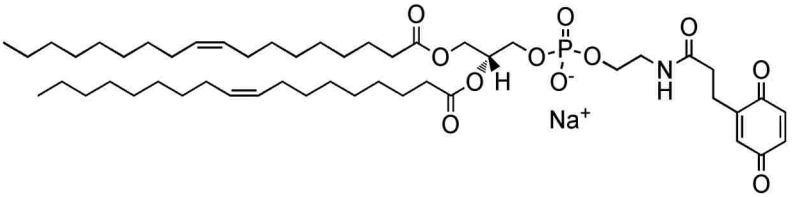

(1) Avanti Polar Lipids. http://www.avantilipids.com (accessed May 2011).

VITA

Jerimiah Forsythe was born in Fort Collins, Colorado. He received his Bachelor of Science degree in chemistry from Colorado State University in 2002 and a master's degree from Washington State University in 2005. He enrolled in the doctoral program in the Department of Chemistry at Louisiana State University in the fall of 2006 where he joined the research group of Dr. Robin L. McCarley. The degree of Doctor of Philosophy will be conferred at the Summer 2011 Commencement.